University of Stavanger

FACULTY OF SCIENCE AND TECHNOLOGY

MASTER'S THESIS

Study programme/specialisation: Petroleum Technology/ Drilling and Well Engineering	Spring semester, 2021 Open
Author: Melissa Rezende Magalhães	
Programme Coordinator: Anita Malde Supervisor(s): Dan Sui	
Title of master's thesis: Digital Twin Development for an In-House Drilling Simulator	
Credits (ECTS): 30	
Keywords: Digital Twin Drillbotics Trajectory Design Trajectory Optimization Sensitivity Analysis	Number of pages: 118 + supplemental material/other: 26 Stavanger, 15 June, 2021 date/year

Abstract

Digitalization is a process that has become inevitable due to the broad economic benefits brought to its assets. The automation and digitalization of the drilling process have advanced greatly throughout the years. The idea behind them aims to increase drilling safety, improve efficiency and decrease the costs associated with said process.

However, drilling a well is an extremely complex operation involving many different systems and drilling parameters that should be taken into account. Dealing with each aspect of the drilling chain is highly challenging, if at all possible. To try and provide the industry with optimal solutions to automate and perform all drilling processes is one of the tasks of the Drillbotics Competition organized by the Society of Petroleum Engineers (SPE).

Therefore, this thesis intends to present the main work done by the University of Stavanger (UiS) Drillbotics Team A, 2020, on its two In-House Simulators, the Well Design simulator, and the Real-Time Drilling simulator. The Well Design simulator was developed to provide its users with a simple and optimal drilling design. In contrast, the Real-Time Simulator aims to integrate methodologies of well design, drilling dynamics, and optimization to provide an automated and intelligent digital twin for helping users to make decisions during real-time operations.

Along with presenting analyses on cases using the rotary steerable system (RSS) simulator developed by the UiS Drillbotics team, the trajectory optimization and control analyses were performed to investigate how accurate the current simulator provided by the UiS Drillbotics team can perform and how its inputs can affect the optimized trajectory.

Acknowledgments

I would like to show my gratitude towards Professor Dan Sui from the University of Stavanger for the commitment dedicated to my thesis and for all the advice and help during the process of writing it. She has always shown me great support, being available at any hour and kindly and politely guiding me through this process.

Likewise, I want to thank all members of the Drillbotics Team from the University of Stavanger for backing up my research, providing me with the necessary material for the composition of this thesis, and always being accessible when I needed it.

To all my friends for sharing with me all their knowledge and supporting me throughout this process. For being kind and generous, and always being by my side, making me laugh and relieving me of all the stress and loneliness I have felt throughout the pandemic.

Finally, to my family for providing me with the means to be here, for all the encouragement they have shown me, and for all the love and nurture they have granted me. Even from across the globe, their positive feeling has always reached me.

Contents

List of Figures

List of Tables

List of Symbols and Abbreviations

AI	Artificial Intelligence
AI lab	Applied Industrial
API	Application Programming Interface
AZ	Azimuth
BHA	Bottomhole Assembly
BHP	Bottomhole Pressure
BSEE	Bureau of Safety and Environmental Enforcement
BUR	Build-Up Rate
CDF	Cumulative Distribution Function
CP	Correction Path
CtC	Center-to-Center
D	Bit Diameter
DL	Dogleg
DLS	Dogleg Severity
DMS	Drilling Modeling and Simulation
DOC	Degree of Curvature
DOF	Degrees of Freedom
DSATS	Drilling Systems Automation Techinical Sections
DT	Digital Twin
E&P	Exploration and Production
ECD	Equivalent Circulation Density
EDM	Engineer's Data Model
EDT	Engineer's Desktop
EOB	End of Build
EOM	Equation of Motion
GA	Genetic Algorithm
GUI	Graphical User Interface
H normal	Natural Displacement
HD	Horizontal Displacement
HSE	Health, Safety and Environment
I	Inclination
IADC	International Association of Drilling Contractors
ICE	Integrated Cloud Engineering
IDS	Integrated Drilling Simulator
IEP	Institute of Energy and Petroleum
IFE	Institute for Energy Technology
IoT	Internet of Things
IPR	Inflow Performance Relationship
ISCWSA	Industry Steering Committee for Wellbore Survey Accuracy
ISO	International Organization for Standardization
JSON	JavaScript Object Notation
KOP	Kick-off Point
MD	Measured Depth
ML	Machine Learning
MPD	Measured Pressure Drilling
MSE	Mechanical Specific Energy
MW	Mud Weight
MWD	Measure While Drilling

NORSOK	Norwegian Shelf's Competitive Position
NPT	Non-Productive Time
OBM	Oil-Base Mud
ODE	Ordinary Differential Equation
OHTC	Overall Heat Transfer Coefficient
OSDU	Open Subsurface Data Universe
PDC	Polycrystalline Diamond Compact Bit
PDM	Positive Displacement Motors
PI	Productivity Index
ppg	Pounds per gallon
PVT	Pressure, Volume, and Temperature
PWP	Planned Well Path
REST API	Representational State Transfer Application Programming Interface
ROP	Rate of Penetration
S&S	Surge and Swab
SESTEM	Shell Extended Systematic
SF	Safety Factor
SHC	Specific Heat Capacity
SI	International System of Units
SPE	Society of Petroleum Engineers
T&D	Torque and Drag
TC	Thermal Conductivity
TOB	Torque on Bit
TVD	True Vertical Depth
UBD	Underbalanced Drilling
UCS	Unconfined Compressive Strength
UiS	University of Stavanger
US	United States
VR	Virtual Reality
web-GL	Web Graphics Library
WOB	Weight on Bit

1. Introduction

Drilling automation and digitalization have advanced from being applied solely for separated pieces of equipment to an idea of application on the entire drilling process. This idea aims to increase safety, reduce costs and improve the efficiency of the process enabling operations in locations considered unsafe and uneconomical (UiS Drillbotics, 2021a.).

However, a limitation found by the industry so far is the cost of testing and validating these developing technologies. To approach this limitation, the idea of creating a student competition took shape, allowing students to develop a full-scale drilling system and a digital twin that can be used to run several drilling designs tests by the introduction of various parameters provides the industry with an extensive and necessary data library (UiS Drillbotics, 2021a.).

Moreover, student competitors could discover innovative tools and processes capable of assisting drillers in speeding the drilling time. This may encompass more than applying a faster rate of penetration (ROP), such as improving wellbore stability issues and problem avoidance for dysfunctions in the well. These students can create fresh approaches to many different problems faced by the drilling industry while learning about the business itself (Drillbotics®, 2021).

Additionally, the creation of an in-house simulator capable of providing the industry with an optimal drilling design and integrating different methodologies to provide an intelligent and automated digital twin is of extreme importance. Being able to optimize the performance of the drilling design, automatically monitor and detect changes in trajectory and provide an open and integrated system can provide several benefits to the industry, such as reduction in costs, safer operations, and increase in production.

1.1. UiS Drillbotics

Drillbotics is a competition created by SPE to allow students to design a lab-sized drilling rig to compete against one another. In the last years, the competition has broadened into two different groups, Team A, which is in charge of developing a drilling simulator, and Team B, in charge of the physical drilling rig. UiS has taken part in both competitions yearly with support from the AI lab at IEP (UiS Drillbotics, 2021a.).

This thesis focus on the competition pertaining to Team A, the Virtual Rig Team. The goal of Team A is to develop a simulated model for a virtual drilling rig that includes the drill string, BHA, and wellbore interaction. In addition, each Team member must oversee the development, investigation, and creation of a complex code of diverse drilling models that will generate the whole Real-Time Drilling Simulator (UiS Drillbotics, 2021b.).

The team's concepts for the Real-Time Simulator are tested during the Drillbotics® competition. The Drillbotics Committee provides the team with a specific case, which must be solved using the simulator software. The winner can travel and present an article at the next SPE/IADC Drilling Conference, an event organized by DSATS (UiS Drillbotics, 2021b).

1.1.1 Guidelines

The challenge given by the Drillbotics Committee is to develop a drilling system model representation of a full-scale system and its control scheme to drill a directional well to a given trajectory. In addition, the teams are expected to perform basic realistic calculations of the system. The scope includes selecting essential parameters such as:

- Drive mechanism;
- Drill pipe;
- Bottom hole assembly (BHA);
- Surface systems for applied rotations per minute (RPM), weight on bit (WOB), among others.

Each system must be modeled according to the guidelines. For example, the rig model should consist of a drum controlling the draw-works and a top drive regulating the torque and the RPM. The downhole drilling system model must predict the bit trajectory for given WOB, RPM, rock strength, and other drive mechanisms given the measured depth (MD).

The bit model must present an applicable framework for steerability and the effect of key parameters, such as drilling efficiency and gauge length. However, this model shall be provided by the judges. The rock model should present specifications for the type of rock, unconfined compressive strength (UCS), and confining pressure. In addition, the change in build-up rate (BUR) due to wellbore geometry must be taken into effect.

The BHA model must compute the contact force at the bit, and the bit tilt using the steering model. It should also measure parameters as inclination, RPM, and vibration. In addition, the design must provide configurable parameters of bit-to-sensor distance and its measurement frequency. The steering system shall take inputs from the Bit and BHA models to predict the well trajectory. As for the drill string model, it may be expressed by one or more models, as long as they follow these specifications:

- Torque and drag (T&D) calculations for a 3D survey, with hook load, drill string/BHA dimensions, mud weight (MW), and variable friction factors as inputs. It should predict downhole WOB and torque on bit (TOB) to be used as inputs on the bit model.
- The drill string model should calculate buckling conditions, and it should simulate torsional oscillations like stick-slip.

The control system may provide automatic drilling optimization, a trajectory control system, a rig display, and a setpoint control system. Therefore, the written code should be of modular design with a separated application for the drilling system to interact with the control system.

The rock properties for the models will be provided as a function of MD by the competition judges. In addition, data will be given to calibrate sub-models, such as the bit model. Teams will be evaluated per model; points will be distributed for each presented model. The purpose is to model a realistic behavioral model with its sub-models. All this information can be found in more dept in Drillbotics® (2021).

1.2. Objectives and Outline

This thesis's general objective is to present the UiS Team A's work throughout 2021 for the Drillbotics Competition, the models designed, and their integration in the Well Design Simulator and the Real-Time Drilling Simulator. Correspondingly, the specific objectives are as following:

- To provide an overview of the industry's current software developments for trajectory optimization and well design.
- To present the methodology used by the UiS Team A to design its models for the well design and real-time drilling simulators, the relations between these models, and their integration in a digital twin.
- To analyze the limitations of the RSS simulator and its correction parameters (dog leg severity [DLS] and tortuosity) for the trajectory optimization by changing its mean values of WOB, RPM, and sliding factor (μ).

To accomplish its objectives, this thesis outline will start by providing a literature review on the digitalization and automation of the drilling process and present information on the commercial softwares for well design and real-time drilling designed by different companies.

Progressing with the definition of the trajectory design, where the concepts of well design, well trajectory, directional drilling, and 3D trajectory design will be disclosed. It will also analyze the wellbore trajectory optimization account for the principles of anti-collision, DLS optimization, and ROP optimization.

Moving forward, the models for the In-House UiS Well Design Simulator will be described, as well as their integration through the Well Design web application. Furthermore, the In-House UiS Real-time Simulator shall be presented with its models, the drilling optimization and real-time control elements, and the models coupled and interacted explanations.

Lastly, a case study will analyze the performance of the RSS Simulator for two different wells and its limitations, accounting for its correction parameters when changes of WOB, RPM, and sliding factor occur. Finally, the results for these simulations will be presented, along with a discussion over them and an evaluation of the necessary further work that should be applied to said model for the following years.

2. Literature Review

2.1. Digitalization Development in Drilling

Digitalization involves using digital technologies to improve or create new business processes capable of driving operational efficiencies (Farmanbar et al., 2020). It may also be defined as the process of using data to simplify the workflow or the use of technology in order to make a process faster, more secure, and more efficient (Nadhan et al., 2018).

Digitalization of the drilling and non-drilling operations is becoming inevitable due to the vast economic rewards brought by such assets. The IoT is pushing for digital enhancement across multiple industries. The oil and gas industry has just start adhering to this transformation, progressively looking towards data-driven solutions to enhance efficiency, increase performance, and ultimately reduce costs (Siemens, 2020).

Equinor's digitalization program is an example of how the application can succeed in the oil and gas industry. As stated by Equinor (2021), digitalization provides:

- Digital security and sustainability: Utilize data to diminish security risks, improve apprenticeship from past incidents, enhance security, and diminish the carbon footprint of the business.
- Process digitalization: Streamline work processes and reduce manual input over the value chain.
- Subsurface analysis: Used to improve data access and analyze tools for subterranean data, thus facilitating better decision-making.
- Next-generation well delivery: Strengths the use of well data for real-time analysis, planning, and enhanced automation.
- Fields of the future: Smart concept and design choices through maximizing the use of accessible data and assimilating digital technologies into future fields.
- Data-driven operation: Using data to maximize the value of the installations through production optimization and maintenance enhancements.
- Commercial insight: Used to improve analysis tools and data access in commercial areas to enable better decision-making.

2.2. Drilling Modeling and Automation

The process of drilling a wellbore is extremely complex, it involves many different drilling systems, which interact among themselves and with the drilling fluids and the formation surrounding it. DMS concerns modeling and simulating the nature of drilling systems and processes. It can provide decisive information about the drilling system without the construction of a physical well. As a result, Drilling Modeling and Simulation (DMS) methods can be devised to help increase drilling efficiency, performance, and productivity, besides managing various risks effectively, therefore, improving the safety of operations and personal (Wilson A., 2015).

Automation establishes a control system to diminish the physical and/or mental workload of operators in charge of running a specific process. It is motivated by increasing economic and/or operational performance while maintaining a safe environment (Breyholtz & Nikolaou, 2012). For example, drilling automation focuses on the downhole activities fundamental in the actual drilling of a well. This process involves linking the surface and downhole measurements to a real-time predictive model visioning improving the drilling process's safety and efficiency.

Tackling every single aspect of a process such as drilling is extremely demanding, if at all possible. In order to put drilling automation into a general workflow, the use of a 'modes-of-automation' approach is necessary. "The role of the driller and the automation system is dependent on the chosen automation strategy". Table 2.1 shows the different modes-of-automation used for such a process; they are listed from Mode 0 (lowest degree of automation) to Mode 6 (highest degree of automation) (Breyholtz & Nikolaou, 2012).

Table 2.1: "Different Modes of automation and the resulting tasks for the automation system and the driller". Source: (Breyholtz, Ø., & Nikolaou, M., Table 1, 2012).

Mode	Management Mode	Automation Functions	Drillers Functions
6	Autonomous Operation	Fully autonomous operation.	No particular function. Operations goals are self-defined. Monitoring is limited to fault detection.
5	Management by Exception	The automation system chooses operations and defines operation goals. Informs the driller, and monitors responses on critical decisions.	The driller is informed of the systems intent. Must consent to critical decisions. May intervene by reverting to lower mode of management.
4	Management by Consent	The automation provides coordinated control of multiple control loops.	The driller feeds the automation system with a chosen operation, operation goals, and desired values for key variables (e.g. circulation rate)
3	Management by Delegation	The automation system provides closed loop control of individual tasks. (E.g. Choke pressure control in an MPD system; automated tripping module)	The driller decides setpoints for the individual control loops. (E.g. setpoint for pressure in MPD operations). Some tasks are still performed manually (envelope protection active).
2	Shared Control	The automation system could interfere to prevent the driller from exceeding specified boundaries. Should predict the outcome of the driller's choices.	Envelope protection systems are enabled. Decision support/advisory systems are available.
1	Assisted Manual Control	Provides down-hole information trends, and detects abnormal conditions in the well. Does not intervene.	The driller has direct authority over all systems. Decision-making is computer-aided.
0	Direct Manual Control	Normal warnings and alarms.	The driller has direct authority over all systems. Unaided decision-making.

Breyholtz & Nikolaou (2012) stated that the understanding that the mode of automation does not need to be permanent is fundamental; in fact, the driller should be able to change between different modes during a single drilling operation having absolute authority over the whole process. Thus, the driller should have the means to override the automated process if necessary. Each automation has its pros and cons, and those must be balanced to provide the best outcome for the operation.

2.3. Digital Twins

Digital Twin (DT) is the virtual portrayal of an asset, i.e., DT is a digital copy of a physical system and serves as a bridge between the digital and physical words (Nadhan et al., 2018).

According to Nadhan et al. (2018), combining real-time data and digital data with predictive diagnostic reports is advantageous in improving accuracy in decision-making and results. That helps the industry improve efficiency, achieve economic-value-based resolutions, and increase safety.

Grieves M. (2006) stated that the main fundaments of the DT are "real space, virtual space, the link for a data flow from real space to virtual space, the link for information flow from its virtual space to real space and virtual sub-spaces". As Nadhan et al. (2018) depicted, using a DT helps to understand the concept, functionality, and failure of a complex system by implementing the virtual models of all physical parts interactions.

Digital twins drove by real-time data assist by giving operations an optimal plan focusing on, risk reduction, safety and enhanced performance. Additionally, DT allow companies to run risk analyses, create what-if scenarios in real-time, and provide health assessments. As a result, they can detect faults early before control limits are reached and contribute to hazard prevention, non-productive time (NPT) avoidance, and performance optimization (Nadhan et al., 2018).

DTs may have different applications in drilling and well operations, for example (Nadhan et al., 2018):

- Real-time monitoring of a well allows real-time predictions of downhole NPT and HSE-related events. It also allows faster real-time optimization and improved decision-making for safer and more efficient drilling operations.
- Post well analysis allows a better understanding of historical events for knowledge application in futures wells.
- Pre-operation allows crew practice and trial runs before drilling the actual well. This allows for making mistakes while testing out the procedures, practice communication, respond to well related and topside related malfunctions, test out new drilling concepts and fulfill regulatory requirements.

The drilling models design by the automation process and incorporated into the digital twins can interact and be used in the full drilling value chain from the planning and design, followed by the development of scenarios for trial runs, real-time optimization, and post well analysis and experience transfer. These systems are part of the Life Cycle Drilling Simulation concept, shown in Figure 2.1, implying an advanced dynamic drilling model and diagnostic technology merged with 2D and 3D visualization into a virtual wellbore (Nadhan et al., 2018).

The current industry is moving forward and including more automation and automated real-time monitoring instead of manual work in its processes. The automated real-time monitoring encompasses real-time transient simulations, automated comparison of simulation results with real-time measurements, automatic diagnostics, and early self-detection of wellbore deterioration. Thus, by applying real-time process-driven transient simulations, forward-looking and what-if simulations, the drilling process can improve beyond its monitoring practices (Nadhan et al., 2018).

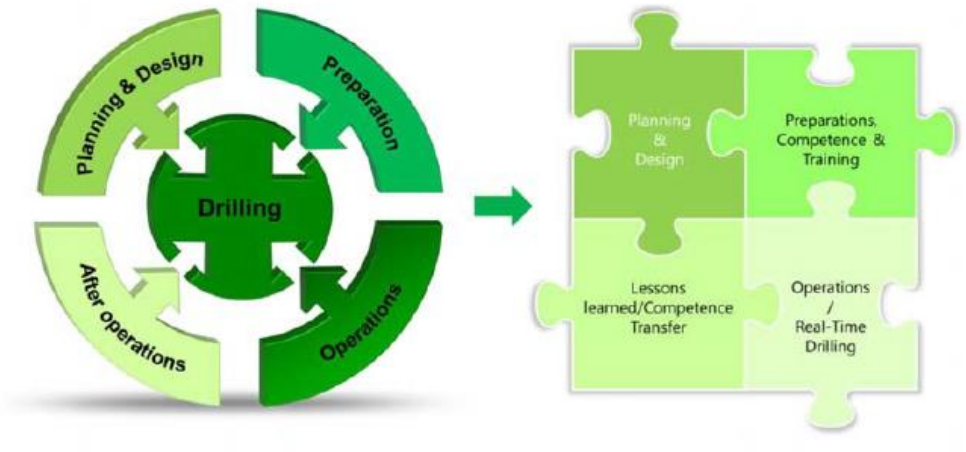

Figure 2.1: Life-cycle of the drilling process.
Source: (Nadhan, 2018.)

2.4. Commercial Softwares

In order to suppress problems in drilling and completion of wells and decrease costs and time, many companies have created their software for well design and real-time simulation. Some of this commercial software and its utilities will be presented in this next section.

2.4.1. eDrilling Softwares

eDrilling AS is a world-leading supplier of machine learning, AI and analytical solutions to the oil and gas industry and applies these technologies on well construction to save costs, improve safety, and increase the efficiency of drilling operations (eDrilling, 2021). The company has four major softwares: wellAhead™, wellPlanner™, wellSim™ and wellBalance™.

The company has created a Life Cycle Drilling Simulation concept, diagnostics technology merged with a 3D graphics into a virtual representation of a wellbore and advanced dynamic drilling models. All the models can interact with one another and be used in the whole drilling value chain. The solution is integrated in a transient drilling simulator named Intellectus™, with a decision support system capable of supporting the life cycles of production: planning, training, drilling, and post-analysis/learning (PetroMehras Directory, 2019a).

2.4.1.1. WellAhead

The wellAhead is a software for automated monitoring, live well support, and real-time optimization. It enables a better understanding of the well's status and the formations in its surroundings, allowing for better and faster solutions. The software uses all available drilling data combined with modeling and operational plans to monitor the well and provide counseling for more optimal drilling. Its graphic user interface provides real-time information visualization (PetroMehras Directory, 2019a).

According to the PetroMehras Directory (2019a), the significant benefits of the wellAhead software is the fact that its real-time mathematical models supplied with real-time drilling data create an embodiment of the well and enables features such as diagnosis, what-if scenarios, forward-looking, and a virtual wellbore with full visualization of the downhole process.

The problems that the wellAhead can address are hole cleaning, lost circulation, kick detection, problems with connections, and tripping in/out of the well. The models adopted by this software are "Flow & Temperature, T&D, Operational Status, Diagnostics, Wellbore stability, Pore pressure, visualization" (PetroMehras Directory, 2019a).

2.4.1.2. WellPlanner

The wellPlanner™ software addresses problems with safety margins and risk associated with them and reduces planning time by using dynamic simulations to provide accurate modeling. (eDrilling, 2021)

As stated by the PetroMehras Directory (2019c), the main benefits of this software are the increase of the drilling productivity, the improvement in well-planning accuracy, the reduction of drilling risks and uncertainty, the improvement in drilling safety, and quicker well planning.

The wellPlanner features "dynamic models verified in wellAhead and wellSim by operators, unique combination of models and functionalities, an all combined in one IDS named Intellectus, all flow-related dynamic functionalities, and responses combined in one IDS, integrated part of Life Cycle Simulations with wellAhead and wellSim products seamless link" with each other (PetroMehras Directory, 2019c).

The main applications found in the wellPlanner software are the "Flow Model; Dynamic Hydraulics and Temperature; ECD/pressure and temperature profiles, the Well Control Evaluation and Optimization, Kick Tolerance, T&D planning Evaluation, Well Positioning planning, ROP and WOB optimization, Pore pressure, Wellbore stability" (PetroMehras Directory, 2019c).

2.4.1.3. WellSim

The wellSim™ is "the software for engineering and training of all disciplines by improving judgment and understanding of the dynamic well behavior; it is likely to change the ways companies plan and drill their several complex wells" (eDrilling, 2021).

This software uses Intellectus, to include a dynamic ROP model coupled with a Flow and T&D model. It provides the user with a model of the time development of each operation and takes into consideration dynamic effects like inertia, effects of temperature and pressure changes on bottomhole, acceleration and retardation of the string, among others. It provides an embedded reservoir model in the "multi-phase hydraulic model for realistic influx behavior" (PetroMehras Directory, 2019d).

Conforming to PetroMehras Directory (2019d), "the simulator models dissolved and free-gas realistic during a killing operation. The T&D model includes an ROP model for realistic ROP

related to WOB based on formation properties". It can be conveyed with different front ends, such as:

- wellSim™ hiDRILL – VR topside simulator for rig floor team collaboration training;
- wellSim™ Interact – Desktop control of common drilling parameters;
- wellSim™ Third-Party – the wellSim™ API facilitates the interface to any third-party top side drilling simulator.

The main benefits of the wellSim software are to reduce the non-productive time by better planning, improvement of risk management both in planning and operation, improvement of operational decision with a distributed decision support alternative and sharing of simulations across teams and disciplines, providing great dynamic feedback of the well, supplying real-time response on interactive user input, exceptional insight of well behavior and the provision of a 'Virtual Well' concept, where wells and simulations can be transferred between different softwares (PetroMehras Directory, 2019d).

Apart from that, the PetroMehras Directory (2019d) states that the interactive ROP model and the Flow and T&D model the software bears other features such as a 3D visualization with informative messages of risk, proximity wells, malfunctions, kicks and losses scenarios, model state handling that provides transfer of simulations between the eDrilling Softwares.

The primary operations performed by the wellSim are drilling operations, tripping in/out with dynamic S&S, stripping operations, multi-fluid operations, deepwater drilling operations, well control operations, and high-pressure-high-temperature (HPHT) operations (PetroMehras Directory, 2019d).

2.4.1.4. WellBalance

The wellBalance software "improves any Measure Pressure Drilling (MPD) control system to keep a constant bottom hole pressure during MPD operations and perform planning with an offline model". It provides with "real-time set points to the MPD control system, based on a dynamic real-time simulation calibrated against downhole measurements. It is complemented with an offline simulation tool, the wellBalance™ Offline, used to test and analyze operations and procedures" (eDrilling, 2021).

This tool is enforced by enclosing a real-time dynamic model into a 3rd party control system, inputs from the rig are continuously updating the ECD and the temperature profile in the well. The following features are added by acquiring a license that provides the offline tool: "dynamic two-phase transport of fluids up the annulus, batch simulation of long pre-defined sequences, can be run on separate computer or "real-time" computer system, reports from the simulations will be on the same format as the real-time system, and provides an integrated tool with real-time and simulation capabilities" (PetroMehras Directory, 2019b).

The wellBalance software supports the following operations: “circulation at different pump rates, with and without rotation, static periods, drilling, reaming, tripping in and out, handles connections with or without backpressure pump and displacements with different fluids or one fluid with different densities” (PetroMehras Directory, 2019b).

According to the PetroMehras Directory (2019b), the models utilized in this software are: dynamic mass transport, pressure, and temperature-dependent density, pressure and temperature-dependent rheology, rheology model, cuttings load, S&S, rotation are taken into account while calculating the heat transfer and the frictional pressure loss in the well, multiple fluids can be tracked in the system, estimated pressures should change depending on details of different parameters , such as: inner and outer diameters, angle of inclination, rheology, and operational parameters having a 2D dynamic temperature model integrated with the 1D dynamic model.

2.4.2. Oliasoft Softwares

“Oliasoft was formed in 2015 by energy sector and software professionals dedicated to using the best digital technology to automate the well planning workflow. The result is Oliasoft WellDesign, an Integrated Cloud Engineering (ICE) platform that transforms the process of building cost efficient, safe and effective well design systems” (Oliasoft AS, 2021a).

This software establishes new ground by associating every link from the well planning into a cloud software application and providing calculation engines that are entirely manageable with industry-standard well integrity regulations (Oliasoft AS, 2021a).

WellDesign’s advanced simulation engines automate well planning and operations, improving safety and enhancing efficiency; the open API allows users to build their own solutions by working any 3rd party application granting the user free range to design and automate their well planning ecosystems, and providing real-time collaboration between different virtual teams (Oliasoft AS, 2021a).

Conforming to Oliasoft AS (2021a), the main features from WellDesign are its integrated workflow, which allows all calculations to update according to the latest data, its comprehensive solution that makes sure all required well design calculations included are fully documented, reducing dependencies on consultants, its digitalization, that allows complete control over the data potential, proving free to use data anywhere, anytime and for any application, and its integration system, allowing seamless integration with third-party applications and connecting to real-time data streams from operations to update designs and monitor critical parameters automatically.

Oliasoft’s Well Design Simulator is divided into six modules: Trajectory Design, Casing Design, Hydraulics & S&S, Torque & Drag, Tubing Design, and Blowout & Kill.

2.4.2.1. Trajectory Design

The Well Trajectory Design Module allows the user to generate various planned renditions of different well trajectories, with a revision tracking and management of each well, field, and analysis. It supports all well configurations such as J-shape and S-shape, error modeling, well

paths and positioning mathematics, and anti-collision functionalities based on mathematical formulas (Oliasoft AS, 2021f).

According to Oliasoft AS (2021f), the key features of this module are integrated access and collaboration features, parametric design capabilities counting automatic trajectory design, error modeling and anti-collision, web-GL 3D real-time trajectories, "full REST API support", return trajectories, error ellipses/ellipsoids, real-time plots of operational path vs. planned path and trajectory and anti-collision reporting".

This module is a fully-fledged engineering and data management system that can be managed from any browser, providing accessible data and designs; it offers a Web-GL 3D real-time interpretation of trajectories and industry-standard graphs like section and plans view, traveling cylinder, ladder plots, and more (Oliasoft AS, 2021).

The module presents a wide range of parametric build choices for construction well trajectories combined with path and positioning mathematics, including "including the Constant Turn Rate, Constant Curvature, Radius of Curvature, Minimum Curvature, Tangential, and Balanced Tangential methods. It also Includes complex build features, including linear, quadratic, and higher-order Bezier curves for optimization, and automation of 'path to target' with continuously varying doglegs." (Oliasoft AS, 2021f).

Apart from those, it also includes full geodetic support; it allows geomagnetic parameters to be applied to the excellent design through a 3rd party provider, it has an error modeling. Anti-collision functionality, including support for continuous gyro and its trajectory model, can be associated to real-time data during drilling for real-time visualization of planned path vs operational path (Oliasoft AS, 2021f).

2.4.2.2. Casing Design Module

Oliasoft AS (2021c) reported that the Oliasoft Casing Design Module offers the user a complete casing design suitable for all industry standards and support of pre-defined load cases meeting all requirements and custom loads.

This module has a full machine learning proficiency, allowing calculations to be performed with 3rd party solutions. The user can pre-define the "internal and external pressure profiles, and integrate these with the temperature and production simulations". Its main features are its complete casing design, its advanced pressure profiles, full support for all custom load cases, its safety factor for all dimensions, its endless configuration options, and its automated design (Oliasoft AS, 2021c).

According to Oliasoft AS (2021c), its Casing Design Module provides with an automated well design and material selection run on unique rules generated by Oliasoft API and the Module interface. It provides a complete casing design compatible with NORSOK, ISO, and American Petroleum Institute (API) standards, where its engine manages point loads, anisotropy, and asymmetry. It also presents the user with pre-defined load cases and generic load cases besides giving the option to customize your own loads. Furthermore, external loads and its temperature profiles can be modified for each load case.

2.4.2.3. Hydraulics & S&S Module

Oliasoft AS (2021d) states that with its Hydraulics and S&S Module, the user can accurately model any rheology profile in several well configurations; it handles ECD estimation from circulation and incorporates pipe eccentricity, rotation, and cuttings transport.

The user can also combine this module with the Oliasoft Torque and Drag Module by using buckled string analysis to calculate the pressure drop in the well. It is also possible to connect its thermal simulation module to generate detailed temperature profiles as a ground for the calculations (Oliasoft AS, 2021d).

The Hydraulics & S&S Module key features presented by Oliasoft AS (2021d) are its drill string eccentricity, the assessment of pressure and temperature impact on rheology, and the predictions on hole cleaning and cuttings bed, its convert rheology from custom apparatus mode, the possible use of the module with the T&D Module for hole cleaning and pressure drop considerations, its holdings on BHA components, and the inclusion of the Newtonian, Bingham Plastic, Power Law and Herschel Bulkley rheology models.

This module allows the user to model fluids with any rheology profile in several well configurations and model pressure losses across the whole circulating system. It supports BHA design, wellbore cleaning, S&S, and integrated load cases. It provides efficient ECD estimative from circulation with cuttings transport model. It optimizes bit nozzle sizes to maximum ROP and gives S&S calculations for BHA completion and casing strings (Oliasoft AS, 2021d).

The module's hydraulic engines fuse "analytical and numerical finite-difference mathematical models" to forecast responses for ECD, reverse-circulation, injection, and drilling (Oliasoft AS, 2021d).

2.4.2.4. Torque & Drag

According to Oliasoft AS (2021e), its Torque and Drag Module provides T&D calculations through analysis of drilling, casing, and completion operations. The calculations can be performed with soft and hybrid string analysis to predict loads accurately. In addition, the user can utilize Oliasoft API to calibrate the friction factor and the T&D calculations in real-time. It is also possible to perform automatic T&D calculations and run iterative T&D analysis on several well and string configurations.

The main features presented by Oliasoft AS (2021e) of this module are, "perform torque and drag calculations for drilling, casing and completion operations, full BHA editor including motors and other torque and drag generating components, complete buckling and stress analysis including Yied and Von Mises stress, full 3D view of downhole string analysis, bulk calculation of multiple scenarios based on trajectory and casing design, supports full soft string, hybrid and stiff string analysis." (Oliasoft AS, 2021e).

This module allows its user "to analyze drilling, casing, and completion operations, and assess the impact of predicted loads related to torque and drag in soft string, stiff string, and hybrid configurations, and calculate scenarios including tension, fatigue, buckling, and triaxial stress, at any point of the string for multiple scenarios." (Oliasoft AS, 2021e)

It provides visualization of standard plots, including “hook load, tension, stress analysis”, buckling, and access to 3D views of bottom hole drill string providing with its “side forces, string clearance, and torque and drag levels”. The module can “perform torque and drag in real-time operations for stress predictions and friction factor calibration, run calculations during drilling to get the optimal views of every stage of the drilling operations process”. (Oliasoft AS, 2021e)

2.4.2.5. Tubing Design Module

Oliasoft AS (2021g) stated that its Tubing Design Module is an advanced simulator that provides the ability to calculate the temperature and pressure profiles for each well design. In addition, this module supports multi-string analysis, including “wellhead growth and annular fluid expansion, ensuring analysis of advanced temperature effects of dynamic systems compliant with all industry standards” (Oliasoft AS, 2021g).

These simulations can be integrated with the rest of the Oliasoft WellDesign suite; adjustments can be made in other modules triggering re-calculations that automatically update tubing design calculations (Oliasoft AS, 2021g).

The key features presented in this module by Oliasoft AS (2021g) are “transient temperature and pressure simulation of production, injection, circulation and shut-in scenarios multi-string analysis including annular fluid expansion and wellhead growth, simulation for unlimited number of nested operations, packer loads on tubing and casing, multiphase flow correlations, automatic phase envelope generation from PVT specifications”.

Oliasoft Tubing Design’s transient simulator “handles operations from multiphase fluid production through tubing and annulus injection, and circulation and shut-in scenarios. The simulation model is built on an advanced finite volume thermal simulator able to calculate temperature and pressure development for any annuli, cement and formations, in any well configuration. The Module allows unlimited nested operations, ensuring accurate simulations of every individual operation, and thermal profile development. The transient thermal profiles it produces can be used in any other Oliasoft WellDesign module” (Oliasoft AS, 2021g).

Another component offered by this module is, as reported by Oliasoft AS (2021), “its tubing string design, can be defined through a variety packer configurations, with temperature simulations linked to casing and tubing load selections.” In addition, “the annular fluid expansion with a range of mitigation effects, and wellhead growth and other multi-string effects can be simulated, ensuring that designs are compliant with NORSOK-D010 and BSEE requirements” (Oliasoft AS, 2021g).

2.4.2.6. Blowout & Kill Module

Conforming to Oliasoft AS (2021b), its Blowout & Kill Simulation Module can perform “stochastic blowout, and dynamic kill calculations according to the latest industry guidelines. The module’s integrated workflow automatically updates changes and results through the entire dataset.”

The key features presented in this module by Oliasoft AS (2021) are: “stochastically limit blowout duration by incorporating probabilities for well kill mechanisms, zero derivative and finite volume dynamic kill methods, automated model selection based on well configuration, full probabilistic event model compliant with latest guidelines and NORSOK D-010, a variety of inflow models, such as oil, gas, fractured reservoirs, and explicit definition of PI and IPR, multiple reservoir definitions for both two-phase oil & gas and gas condensate fluid characteristics.”

The Oliasoft Blowout & Kill Simulation Module allows the user to resolve the blowout potential of a well accurately. “Its engine is built on the BlowFlow engine developed by NORCE, Equinor, and a consortium of other oil companies” (Oliasoft AS, 2021). As reported by the Norwegian Oil and Gas Association guidelines, the Oliasoft Blowout module is presently the only commercially available solution to perform a stochastic blowout calculation (Oliasoft AS, 2021b).

This module can also be used in order to verify that oil companies drilling in the US are complying with American Petroleum Institute (API) standard 53 regulated by the BSEE (Oliasoft AS, 2021b).

As reported by Oliasoft AS (2021b), its engine was developed with IFE, and “it simulates dynamic kill rates for kill operations through existing drill string or through a relief well intersecting the blowing well at a chosen depth, combining the static head of a kill fluid with frictional pressure losses.” Furthermore, it provides its users with a way to express all reservoir parameters by performing probability distributions, cultivating the uncertainty related to the subsurface data and enabling probabilistic Monte Carlo simulations.

Conforming to Oliasoft AS (2021b), “the Kill Simulation engine calculates upper and lower kill limits using zero-derivative and advanced finite volume methods, presented in industry-standard formats to determine if the kill operation can perform, preferably, through injection point”.

Its technology authorizes simulations to be performed on all sides for computationally heavy scenarios. Furthermore, integrating different modules enables automatic re-calculation of a blowout and kills when performing changes at any mark in the estimations. Also, by integrating the blowout and kill simulations with the well planning software, the drilling engineer is provided with maximum control over all choices being made regarding any inputs and settings related to the simulations (Oliasoft AS, 2021b).

The reduction of the simulation time is also achievable, thus optimizing the well design over many iterations and investigating distinct design options, reducing the number of overdesigned wells. The company’s latest update in this module is the “parallelization option” – a feature that allows the user to run many kill simulations by pushing one button (Oliasoft AS, 2021b).

2.4.3. Schlumberger Softwares

Schlumberger is a very well-known company in the industry, with a large bank of data and different software solutions for the whole of the petroleum chain. The company has also created a cloud-based environment called DELFI.

DELFI's cognitive E&P environment is a cloud-based software built on crucial premises that make it unique in Schlumberger's portfolio. It harnesses data, domain expertise, and scientific knowledge changing the way to perform in every part of the E&P value chain. The DELFI environment creates workflows and applications attainable to every single user. It provides members with access to build shared workspaces for models, interpretations, and data while respecting proprietary information boundaries (Schlumberger, 2021).

According to Schlumberger (2021), the DELFI environment displays a shared space for employees to work together. The result is an association where all are benefit directly from each other's proficiencies and insights. In addition, the environment's openness and extensibility integration simplify sharing and building on all available data sources, applications, workflows, and intellectual property.

The DELFI environment puts the full scope of available technologies to work from AI to analytics. "Powerful cognitive systems recognize each user to deliver a uniquely personalized experience. Intelligently searching, proactively learning and automating tasks, enabling you to predict, prioritize, and advise. Live with new data automatically shared between tasks across the DELFI environment, each live project is dynamically optimized with the latest information. Now the whole team can work concurrently on the same project, confident that the information they're using is always current and accurate. Duplication is reduced, team productivity and efficiency are increased, while business continuity is secured" (Schlumberger, 2021).

Apart from the DELFI environment, the company also provides software for drilling design, such as the DrillPlan and the DrillBench software. Each one will be presented in the following sections.

2.4.3.1. DrillPlan

The DrillPlan solution is a digital well construction planning software that maximizes the results found by each team by providing access to the data and science needed into a shared system. In addition, the automation of monotonous tasks and validation of workflows enables better quality designs to be performed quickly and ensures a coherent plan of action (Schlumberger, 2020).

Schlumberger (2020) reported that the software includes a circular workflow; thus, plans are revised as data is added. Future programs improve from the know-how of all wells designed before it. The DrillPlan solution was designed for the cloud and is accessible in the DELFI cognitive E&P environment, providing easy access to all the users' projects. Some of the features taken from presented Schlumberger (2020) for this mechanism are:

- Oversight of overall projects and well-planning workflows for completeness and quality;

- Mapping and customization of company's well construction workflow process, including all required stage gates and standards;
- Implementing themed workflows and templates to drive planning efficiency and consistency across the organization;
- Inbuilt digital review and approval systems for technical and management sign-off;
- Live activity feed showing all the latest updates to the active projects from all team members.

This solution allows its users to access all drilling engineering applications and data in a standard system, integrating the well construction frameworks from the "trajectory and casing design to fluids and cementing through operational activity planning", and creating cross-domain collaboration break down silos, thus increasing team productivity (Schlumberger, 2020).

The automation of repetitive tasks frees domain experts to focus on creating new engineering insights. The user is capable of running several simulations to find the best solution in their design constraints while being able to review updates on the project's life and learning how to design changes by using its design traceability, improving the drilling program coherency and operational reliability, as shown in Figure 2.2 (Schlumberger, 2020).

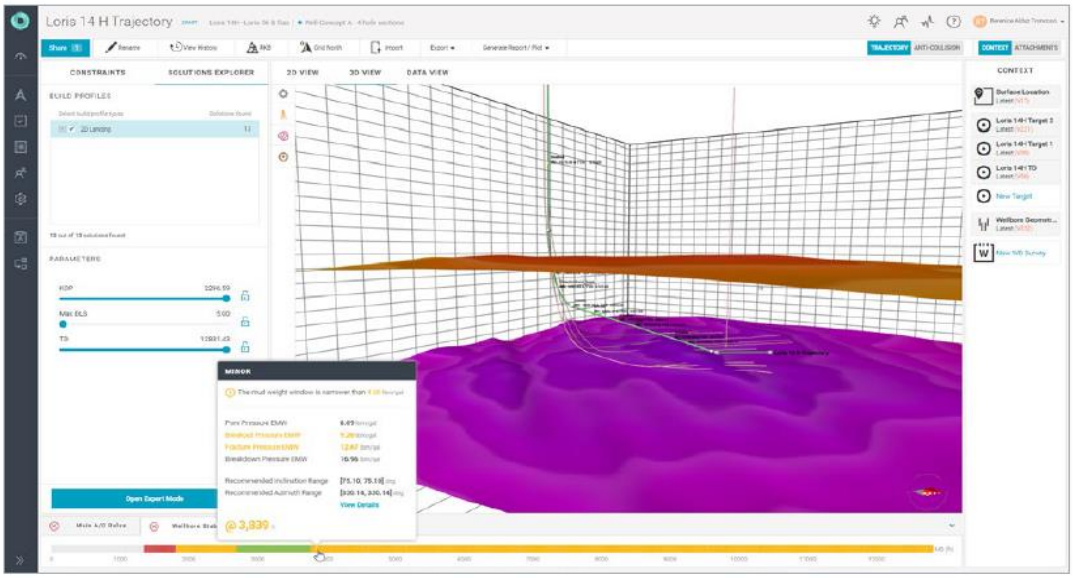

Figure 2.2: Multiple simulations example in DrillPlan software.
Source: (Schlumberger, DrillPlan Product Sheet, 2020).

According to Schlumberger (2020), the solution also presents different features in order to improve the design validation of the well drilling program, such as its single data source and models maintaining consistency across frameworks and tasks, the shared information between applications is able to ensure the user is always providing the latest engineering outputs, the validation engines like torque and drag hydraulics and load case analysis allowing automatic cross-check with the designed plan, an engineering flags highlight, that dictates the need to

interrogate detailed engineering outputs and the ability to observe how an instant design change affects the plan and review and validate the final results.

The new features presented by Schlumberger (2020) for the DrillPlan solution and its functionalities are:

- Dynamic well template: leverages offset constraint correlation to automate multi-well design.
- Activity plan with estimated best composite time: Enhances the operational forecasting by identifying offset wells' best composite time and probabilistic analysis of non-productive time.
- Multi-Plan Optimization: Enables well concept evaluation and selection by quickly duplicating the master plan.
- Multi-Dimension Sensitivity Analysis: Offers insight into the designs by performing multi-dimensional sensitivity analysis for hydraulics and torque and drag.
- Automated Engineering Analysis and Validation: Maximizes the efficiency of the well planning team with the automated engineering analysis and validation.
- Casing and Liner Running Analysis with Automated Validation: Ensures successful casing and liner running operations with engineering validation every time a design change occurs.

2.4.3.2. DrillBench

The DrillBench Dynamic Drilling Simulation Software is a Schlumberger software that provides the user with dynamic simulations for pressure control, blow out control, managed and underbalanced operations, and well control (Schlumberger, 2015a).

According to Schlumberger (2015a), the software's simulations are a feature to provide an accurate drilling operation and implement accuracy that simpler steady-state models cannot provide. The software consists of a user-friendly tool and targets all drilling engineers working with difficult well profiles. Its build around a well-control workflow, covering pressure control, well control, and blowout control.

The company's recent enhancements on this software include the integration of well paths directly from the Petrel platform, being able to read "pore and fracture pressure from the Techlog platform, the support for dual gradient drilling with improved modeling of managed pressure drilling, the strengthened dynamic S&S calculations, subsea pump, and the rig site Kick, which is a standardized kick sheet for operational rig site use, based on robust well control modeling and simulation" (Schlumberger, 2015a).

This tool provides its user with five different applications, the DrillBench Blowout Control system, the DrillBench Dynamic Hydraulics system, the DrillBench Dynamic Well Control system, the DrillBench Rig site Kick system, and the DrillBench Underbalanced system (Schlumberger, 2015b).

The DrillBench Blowout Control system has as main applications the planning of dynamic kill operations, the evaluation of relief well geometries, calculating worst-case discharge rate and total discharge volume, the prediction of required kill mud volume and time to kill, and the evaluation of the bull-heading operations and other well control options (Schlumberger, 2015b).

Its major benefits are proactively planning relief wells, establishing required contingencies and fluid volumes required to kill well, and using "what-if" analysis for support. Its key features are a powerful and dynamic multi-phase model, flexibility, intuitive interface, link to Petrel Well Design Module, multiple simulations run simultaneously, planning, training, and post-analysis of operations (Schlumberger, 2015b).

Figure 2.3 presents a typical blowout control simulation showing how pumping kill mud through a relief well can control and kill the blowing well.

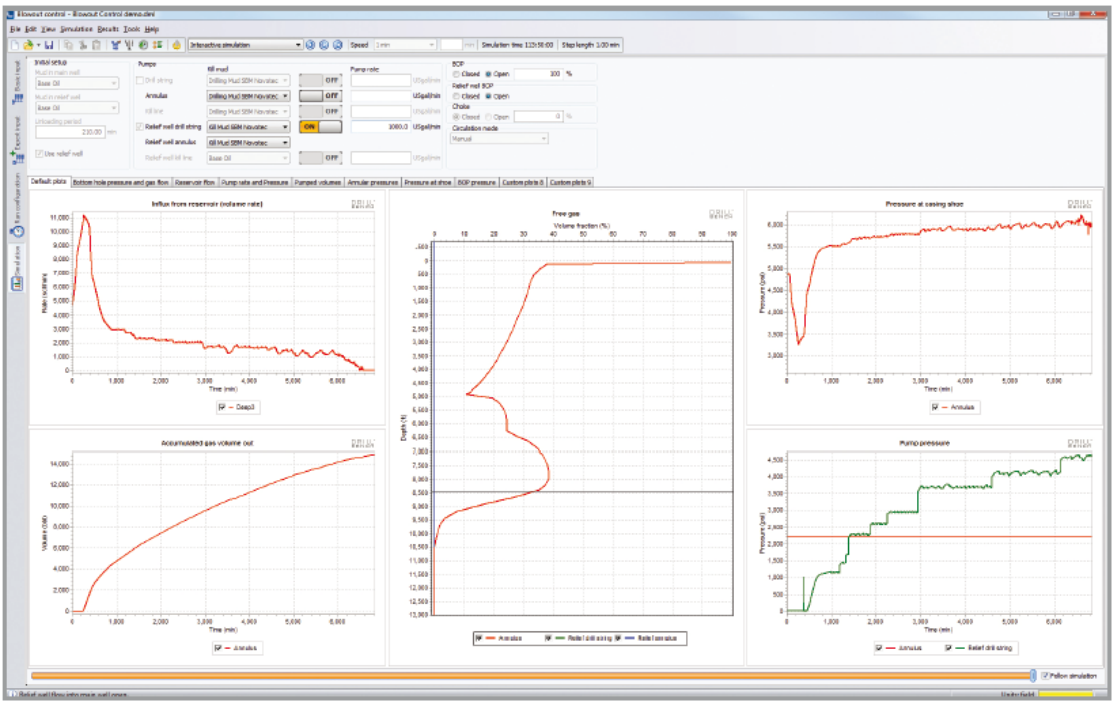

Figure 2.3: DrillBench Blowout Control system example.
Source: (Schlumberger, DrillBench Blowout and Kill Product Sheet, 2015b).

The DrillBench Dynamic Hydraulics system is used to optimize mud weight and maintain proper overbalance, identify and avoid drilling conditions outside the safety margins, evaluate the impact on mud window of new drilling methods, evaluate thermal effects and flow or pressure buildup caused by temperature-induced changes in mud volume, and monitor local pressure and temperature conditions (Schlumberger, 2016b).

The significant benefits of this system are the optimization of procedures to drill efficiently while maintaining pressure control for all operations, drilling virtually to identify hazards and prepare for efficient operations, usage of "what-if" analysis for support, and train the drilling crew (Schlumberger, 2016b).

Its main key features are transient flow and temperature models, multiple fluid options, accurate PVT modeling, including thermal expansion, pressure, and temperature-dependent rheology, evaluation of thermal effects and changes in mud weight in static wells, S&S modeling, modeling for calculation of gel-breaking pressure, efficient simulation workflow, and a flexible user interface. Figure 2.4 shows an example of a model of the equivalent circulating density relative to the mud-wight window when forecasting the operational pressures to ensure that the well integrity boundaries are not exceeded (Schlumberger, 2016b).

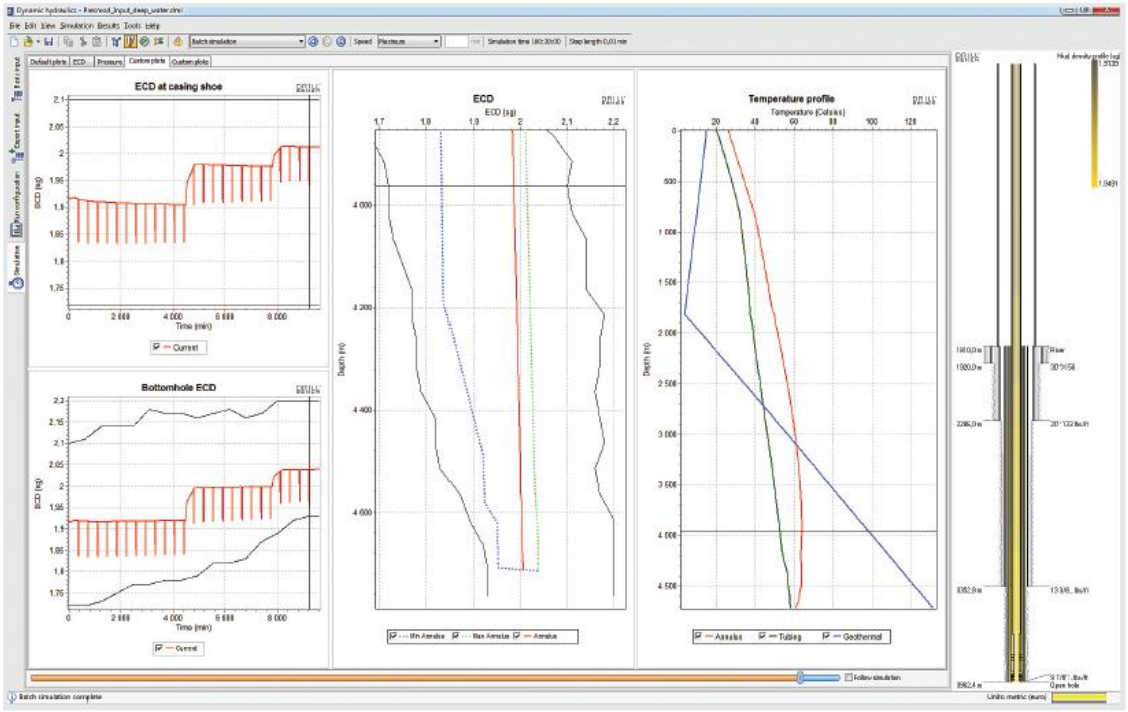

Figure 2.4: DrillBench Dynamic Hydraulics system example.
Source: (Schlumberger, DrillBench Dynamic Hydraulics, 2016b).

The DrillBench Dynamic Well Control System is used to "assess well control procedures and casing setting depths, study kick tolerance, evaluate surface equipment limitation, analyze kicks after incidents occur, train personnel prior to challenging drilling operations, obtain operational decision support through "what if" analysis" (Schlumberger, 2016a).

Its major benefits are improving the understanding and awareness by using its visualization process, obtaining a realistic evaluation of maximum drilling depth, optimizing well control procedures, and assessing and managing risks. The main key features of this system are its intuitive interface, the multiple simulations that can run simultaneously; it is interactive; batch, and sensitive modes, the determination of maximum pressure loads, free-gas-breakout depth, water-based gas migration, gas dissolution in OBM, and horizontal kicks, its mud-gas separator capacity evaluation, and its planning; training and pot-analysis of operations (Schlumberger, 2016a).

Figure 2.5 is an example of how this system can be used and shows the "dissolution of methane in a synthetic mud. This is a unique feature in the DrillBench Dynamic Well Control that has a significant impact on kick tolerance" (Schlumberger, 2016a).

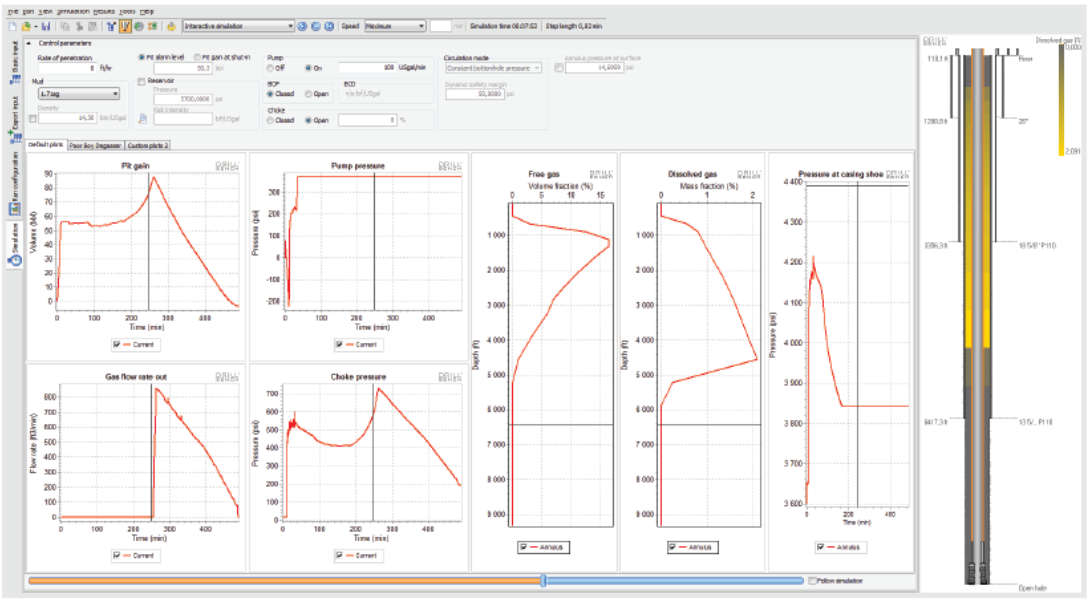

Figure 2.5: DrillBench Dynamic Well Control System example.
Source: (Schlumberger, DrillBench Dynamic Well Control Product Sheet, 2016a).

The DrillBench Rig Site Kick system is used to plan for potential well control incidents; its benefits are the enhancement of the understanding of well control incidents using unique visualization features, the avoidance of error by entering operational data only at the rig site, and the improvement of simulation accuracy and save time. Its main features are the intuitive interface, fully dynamic simulation, handling of all well profiles and mud systems, multi-phase modeling with advanced PVT model, the inclusion of dissolved gas effect, output versus strokes or time, dependable for engineering work, and IADC kick report (Schlumberger, 2016c). In addition, its workflow provides full collaboration between the office and the rig site, as shown in Figure 2.6.

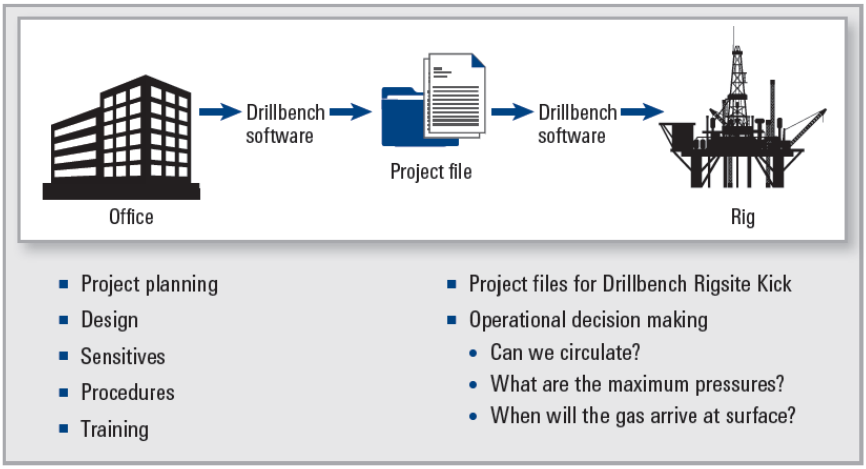

Figure 2.6: DrillBench Rigsite Kick workflow schematic.
Source: (Schlumberger, DrillBench Rig site Kick Product Sheet, October 6, 2016c).

The last system presented by Schlumberger (2016) is the DrillBench Underbalanced and Managed Pressure Drilling system that has as critical features the prediction of how operational conditions and fluid properties influence pressure, ECD, and temperature, its dynamic

temperature calculations in the hydraulic model, the investigation of both static and hydraulic UBD problems and its steady-state solution for accurate screening and sensitivity analysis.

2.4.4. Halliburton Softwares

Halliburton is another well-known company in the industry, with a large bank of data and different software solutions for the whole of the petroleum chain. The company provides E&P professionals with a software-driven life-cycle named Halliburton Landmark Solutions. Landmark Solutions is a hybrid cloud environment with seamless connectivity that uses a digital twin technology to provide the user with a faster, more open, and collaborative open industry platform (Halliburton, 2021).

Two of the central systems in Landmark Solutions are the WellPlan software and the DecisionSpace® 365. The WellPlan software is the latest evolution in Halliburton's well-construction information solutions. It is integrated with EDT and EDM applications, providing a complete well engineering software tool kit capable of designing complex well string operations and navigate different challenges found in the well construction.

The DecisionSpace® 365 is a cloud-based subscription service for E&P applications found on OSDU that provides high throughput, low latency, and self-cleaning solutions to large quantities of data from various sources into the OSDU. Once the data is loaded, the DecisionSpace® 365 cloud provides modular, open, and plug-and-play solutions with an intelligent workflow to provide efficiency and insight (Halliburton, 2020a).

2.4.4.1. WellPlan

The WellPlan Software is used to design complex well string operations requiring meticulous analysis to define critical aspects of each string-related operation in the wellbore. It can determine the appropriate rig and equipment specifications, string components, and fluid properties and parameters to drill safely and efficiently. The software values drilling faster without compromising safety, simplifying processes leading to more accurate analysis and opportunity for better decision-making, and offering a comprehensive tool kit to optimize the well design and mitigate the risks in common or complex drilling scenarios (Halliburton, 2016).

The significant benefits of the WellPlan Software, according to Halliburton (2016) are, well engineering integration, the possibility of configuring the right tools for any job, a simplification of the process; leading to better well decision-making, and the possibility of performing a sensitivity analysis, where users can model any directional well profile and pipe strings and the ranges can be defined for any relevant parameter to perform sensitivity analysis efficiently, as shown in Figure 2.7.

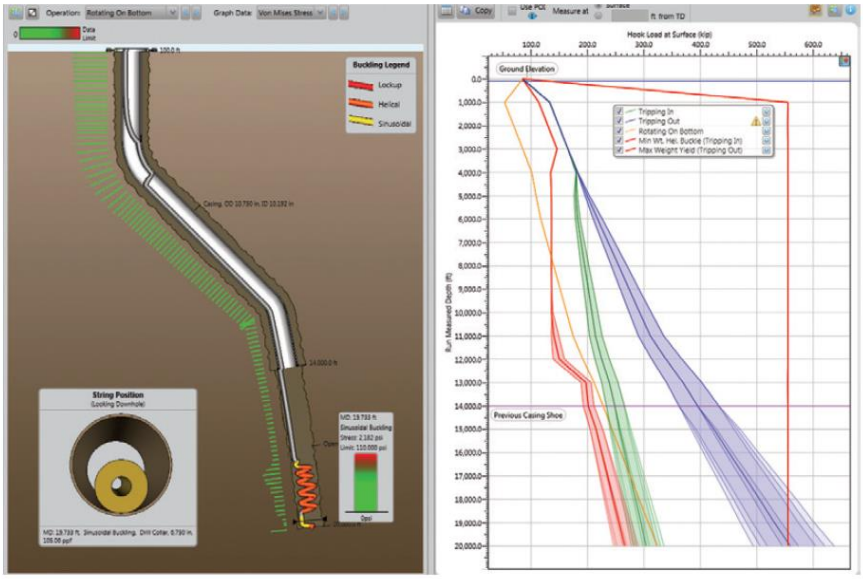

Figure 2.7: Sensitivity analysis in WellPlan Software example.
Source: (Halliburton, WellPlan Software, H012161 datasheet, 2016).

The main features of the WellPlan software, are taken from Halliburton (2016), and they are:

- **T&D analysis**: "plan and analyze drilling, casing, and completion, running operations, and assess the impact of predicted loads related to torque and drag. The main calculations are tension, torque, side force, fatigue, and tri-axial stress." Soft, stiff, or hybrid string models can be used for the analysis.
- **Hydraulic analysis**: "model pressure losses across the circulating system and pipe string, estimate ECD across the annular space, and analyze formation cuttings transport and its effect on pressure and ECD calculations." The module "considers string eccentricity effect, pipe roughness, returns to seafloor for dual-gradient operations, and backpressure for underbalanced operations."
- **Underbalanced Hydraulic analysis:** Using UBD and "MPD to improve circulation, ROP, and reduce formation damage and stuck pipe events" requires control of bottom hole and surface pressures, making it critical to model multi-phase fluids.
- **Transient S&S analysis:** "offers the capability to calculate transient pressures within the wellbore caused by pipe movement during tripping and cementing operations".
- **Well Control analysis:** "offers a large set of modeling capabilities and variable effects such as temperature, complex wellbore, and string geometries to reduce uncertainty when planning a well and/or performing a well control operation."
- **Cementing Job and Centralization design:** "This allows users to identify potential difficulties and tune the cementing design before pumping begins", starting with the casing centralization workflow, which is a crucial factor in "completing an optimal and safe cementing job."

- **Stuck Pipe analysis:** locates the sticking point and conducts brief, "accurate failure analysis" by calculating "back-off force, force delivered to stuck points, and forces required to set and fire jars."
- **BHA Dynamic analysis:** uses finite element analysis to visually identify drilling parameters (WOB, RPM, and Torque) that produce high-stress concentrations. It also helps predict the directional tendencies of the BHA.
- **Output-driven-input:** "provides clear step-by-step guidance to the user on what data is required and leads them through the input panels in just a few clicks."
- **Interactive wellbore representations:** "results illustrated graphically as part of interactive wellbore portrayals, making the results easier to visualize and understand."

2.4.4.2. DecisionSpace® 365

The DecisionSpace® 365 has four modules, Exploration & Reservoir Development, Well Construction, Production, and Information Management. This thesis will focus on the well construction module, which has five applications, Digital Well Program, Holistic Field Development Planning, Real-time Control-Edge, Real-Time Well Engineering, and Well Operations Monitor, which will be discussed in this section (Halliburton, 2020a).

a) Digital Well Program

The first application within the Well Construction Module is the Digital Well Program. This application offers an integrated digital well program software; it allows the user to co-innovate with the machine learning algorithm to create a customized solution for a unique workflow need while helping the user plan, design, and deliver safe, cost-effective productive wells (Halliburton, 2020b).

The significant benefits found in this application are the optimization of good operations, the predictability of well operations, the maximization of reservoir contact, the connection between the digital twin and the well operations, its improved drilling performance, and its flexibility. Its main features are well feasibility and detailed design, integration and collaboration, real-time connections, customized solutions, and automated workflows and calculations, which include: well trajectory anti-collision check, geological prognosis, basic and advanced well integrity analysis, operations planning analysis, well completion analysis and well time and cost (Halliburton, 2020b).

b) Holistic Field Development Planning

The second application is Holistic Field Development Planning; according to Halliburton (2020c), this application addresses problem that happens when the field development falls short of the actual plans and compromises return on capital. In order to accomplish this, this cloud application updates as constraints appear from the field and office during the project's design and execution. Therefore, allowing more optimal decisions throughout the well construction process and improved development plans. In addition, it allows its user to maximize its value and optimize well placement to achieve the economic goal wanted.

The major benefits found in this application are the increasing confidence in performance forecasts, integrated data, automated workflows, and collaborative workspaces that enables transparency between technical, operational, and economic teams. The reduced planning cycle time diminishes human error and optimizes the efficiency through collaboration by connecting the software used for field planning and rerunning planning scenarios. Moreover, last but not least, it accelerated informed decision-making that digitalizes the approval process, allowing for better and faster design making (Halliburton, 2020c).

c) Real-Time Control-Edge

The third application is the Real-Time Control-Edge drilling automation platform which integrates and automates drilling data allowing for a single set of actionable constraints, setpoints, and commands. The main benefits of this platform are its connectivity with digital advisory and rig automation systems for improved efficiency, it grants a synchronized and more accurate decision making, it creates a user-specific innovative workflow, it stays in control of the drilling operations; providing integration of drilling parameters set points, constraints, and events notifications, it has a multi-discipline collaboration data system, and it allows users to connect with remote operations and well sites (Halliburton, 2020d).

As stated by Halliburton (2020d), the main features of this application are, orchestrated intelligence and integration; in which the platform provides the means to aggregate the well plan with a high frequency, low latency real-time data from many sources at the rig site, listen to and orchestrate several set points and constraints coming from both remote and wellsite advisory solutions; has connectivity to several different rig interfaces, feature functionality; delivering core platform functionality modules that enable customers and service lines to configure and match various inputs from both models and set points with procedural sequences for drilling advisory and automation systems; and rig-site advisory services such as maximum ROP, maximum trip, steering automation and vibration mitigation.

d) Real-Time Well Engineering

The fourth application is the Real-Time Well Engineering, as described by Halliburton (2020e), the user can rely on the said application to help in the management of rig site operations, building from a project from the beginning using their computational algorithms, the system automatically detects rig state and couples engineering and system uncertainty models in real-time closed looped systems. It also facilitates the automation of broader, more complex E&P workflows, and effective operational decisions, improving drilling efficiency and downhole performance, reducing costs.

The main benefits of these applications are the increase of drilling efficiency with automated processes, the reduction of data analysis run time from days to minutes, the achievement of better drilling outcomes, and the delivery of dynamic data on intelligent dashboards. There are two main features in the Real-Time Well Engineering, the torque and drag model, which helps detect irregularities to facilitate operational decisions. The anti-collision model helps users visualize and monitor the well and avoid no-go zones nearby offset wells (Halliburton, 2020e).

e) Well Operations Monitor

The fifth and final application from the Well Construction Module is the Well Operations Monitor, which provides the user with a virtual window to use on the rig site, thus helping optimize the well monitoring and operations reporting with an automated process for safe, efficient, and efficient, cost-effective outcomes (Halliburton, 2020f).

Halliburton (2020) stated that the major benefits of this application are its connected workspace, remote operations, minimization of disruptions, minimization of unplanned deviations, safer operations, efficient collaboration, and streamline reporting, top-quality efficiency, and just-in-time information. The main features of the Well Operations Monitor are activity program planning and monitoring, barrier planning integrated with operations, visual reporting to the plan, digital well exchange for automated reporting, and a digital twin of the "live plan" that provides a shared digital representation of the planned and current as-built status of the well throughout the operation (Halliburton, 2020f).

3. Trajectory Design

3.1. Well Design

Throughout the years, the drilling industry's main objective has been drilling wells faster and more accurately, hitting its wanted geological target. In trying to accomplish such a purpose, the improvement of the trajectory design was necessary, thus, opening the way for directional well trajectory design to appear (Farah, 2013).

The intention of steering a well trajectory into the right location several kilometers below ground has compelled the industry to focus on new tools and methods to analyze wellbore target location and its path during drilling. It has been of common ground to set the drilling rig above its target and drill a vertical well into it in the past days. Now, it has become necessary to reach targets that deviate from the reference location in the surface; thus, many tools and methods have been developed for directional drilling (Farah, 2013).

The directional well trajectory design is essential to drilling; it must, therefore, consider various factors from "surface and subsurface restrictions, challenges to available technology and equipment, and most importantly, economics" (Okpozo & Samuel, 2016). It requires meticulous mathematics to ensure the proper execution of a drill path that can safely contain the tools being used in the well planning (Okpozo & Samuel, 2016).

Farah (2013) stated that the directional survey measurements used in the trajectory design are given in terms of I, AZ, 2D and 3D coordinates, TVD, and northing and easting at a depth of the survey station. The precise position and direction of the wellbore should be determined at depths that may not coincide with those of the survey stations when those are designed by applications. Therefore, a mathematical tool for interpolating between survey data and calculated data is required.

According to Okpozo & Samuel (2016), a few practical reasons why one should use directional drilling are; to sidetrack out of an existing well, to develop multilateral wells using one drill pad, to use a single well string to cut across pockets of layered reservoirs, to avoid existing well collision, to avoid unnecessary exposure to the unstable formation and to explore a reservoir beneath an obstructed surface.

Planning a well with the aid of geological structure and information, the depth and horizontal departure of the target, and its dimensions are incredibly important. Various trajectories are constructed in order to meet the planned target from which only the best is selected (Okpozo & Samuel, 2016).

When planning a well, all parts of the drilling procedure must be assessed, and all fundamental and related data should be incorporated into the well program. First, to decide the best regions that shall give reasonable access to the hardware transportation, drilling apparatus settings, and so forth, the land areas should be overviewed. Then, different sorts of projects should be set up, including the casing program, the mud program, the directional drilling project, the bit

design, and different kinds of reports relying upon the specific kind of well wanted. Some of these are summarized below:

- The drilling mud program is created to provide the mud parameters that will ensure effective wellbore cleaning, little harm to the environment, appropriate improvement of channel cake, and hydraulic isolation under given bottom hole pressure and temperature.
- The cement system provides properties that will keep up well integrity, satisfactory well control, and hydraulic isolation for production formations and pay zones.
- Significant time should be spent on bit program preparation to drill the well in the best way and have the highest ROP as could be allowed.
- Information and data about the problems that could be faced to improve drilling the well should be collected from the offset wells.
- Cooperation with service companies to check on equipment limitations: mud properties should be compatible with the MWD equipment and steerable motors. The design of BHA should give the highest possible ROP.

Selecting bit types depends on many things: type of well, type of formation, and hole condition; it all will affect the bit-type which will be used. The most effective bit is that which gives the optimum ROP defined by the engineers.

Well trajectories can be bidimensional or three-dimensional. Each type is used for specific reasons in a well trajectory design for directional drilling. In the next sections, both trajectories will be addressed and explained, but first, the concept of directional drilling should be presented.

3.2. Well Trajectory Design

Directional drilling is an essential part of modern drilling operations. It is mainly defined as the act of controlling the direction and deviation of the well in order to reach a predetermined target.

Some important directional drilling concepts were presented by Khadisov (2020) and by Strømhaug (2014); these are essential to the development of the well trajectory and are as follow:

- I: The angle(º) between the tangent to the wellbore and the vertical.
- A: The angle(º) measured, clockwise, between the geographical north and the survey point. It ranges from 0º to 360º degrees in angle.

Figure 3.1 shows the inclination from two points in a deviated well.

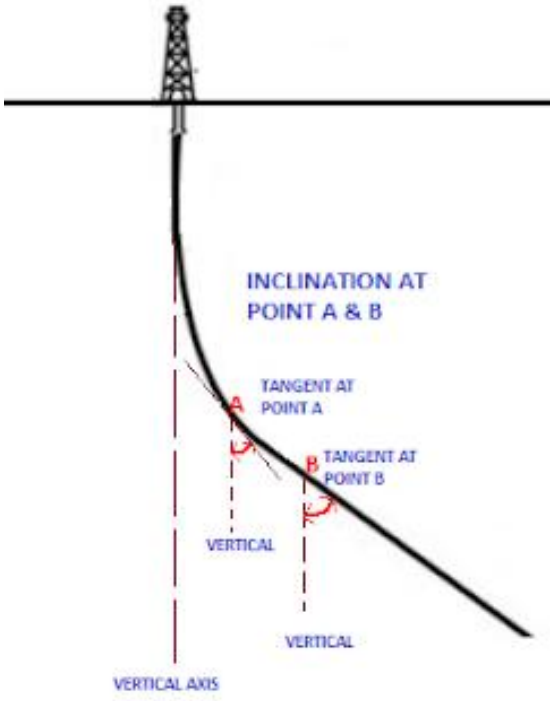

Figure 3.1: Schematic showing the inclination at two points (A and B).
Source: (Sunny, 2015a).

Figure 3.2 shows azimuth in a deviated well. Here, the azimuth or well path changes in the horizontal plane regarding the plan view and the actual well path.

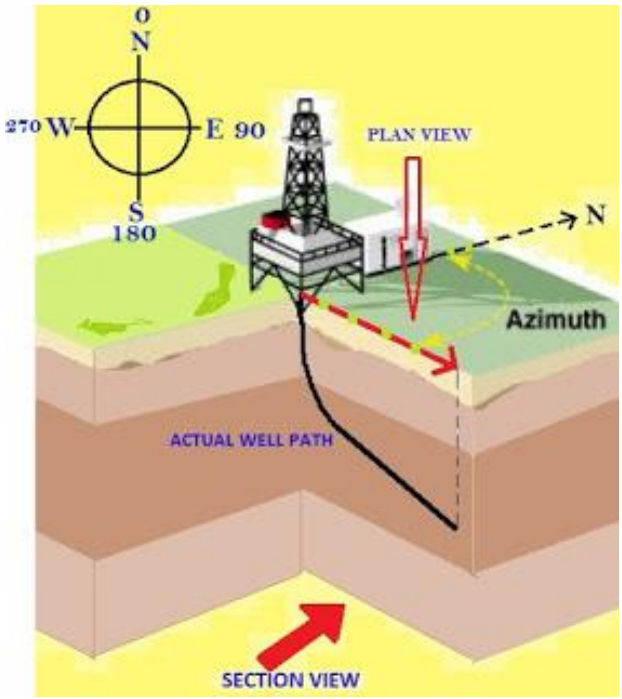

Figure 3.2: Schematic of the well path regarding the azimuth and the plan view.
Source: (Sunny, 2015a).

- TVD: Vertical distance amid the top and the bottom of the well.
- MD: Absolute length of the well, measured along the well path.

- KOP: is described as the depth at which the wellbore first deviates from the vertical section, and the build section is initiated.
- Build section: Section of the well in which the angle is being built.
- Hold section: Section of the well where the inclination is kept constant.
- Drop-off section: Section of the well in which the inclination is dropped.

The concepts presented above can be seen in Figure 3.3.

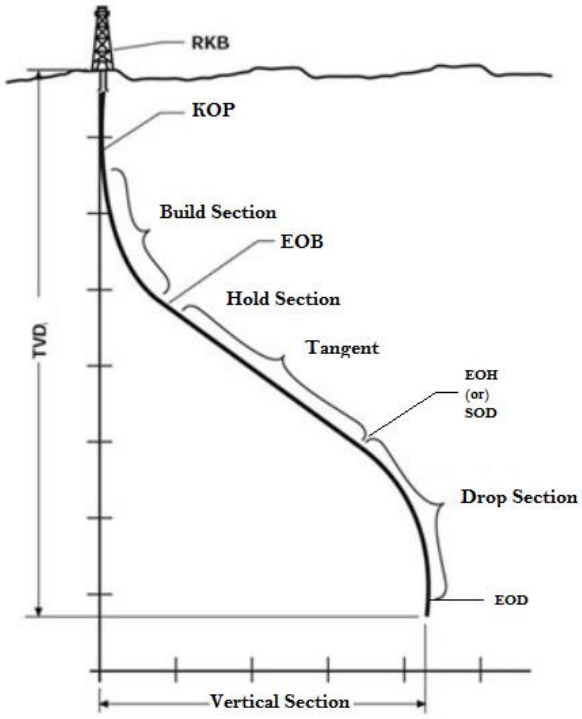

Figure 3.3: Schematic of the well trajectory design and its main concepts.
Source: (Sunny, 2015a).

- BUR: Rate at which the angle is being built, measured in º/30m or º/100 ft.
- DL: the angle formed between two vectors tangent to the trajectory of the well in two considered points. It represents how much the trajectory bends.

$$DL = \cos^{-1}(\cos I_1 \times \cos I_2 + \sin I_1 \times \sin I_2 \times \cos(A_2 - A_1)) \quad (3.1)$$

- DLS: Represents the combined change in inclination and azimuth. High DLS may cause problems pulling equipment in and out of the well.

$$DLS = \frac{DL}{L} \quad (3.2)$$

Where:
- DL is dogleg [°/30m];
- L is length of wellbore [m].

3.2.1. Well Design Configuration Data

In the interest of offering the best arrangement to a directional well that will be safe and cost-effective, a parcel of data is required. The data can be arranged by collecting such from offset wells, seismic analyses, completion procedures, and enhanced oil recovery (EOR) operations akin to the drillers being able to drill the well with its optimum parameters. The different approaches to acquire data will be discussed below.

a) Geology

The first step in drilling design is to understand the condition of the formation. Much information shall be shared in this section to achieve the best wellbore trajectory and avoid drilling problems. The information below is acquired from studying the geology of the reservoir:

- The lithology of the well (shales, limestones, sand, and so on.);
- Water/oil and gas/oil contacts;
- Geological control quality;
- Target development type and its properties (channel sands, a seismic inconsistency, zenith reefs, infill drill, or investigation);
- Target topographical structures (deficiencies, plunge, shales);
- Regulation issues (Gas/oil limits, against crash, last MD and TVD);
- Well type (investigation, infusion, oil/gas creation).

b) Completion and Production

In order to fulfill the requirements of completion and production program, the following are necessary:

- Completion type (fracking, siphon bars, and so on.);
- Maximum inclination and DLS limits;
- Positioning of well with connection to the future production plan;
- Pressure slopes and temperatures.

c) Drilling

Another strategy, this time for drilling, is the cooperation between drilling companies and operator ones in order to decide and provide the drilling program by using the following parameters:

- Selection of the well slot;
- Number of casing and casing shoes;

- Drilling mud parameters;
- Rig types and drilling equipment;
- Well trajectory and bit program.

3.2.2. Directional Well Profiles

This section will present the well profiles that can be achieved through directional drilling for both types of trajectories, 2D and 3D; a focus will be put on the 3D well profile where the model utilized by the Drillbotics Team, the Bézier curves model will be presented.

3.2.2.1. 2D Well Trajectories

Wells can vary in design/profiles; 2D wells are drilled in a vertical plane that contains the wellhead and the trajectory target. However, the most common bidimensional trajectories, as stated by Khadisov (2020), are:

a) Vertical Wells

Consider to be wells without any inclination; however, in practice, some variations in inclination may exist; its schematic can be seen in Figure 3.4

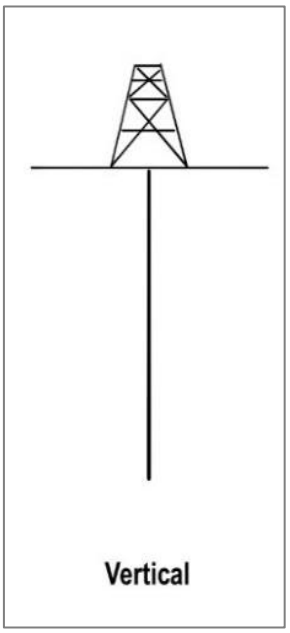

Figure 3.4: Bidimensional well trajectory of a vertical well.

b) J-Shape wells/ Build & Hold

A J-shape well design consists of a vertical section, followed by a KOP, a build section, and a hold section (Figure 3.5).

Figure 3.5: Bidimensional well trajectory of a J-shaped well.
Source: (Sunny, 2015b).

c) S-Shape wells

An S-shape well is more complicated than a J-shape well. They consist of a vertical section, followed by a KOP and a build section. When the desired angle is achieved, such angle is held until the desired target is reached. The last part of the well consists of a drop section, where the inclination is dropped until the well is vertical. Finally, the drilling can proceed as vertical, as shown in Figure 3.6; S-shaped wells are usually used to avoid salt domes, hit multiple targets, or avoid faults.

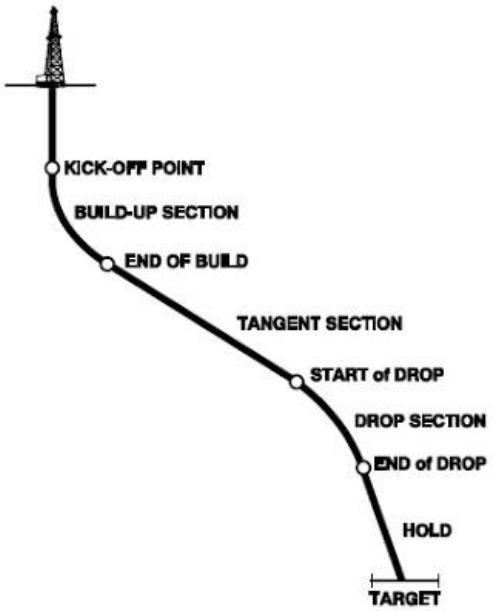

Figure 3.6: Bidimensional well trajectory of an S-shaped well.
Source: (Sunny, 2015b).

d) Horizontal wells

Horizontal wells consist of a vertical section, followed by a KOP. At the KOP, the inclination of the well is built until it reaches 90°, thus turning the well horizontal, as seen in Figure 3.7. These wells are usually used for production in thin layers of the reservoir, avoiding gas and water coning and increasing production in reservoirs with lower permeability, such as shale gas and shale oil reservoir.

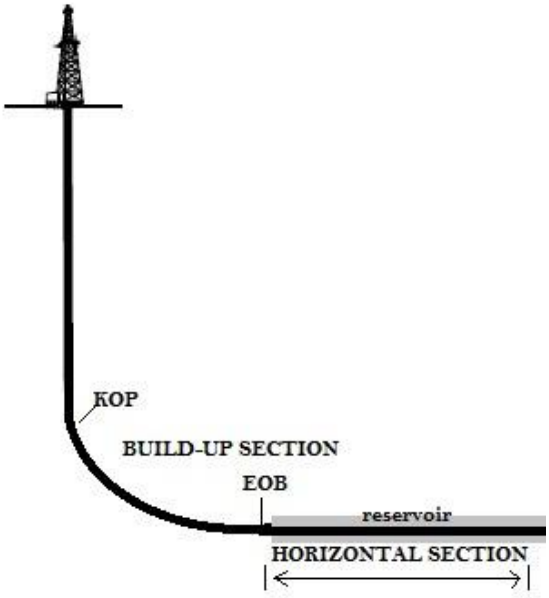

Figure 3.7: Bidimensional well trajectory of a horizontal well.
Source: (Sunny, 2015b).

3.2.2.2. 3D Well Trajectories

The 3D trajectory is usually planned after the preliminary design of the 2D well. The 3D project is essential due to the well not being drilling in a vertical plane consisting of only the wellhead and the target. Many factors should be considered, such as the geology and the BHA composition, making the drill turn and drill in different planes (Rocha, 2011).

Further, these 3D wells can also be applied in situations such as when it is impossible to place the wellhead in the same vertical plane as the target, in the case of restricted rig positioning, or when there is a necessity of reaching multiple targets, in a different plane, with the same well (Rocha, 2011). The 3D trajectory is presented in a X, Y, Z plane, as shown in Figure 3.8.

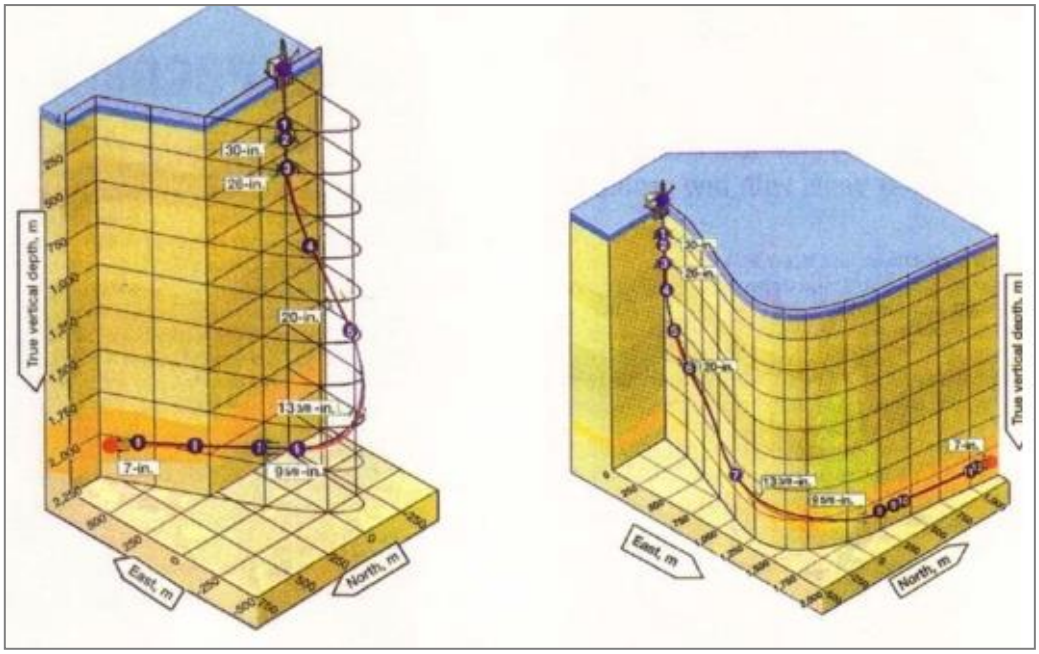

Figure 3.8: 3D Well Trajectories.
Source: (Eid E., 2020).

The model that will be discussed in this thesis for the 3D Trajectory planning is the Bézier Curves. The argument behind such a decision is that the Bézier curves are mathematically simple and have two degrees of freedom, which provides considerable control on the trajectory characteristics. This model is considerably more relevant for real-life application, and the concepts and explanation for the said model were retrieved from Sampaio Jr (2006).

The Bézier curves are capable of solving four specific cases:

i. Free-end trajectory: where both the inclination and the azimuth of the target do not have any restrictions.

ii. Set-end trajectory: where both the inclination and the azimuth of the target are specified.

iii. Set-inclination and free-azimuth: where the target's inclination is specified, and the azimuth does not have any restrictions.

iv. Free-inclination and set-azimuth: where the target's azimuth is specified, and the inclination does not have any restrictions.

a) Free-End Well Trajectories

A second-order Bézier curve is defined by Equation (3.3):

$$B(u) = (1-u)^2 S + 2(1-u)uC_s + u^2 E \qquad (3.3)$$

Where:

- u is a dimensionless parameter in the interval [0,1];
- S is the starting point of the curve;

- E is the ending point of the curve;
- and C_s is the attractor of the starting portion of the curve.

The support line of C_s is determined by the tangent to the trajectory at S. Figure 3.9 shows curves with the same starting and ending point, with attractors at different distances from S. The maximum curvature of a curve moves away from S with C_s (Sampaio Jr., 2006).

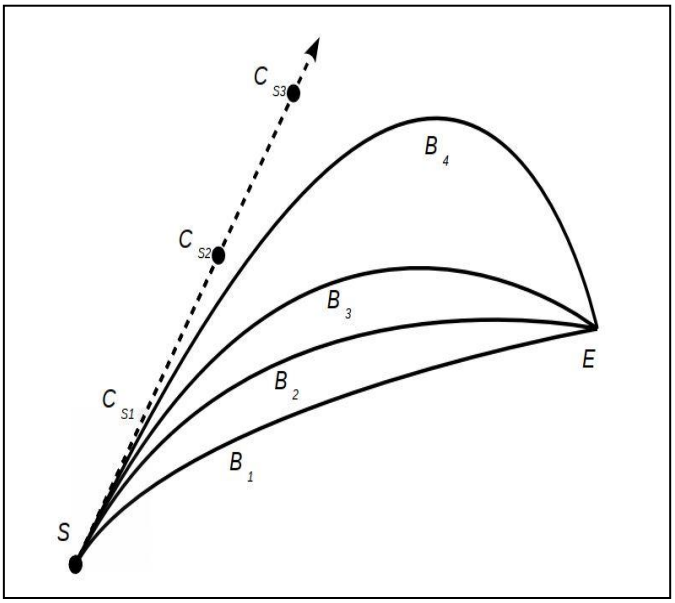

Figure 3.9: Second order Bézier Curves.
Source: (Sampaio Jr., 2006).

The position of the attractor point C_s is given by:

$$C_s = S + d_s t_s \tag{3.4}$$

$$S = (v_s, n_s, e_s) \tag{3.5}$$

$$t_s = (\cos I_s, \sin I_s \cos Az_s, \sin I_s \sin Az_s) \tag{3.6}$$

The parameter d_s is an arbitrary scalar, and it expresses the distance the attractor point is ahead of S.

b) Set-End Well Trajectories

A third-order Bézier curve is defined as:

$$B(u) = (1-u)^3 S + 3(1-u)^2 u C_s + 3(1-u)u^2 C_e + u^3 E \tag{3.7}$$

Where:

- u, S, and E were defined above.

- C_s and C_e are two attractors of the curve.

The support line of C_e is determined by the tangent to the trajectory at E. Figure 3.10 shows a set of curves with the same starting and ending point, with varying C_s and fixed C_e (Sampaio Jr., 2006).

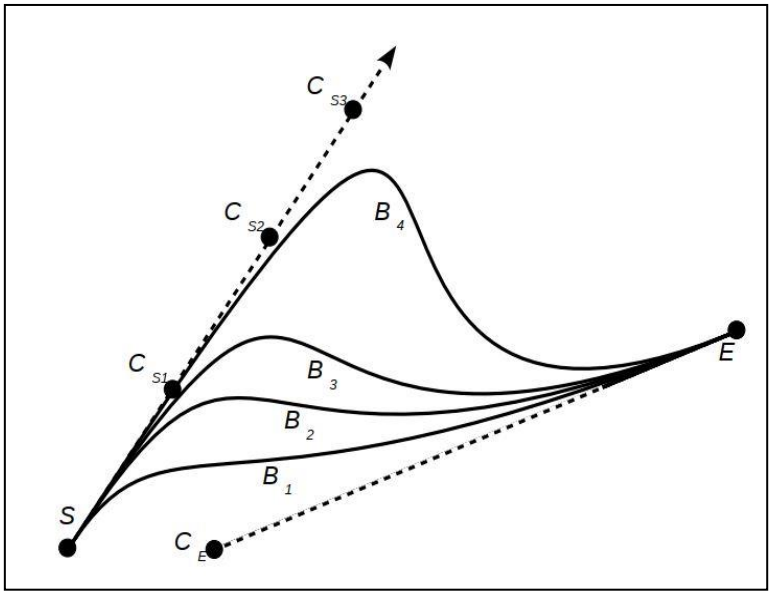

Figure 3.10: Third-order Bézier Curves.
Source: (Sampaio Jr., 2006).

The position of the attractor point C_e is given by:

$$C_e = E - d_e t_e \tag{3.8}$$

$$E = (v_e, n_e, e_e) \tag{3.9}$$

$$t_e = (\cos I_e, \sin I_e \cos Az_e, \sin I_e \sin Az_e) \tag{3.10}$$

The parameter d_e is an arbitrary scalar that expresses the distance between the attractor and the E point. The pair of parameters d_s and d_e can be freely controlled, which provides the degree of freedom required for trajectory design. In cases in which either the inclination or azimuth are not set at E, the well designer has the freedom to choose any appropriate value for it. The designer can run several cases for the free end trajectory and search for an optimum objective such as shortest trajectory length, least maximum curvature, or least torque and drag. (Sampaio Jr, 2006)

c) Other Outputs

The MD of the well can be found using:

$$\Delta MD = \sqrt{(v_i - v_{i-1})^2 + (n_i - n_{i-1})^2 + (e_i - e_{i-1})^2} \tag{3.11}$$

The MD is a function of the Northing (n_i), Easting (e_i), and TVD (v_i) coordinates of each calculated point (i) and the previous point ($i-1$).

The I and Az can be calculated with:

$$t = (t_v, t_n, t_e) = \frac{\dot{B}}{\sqrt{\dot{B}.\dot{B}}} \tag{3.12}$$

$$I = \cos^{-1}(t_v) \tag{3.13}$$

$$Az = \tan^{-1}\left(\frac{t_e}{t_n}\right) \tag{3.14}$$

In which the free-end trajectory and the set-end trajectory can be defined, respectively, by the formulas below:

$$\dot{B}(u) = -2(1-u)S + 2(1-2u)C_s + 2uE \tag{3.15}$$

$$\dot{B}(u) = -3(1-u)^2S + 3(1-u)(1-3u)C_s + 3(2-3u) \tag{3.16}$$

The DLS can be calculated by:

$$DLS = \|k\|\frac{180}{\pi}30 \tag{3.17}$$

$$\|k\| = \sqrt{k.k} \tag{3.18}$$

$$k = \frac{1}{\dot{B}.\dot{B}}\ddot{B} - \frac{\dot{B}.\ddot{B}}{(\dot{B}.\dot{B})^2}\dot{B} \tag{3.19}$$

Where:

- k is the k factor;
- $\dot{B}$ is the first derivative of cubic Beziér curve equation;
- $\ddot{B}$ is the second derivative of cubic Beziér curve equation.

In which the free end trajectory (3.20) and the set end trajectory (3.21) can be defined, respectively, by the formulas below:

$$\ddot{B}(u) = 2S - 4C_s + 2E \tag{3.20}$$

$$\ddot{B}(u) = 6(1-u)S - 6(2-3u)C_s + 6(1-3u)C_e + 6uE \tag{3.21}$$

3.3. Case Study: 3D Trajectory Design Bézier Method

This section will present a focused study on a well path design modeled by the Drillbotics Team UiS for the 3D Trajectory Design applying the Bézier method. A 2D Wellbore Trajectory design specification is also presented (see Appendix A).

Many rules and limits must be applied during the design of the well path between two points, such as:

- Keep DLS as lower as you can, and it is known that 2-3 deg per 30 meters is the optimum one.
- The hold section should be 50 m or longer.
- Drop off rate should be in the range of 1.5-2.5 deg.
- KOP is kept as low as possible.

3.3.1. 3D Wellbore Trajectory

There are many techniques utilized for wellbore profile calculation. However, the cubic function was the one selected for the Competition. In the cubic function, the 3D coordinate functions are generated by solid functions that describe a wellbore mechanical phenomenon. Therefore, it is impossible to assume that this methodology can offer an all-time low force and drag mechanical phenomenon or a more robust mechanical phenomenon than any other methodology.

However, the cubic function provides more advantages comparing to other methods: it supplies a continuous and sleek mathematical 3D curve connecting the position of the outlet at the surface to a target, generally with a given inclination and azimuth, with a DOF that permits a good deal of management on the geometric characteristics of the wellbore trajectory (Sampaio Jr, 2007).

It can be defined as a mathematical method used for designing complex wellbore trajectories. It is used for different end conditions, for instance, the free end, set end, free inclination/set azimuth, and set inclination/free azimuth. The 3D smooth continuous functions are the outcome of this method, and it is found that this trajectory is more fit with the modern rotary steerable deviation tools (Sampaio Jr, 2007). Furthermore, changing the path curve and tool face gradually and continuously will result in a smooth trajectory curve with less drag, torque, and equipment wear.

For the three parametric coordinate functions, the expressions derived for cubic functions are used to construct a 3D cubic trajectory. It is assumed that the initial end of the trajectory's coordinates, inclination, and azimuth are known. Also known are the coordinates of the trajectory's end. There are four cases to be analyzed concerning the final end of the trajectory:

- Free inclination and azimuth;
- Set inclination and azimuth;

- Free inclination and set azimuth;
- Set inclination and free azimuth.

The procedures for cases one until case three are the same. They differ only in how each coordinate is represented by the functions selected and how the final conditions are imposed. Case four, however, requires an iterative process for obtaining the final azimuth due to its existence. To clarify the application of the method, the calculations for the second case, setting of inclination and azimuth, will be shown.

The three functions of the coordinate are set to slope cubic functions in this case. The parameters d_s and d_e are two degrees of freedom. They affect the 3D trajectory form, particularly its overall length and the varying curvature along the trajectory, d_s has a major impact on the trajectory's initial portion, while d_e has a major impact on the trajectory's final portion (Figure 3.11) (Sampaio Jr, 2007).

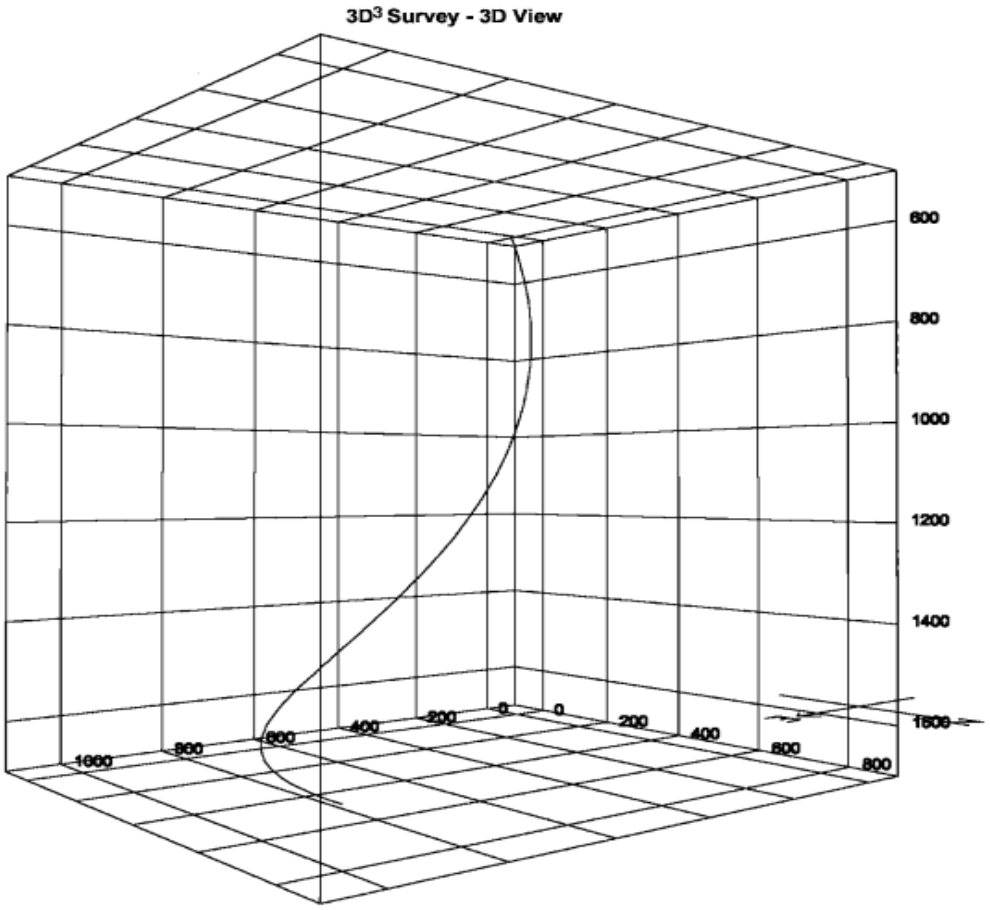

Figure 3.11: 3D Cubic Function Method.
Source: (Sampaio Jr, 2007).

A simple example for 3D well trajectory design:

The condition at the beginning of S and the end of E is given in Table 3.2:

Table 3.1: Conditions of S and E

Points	V [m]	N [m]	E [m]	I [°]	A [°]	M [m]
S (initial point)	500	5	18	30	10	508
E (target point)	1600	800	1000	90	0	

In addition, the model configuration parameters d_s, d_e are designed by users to adjust the trajectory shape, where d_s magnitude is connected to the coordinate functions. The shape of the coordinate functions will decide their general behavior. However, the final shape of the functions depends on the magnitude of d_s, which can be treated as an independent parameter (Sampaio Jr, 2007).

The d_s and d_e parameters will determine the final 3D trajectory design. From the simulation, a result of the 3D cubic trajectory calculation for the above data. The trajectory's arc length is 1933.57 m, and the final depth estimated is 2441.57 m.

The trajectory's free parameters yield several optimizations. For instance, the trail length and curvatures through the mechanical phenomenon square measure littered with changes in d_s or d_e. The arc length incorporates a minimum quantity of the geometer interval between the trajectory's initial and final ends. Nonetheless, increasing the trajectory's arc length usually will increase the curvature close to the ends well.

To attenuate the force, drag, and wear of drilling and production instrumentation, it is vital to avoid points with wide curvatures. One potential improvement approach is to attenuate the quality curvature deviation on the trail. For trajectories with two or additional degrees of freedom, a gradient descent theme may be used. For trajectories with just one degree of freedom, a proportion or a parabolic interpolation theme is appropriate (Sampaio Jr, 2007).

A curvature optimization on the set inclination and azimuth case information is given as an example to clarify the strategy. In this example, $d_s = d_e$ was contemplated offering consistency, thereby reducing the degree of freedom to at least one. By minimizing the standard curvature deviation, the value for d_s is acquired as $d_s = d_e = 2412.19$ m. Within the optimized trajectory, the maximum dogleg frequency is 4.37 deg/30 m at the calculated depth of 2029 m. Comparing this value by the non-optimized one given before with the peak dog-leg severity of 5.01 deg/30 m at 2036 m. If the d_s and d_e are defined as two separate parameters, it is possible to achieve the optimized wellbore trajectory at these values: $d_s = 2045.90$m and $d_e = 2808.68$m.

3.4. Wellbore Trajectory Optimization

3.4.1. Multiple Objectives of Trajectory Optimization

The oil/gas industry has, in recent years, been focusing on optimizing its performance being to reduce cost and time or for safety purposes. One of the areas where this optimal design is being

applied and has become very demanding is wellbore trajectory; this happens due to the many complex and interacted drilling variables, model uncertainties, and design constraints related to said model.

For drilling engineers, well path optimization is of extreme importance. It is usually based on minimizing drilling cost and time, avoiding well collision, minimizing the total wellbore length, improving the efficiency in the transport of cuttings, and increasing the drilling speed. This problem can be solved by utilizing some solutions presented by different optimization algorithms, such as generic algorithms, dynamic programming, and particle swarm optimization.

Drilling direction wells has become challenging for many reasons, such as low ROP, hole cleaning issues, and wellbore stability problems. In this model, we aim to improve performance during drilling by achieving stability and decreasing the time. There are some factors/parameters which should be fed/considered to the trajectory plan module:

- The azimuth of the wellbore trajectory;
- The inclination of the wellbore trajectory;
- Controllable drilling parameters (WOB, RPM, ROP, among others);
- Unconfined compressive strength (UCS);
- Formation pore pressure;
- In-situ stresses of the studied area.

Data input is the first step in this model; the second step involves optimizing the process to obtain max ROP by using a GA. The last step is to predetermine the suggested azimuth and inclination "by considering the results of wellbore stability using wireline logging measurements, core, and drilling data from the offset wells. The present study emphasizes that the proposed methodology can be applied as a cost-effective tool to optimize the wellbore trajectory and to calculate approximately the drilling time for highly deviated wells" to be drilled in the future (Abbas et al., 2018).

Considering the fact that well path and trajectory is a complex optimization problem, we attempted to examine a decision-driven approach to well path design by quantifying key decisions and uncertainties. We aim to develop an analytical decision framework to design an optimal 2D/3D well path while considering drilling bed boundaries uncertainties and the offset wells' uncertain positions to optimize the drilling process.

Some principles such as the anti-collision, DLS, and ROP can be used to optimize the well design trajectory; this thesis will go over these principles and then present their use in a case study.

3.4.2. Anti-Collision Principle

The cluster well drilling technology and infill development drilling technology has been widely used in recent years to meet the requirements of oil field development; more and more drilling occurs in dense well spacing in the existing oil field or the high-density well. However, the risk of drilling such wells was increased by wellbore anti-collision incidents. Suppose one can reliably predict such accidents and take active steps to eliminate the risk. So, these two drilling technologies may have wider prospects for implementation (Olaijuwon, 2012).

Survey data for a given wellbore is never normally considered accurate when defining actual wellbore positions. There is a need to recognize that measurement errors can occur even on the most accurate survey tools. Azimuth reading error, depth error, and inclination error are mainly responsible for wellbore position uncertainty. By considering these errors, it becomes possible to construct a cone of uncertainty around the actual survey data, which better defines the probable boundaries within which the actual position of the wellbore will fall (Ekseth, 1998).

The inclination error creates a high side dimension of the uncertainty ellipse. The azimuth error creates a lateral dimension of the uncertainty ellipse, while measured depth error creates a third component along the wellbore axis. So, they combine and form an ellipsoid of uncertainty (DeWardt and Wolf, 1981).

Several models have been conducted to overcome such errors, namely, cone of uncertainty model, Walstrom error model, Wolff and DeWardt error model, SESTEM error model, and the ISCWSA error model. However, ISCWSA is the more accurate model to eliminate the errors during drilling until it reaches the target. The model starts by finding all error sources affecting measure depth, inclination, and azimuth. Then, it designates the error code to each error source and defines the vector for each error (Ekseth, 1998 & Williamson, 2000).

Then, each error source has a set of weighting functions, which are the equations that describe how the error source affects the actual survey measurements of MD, I, and AZ. Afterward, summing up the errors, where "each error source also provides a propagation mode, that defines the correlation between surveys" (Jamieson, 2012).

Anti-collision is about maintaining a safe clearance between the cones of uncertainty. The anti-touch scan is the basis of collision prevention and scientific decision-making during drilling. Anti-collision scanning starts with a global scan, and then a proximity one takes place. Figure 3.13 illustrates the distance between the cone of uncertainty of two wells (Wolff and De Wardt 1981 and Abughaban et al., 2016).

The global scan is the initial scan made in the anti-collision planning process to scan through the entire database project for all nearby wells that fall within the user-specified scan radius of 12 000 meters. This global scan is required to identify the wells required to be included in the next step of the anti-collision planning process. On completion of the global scan, a proximity scan must be performed on all the wells that have been identified as being "nearby wells." The proximity scan uses the subsurface survey data associated with each nearby well to calculate the distance from each well to the subject well at every point along its length (Ekseth, 2000).

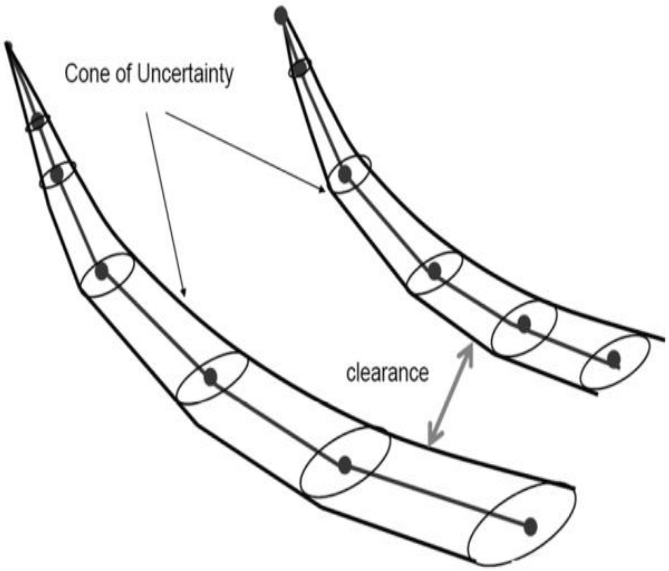

Figure 3.12: Clearance between the Uncertainty Cone of Projected Well and the Cone of Offset Well.
Source: (Olaijuwon, 2012).

The proximity scan has two methods to perform the analysis on the wells, namely, Geometrical Analysis (Centre to center distance) and Statistical Analysis (Separation Factor). Geometrical analysis (CtC calculation) is necessary to scan using both normal plane and 3D least distance to ensure that the closest CtC distance is found.

The separation factor is defined as the ratio of the center-to-center distance between wells and the sum of the radius (major semi-axis) of the ellipsoids of uncertainty between the subject and offsets wells being scanned. "A SF greater than one means that the ellipses are completely separated, and there is no overlap. A SF of one means that the ellipses are touching and a number less than one means that the ellipses are overlapping one another." (DeWardt and Wolf, 1981 and Abughaban et al., 2016). Figure 3.14 shows the SF methods of proximity scan.

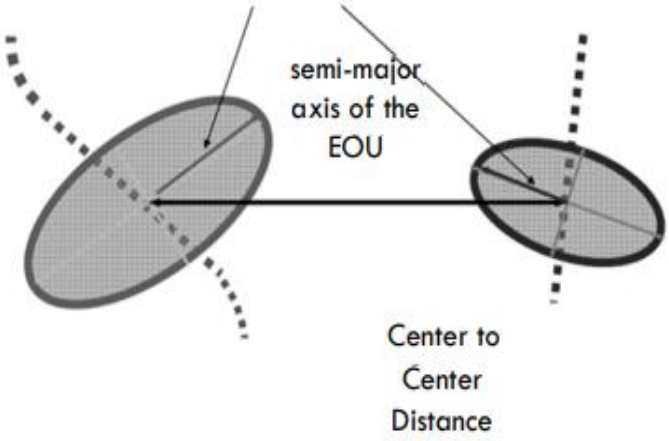

Figure 3.13: The Separation Factor.
Source: (DeWardt and Wolf, 1981).

3.4.3. DLS Principle

Another way to optimize a well trajectory is by optimizing its DLS. This parameter optimization occurs through selecting the most attractive directional drilling conditions to reach the target wanted. High values of DLS imply minimizing well trajectory; however, this factor increases the fatigue on the drill string and the T&D, notably during rotation mode (Hosseini et al., 2014).

According to Hosseini et al. (2014), one way to accomplish the DLS optimization is by selecting the final MD as the objective function to optimize it. This can be done since the DLS and the final MD are associated through well path equations, for instance, the equations in build and hold pattern. This pattern is commonly used in directional drilling and uses three variables with 2-DOFs: DLS, KOP, and maximum well angle. The relationship among these parameters is observed from Equation (3.22) until Equation (3.26), and the schematic can be seen in Figure 3.14.

$$\mathrm{DLS} = \frac{18000}{\pi \mathrm{R}} \tag{3.22}$$

$$\alpha = \arccos\frac{\mathrm{R} - \mathrm{X}}{\mathrm{d}} - \arccos\frac{\mathrm{R}}{\mathrm{d}} \tag{3.23}$$

$$\mathrm{d} = \sqrt{(\mathrm{D_3} - \mathrm{D_1})^2 + (\mathrm{X} - \mathrm{R})^2} \tag{3.24}$$

$$\mathrm{MD_{EOB}} = \mathrm{D_1} + \left(\frac{100\alpha}{\mathrm{DLS}}\right) \tag{3.25}$$

$$\mathrm{MD} = \mathrm{MD_{EOB}} + \left(\mathrm{D_3} - \frac{\mathrm{D_2}}{\cos\alpha}\right) \tag{3.26}$$

Where:

- R is radius of curvature [m];
- X is horizontal displacement [m];
- α is inclination [°];
- $\mathrm{D_1}$ is TVD to KOP [m];
- $\mathrm{D_2}$ is TVD to point EOB [m];
- $\mathrm{D_3}$ is TVD to target[m];
- d is the distance from radius to target [m];
- DLS is dogleg [°/30m];
- $\mathrm{MD_{EOB}}$ at the end of the build-up section [m].

In planned drilling programs, there are usually two know parameters, the horizontal displacement, X, and the TVD, $\mathrm{D_3}$.

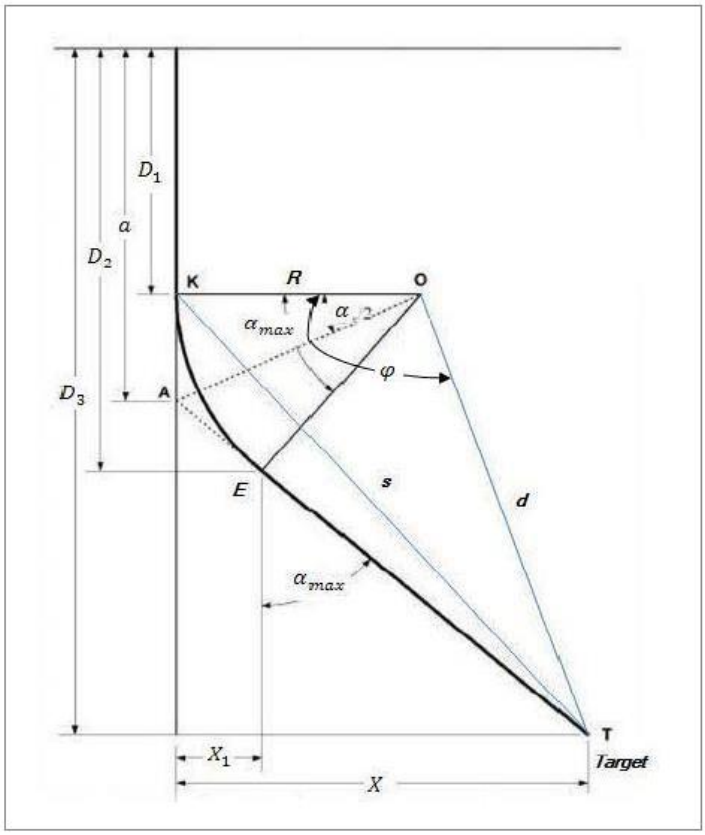

Figure 3.14: Well profile for build & hold pattern equations.
Source: (Hosseini et al., 2014).

3.4.4. ROP Principle

According to Arabjamaloei et al. (2011), selecting the most appliable wellbore trajectory is important in achieving superior drilling performance. Several methods can accomplish such an objective; one is the maximum ROP principle or the ROP optimization.

Accomplishing a higher ROP can lead to a considerable reduction in drilling costs; a higher ROP can be achieved by better planning wells, a better understanding of the drilling process, and implementing advanced well technologies. However, drilling data and predictive models cannot provide absolute values for ROPs. Many uncertainties coming from formation, drill bit and BHA, drilling mud; make the estimation and optimization of the ROP more complex (Wiktorski et al., 2017).

As presented by Kahraman et al. (2003), the difficulties of modeling the ROP come from its dependence on a wide range of drilling variables, such as WOB, RPM, pump flow rate and standpipe pressure, total flow area, bit design and type, mud weight and type, bit diameter, and wellbore trajectory.

Many mathematical models venture to parallel drilling parameters with the ROP; however, due to the intricate and non-linear behavior of the variables with the ROP, these models cannot make an accurate and comprehensive prediction of the penetration rate (Abbas et al., 2018). In

addition, there current model that includes all effects for inclination and azimuth of well trajectory on the rate of penetration (Arabjamaloei et al., 2011).

The ROP optimization can be achieved by constructing a good well path design, new technologies implementation, and real-time operations with manipulating operational parameters, such as WOB, RPM, and flow rate.

3.5. Case Study: Trajectory Optimization

This section will present a case study for the optimization of a well trajectory design using the optimization principles of anti-collision, DLS, and ROP. The model designed was coded in MATLAB®, where an offset well was designed with a 3D trajectory. The North and East coordinate, the vertical depths of point 1 (bottom of the reservoir) and 0 (top of the reservoir), and the measured depth at point 0 are designated by the user, as well as the initial azimuth and inclination. Finally, the trajectories survey points and DLS are calculated, and a graph is plotted as shown in Figure 3.15.

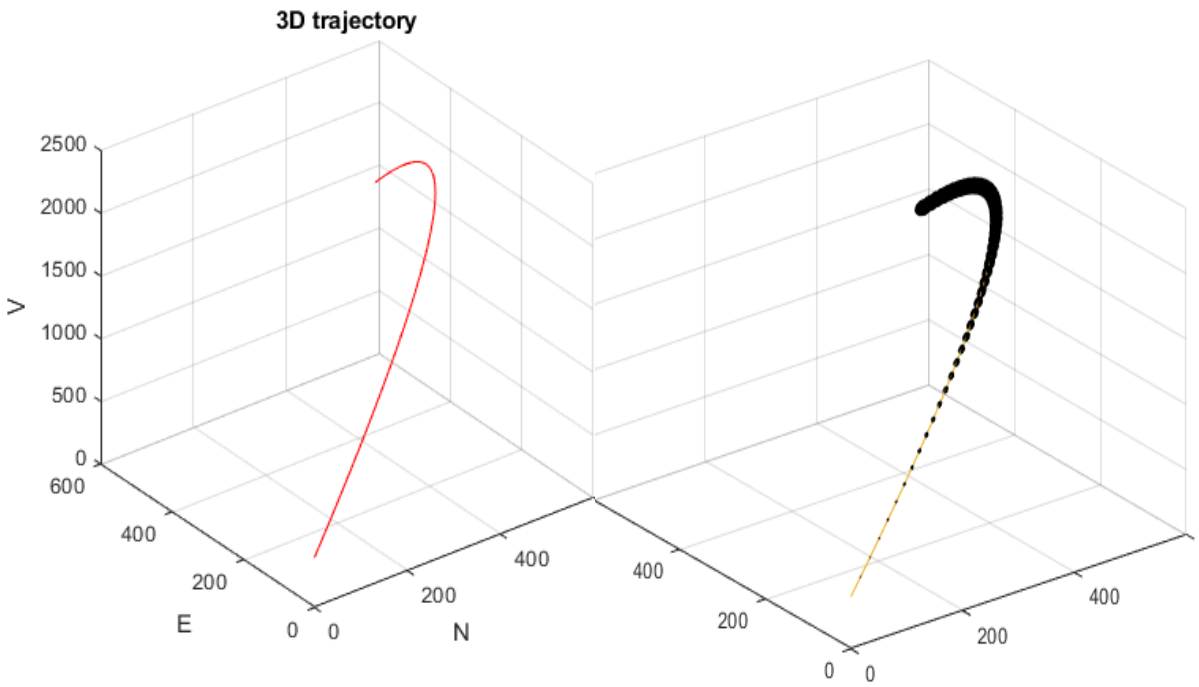

Figure 3.15: Offset Well and Offset with Uncertainties.

After plotting the offset well, the parameters for the bit uncertainty calculation were defined, being the number of measurement errors, dip angle, inclination limit, singular matrix condition, and the SF for the confidential region. Finally, a covariance matrix calculation was created for the offset well, and the offset well uncertainties were plotted, as shown in Figure 3.15.

Subsequently, an arbitrary reference was designed by assigning an arbitrary target point, its vertical, North, and East coordinates, and its azimuth and inclination. Then, a loop is generated to obtain the vertical target point 1 and the anticollision survey calculation. This anticollision survey calculation generates a graph that can be analyzed by two points. At survey point,

anti=1, we have safety factor (SF) >= 1, which means there is no collision between the offset well and the new well, the collision will happen at survey point anti=0, where we have a SF<1, the parameter SF is defined as the separation factor to avoid collision and is calculated as shown in Equation (3.27).

$$\mathrm{SF} = \frac{\text{distance between two points}}{\text{area between both points radius}} \tag{3.27}$$

The first survey done in this arbitrary well presents a collision, as shown in Figure 3.16.

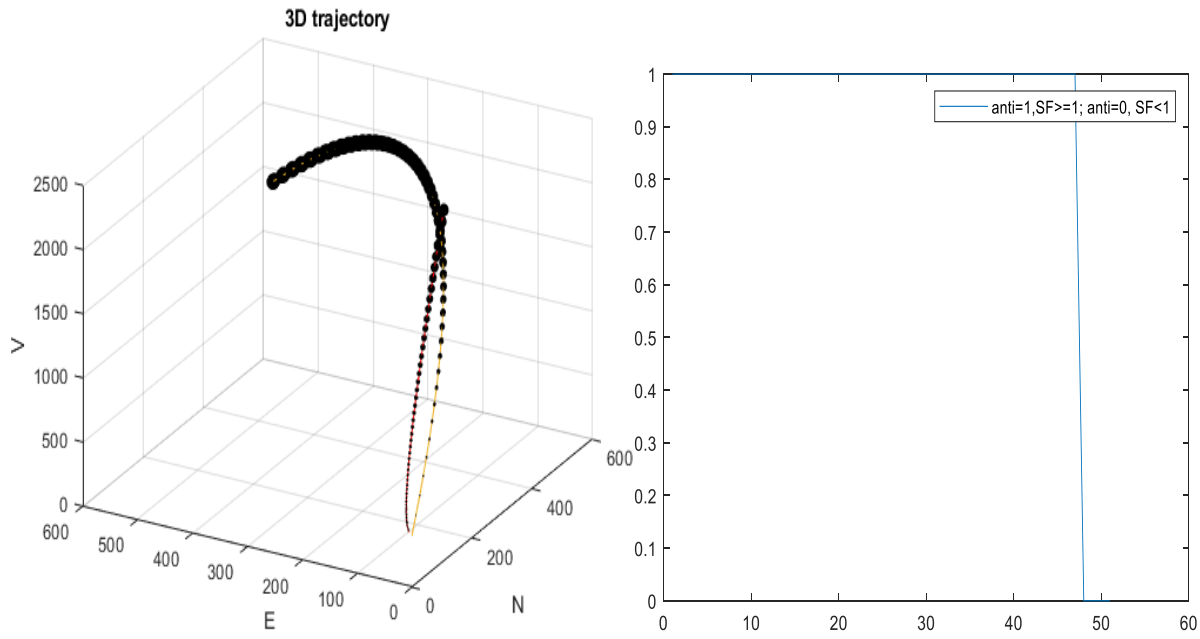

Figure 3.16: Arbitrary Reference Well (Collision Happens) Plot and Collision Points Plot.

In order to fix this collision problem, the well path is redesigned by changing the target point such that we get anti=1 point for all survey points. Then, the new well path is plotted again with anti = 1, i.e.; no collision happens, as shown in Figure 3.17. This step does not consider any optimization inputs.

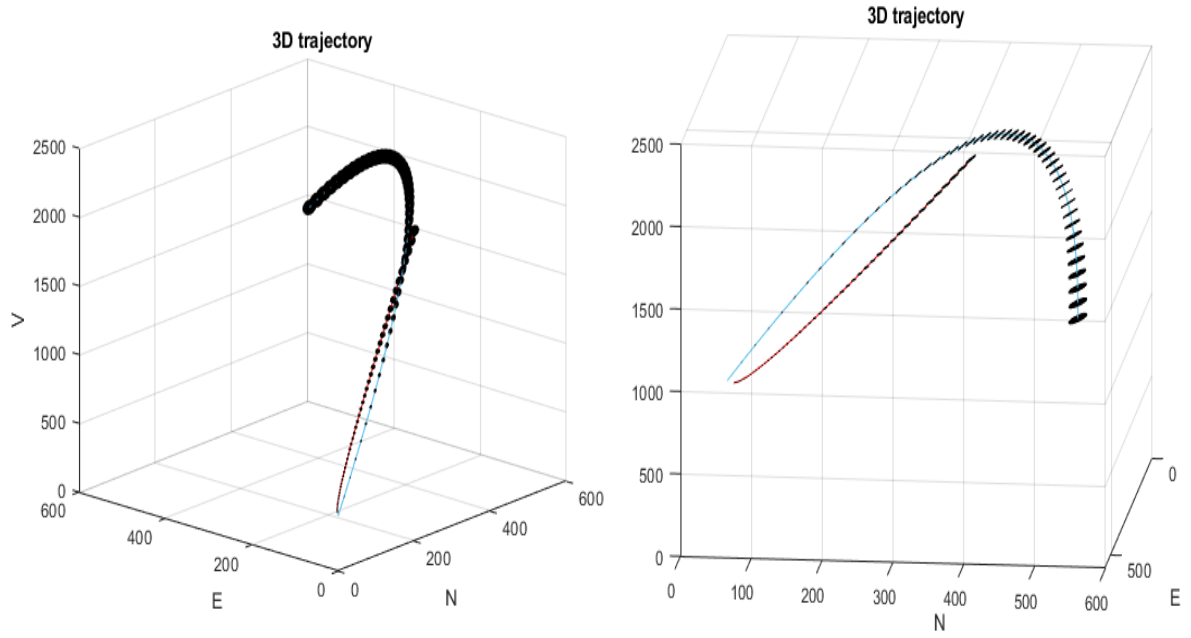

Figure 3.17: New 3D Trajectory with No Collision Plot.

Once the anti-collision model is finished, the optimized well path model, which minimizes the DLS, is designed. This is done by defining the DLS constraints, the coordinate points, azimuth and inclination points, and the rest of the trajectory parameters. It then plots uncertain region values and finds the optimal well path with the optimized DLS, shown in Figure 3.18.

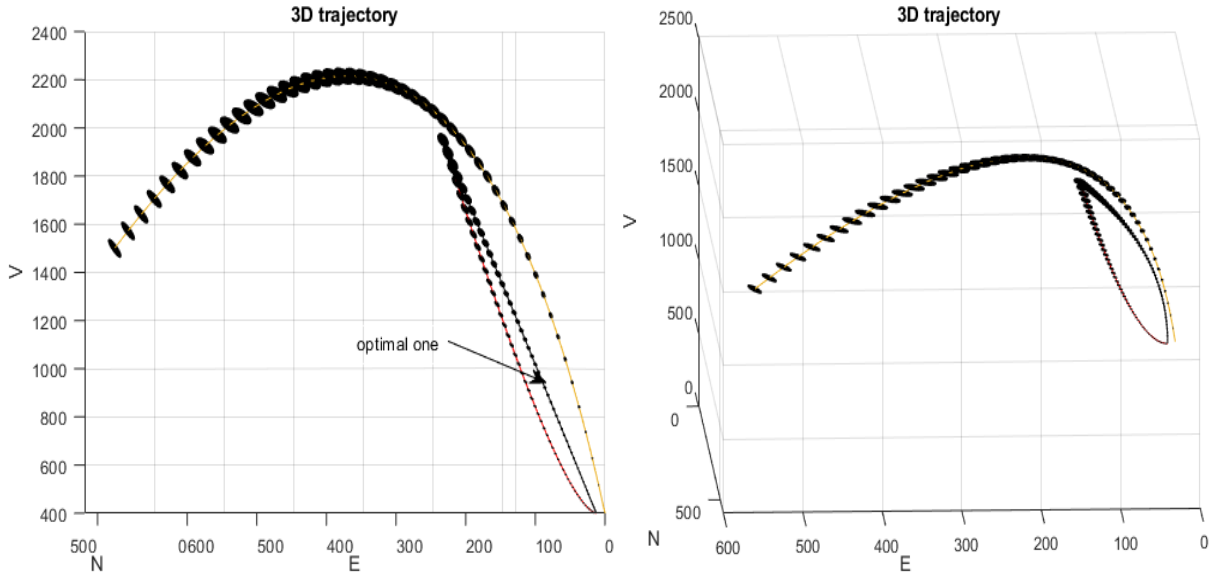

Figure 3.18: Optimal Well Path, with Optimized DLS.

After the well is optimized for DLS, an optimization code for ROP is designed, and an optimal well path for DLS and ROP is created with a sliding mode DLS > 3. Finally, a reference well after ROP optimization is generated, and the separation factors are applied to the model. The graph is plotted in Figure 3.19.

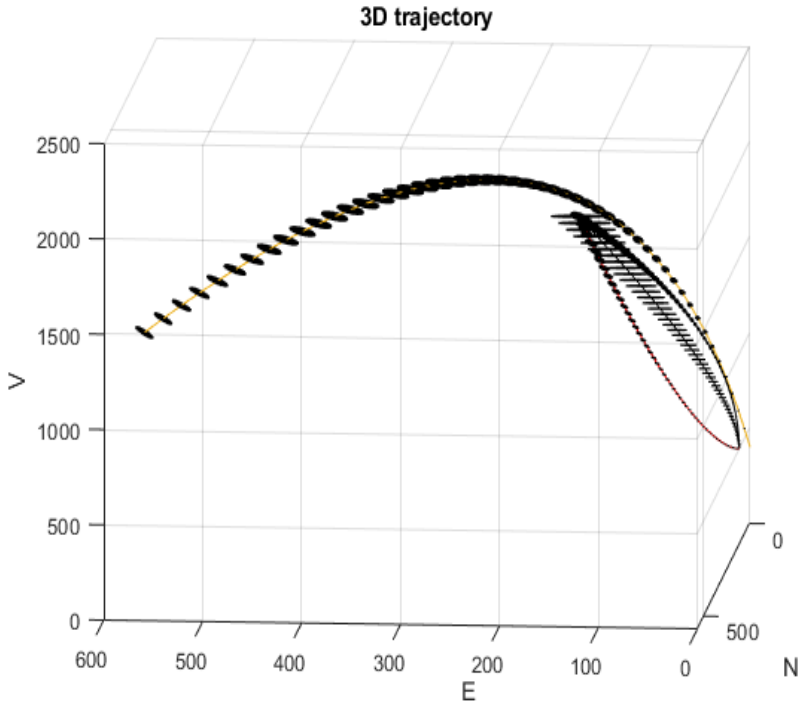

Figure 3.19: Optimal Well Path with optimized DLS and ROP.

The ROP results for the well without ROP optimization are an average ROP $= 42.6$ m/s, while the results find with the ROP optimization are an average ROP $= 43.5$ m/s.

4. Models for In-House UiS Well Design Simulator

This section will provide information about the models designed by the Drillbotics UiS Virtual Team for the 2021 Drillbotics Competition; these models include the T&D model, the Flow model, the Cuttings Transport model, the Buckling model, the Temperature model, and the ROP model.

4.1. Torque and Drag Model

The T&D are the main limiting factors in knowing the depth in which one can drill a well, especially concerning horizontal wells. These forces are intertwined with the friction between the drill string and the wellbore.

Torque is the moment needed to rotate the pipe to overcome its rotational friction and bit friction. When concerning T&D models, the torque is equivalent to the torque loss, or torque that is lost on the way from the top drive to the drill bit due to friction.

Drag is the extra load compared to a free rotating drill string. It is defined as the sliding friction force that appears during drill string or casing tripping operations. The T&D model chosen by this thesis is defined by Aadnoy (2010) and assumes a soft string model, which implies that the pipe bending is so tiny that its bending stiffness can be neglected, meaning the pipe is in constant contact with the wellbore. The equations are separated into two categories: straight wellbore sections and curved wellbore sections.

Straight sections of the well are usually weight-dominated. For arbitrary well orientation or curved borehole sections, the normal contact force between the drill string and the hole is strongly dependent on its axial pipe loading, making it a tension-dominated process. At the string's bottom, the tension is low, and the weight dominates over the friction, a factor also used for curved bends. During trip in/out of the well $F1 = 0$ is used as an end condition, and $T1 = 0$ is used as a wellbore bottom condition. The calculations are made bottom-up in the well.

The inputs and outputs for the T&D model are presented in Tables 1 and 2 (See Appendix B).

4.2. Flow Model

The flow model is used to calculate the change in pressure throughout the wellbore. In order to accomplish these results, the drill string and annulus are discretized into n cells. Next, the hydrostatic pressure and pressure loss are calculated with updated density and viscosity for each cell, where the viscosity can be calculated using Herschel-Bulkley models as:

$$\mu_a = K\left(\frac{3n_a + 1}{4n_a}\frac{8v}{D}\right)^{n_a - 1} \tag{4.1}$$

Where:

- K is the consistency index [Pa.s^n];
- and n_a is the generalized flow index.

The pressure loss is then calculated as being:

$$(\Delta P)_{Frictional} = \frac{fL\rho v^2}{2D} \quad (4.2)$$

Where:

- f is the friction factor;
- L is the pipe length [m];
- v is the fluid velocity (average) [m/s];
- ρ is the fluid density [kg/m²];
- D is the pipe inner diameter [m].

The solution proposed by this model for pressure calculation is to use a numerical shooting method to calculate the pressure profile in the drill string and the annulus, respectively. To specify it, the process starts by defining two initial guesses of BHP_1 and BHP_2, based on such values, the density and viscosity of the bottom cell are updated; thus, the pressures of the above cells are calculated.

The pressure at the first cell is obtained through the repetition of this calculation. Formerly, a comparison between the calculated pressures with the surface pressures is made. If the differences are more significant than a specified tolerance (such as a terminal condition), an adjustment is provided to the initial guesses BHP_1 and BHP_2, the process is repeated until the difference between them is less than such threshold. The shooting method steps for the algorithm are summarized below:

Algorithm

- Step 1: Discretize the wellbore into n cells with the length Δz
- Step 2.: Inputs: flow rate Q, $P_{surface}$, surface mud weight, mud viscosity, wellbore geometry
- Step 3: Determine two initial guesses $P_{guess,1}$ and $P_{guess,2}$ and calculate the pressure at cell (2) in by

$$P_{2,1} = P_{guess,1} - \rho(P_{guess,1})g\Delta z - P_{loss,1,1} \quad (4.3)$$

$$P_{2,2} = P_{guess,2} - \rho(P_{guess,2})g\Delta z - P_{loss,1,2} \quad (4.4)$$

  Where: P_{loss} is the frictional pressure loss associated with each cell.

- Step 4: Repeat steps above for each cell i=2, …n-1 by:

$$P_{i+1,1} = P_{i,1} - \rho(P_{i,1})g\Delta z - P_{loss,i,1} \quad (4.5)$$

$$P_{i+1,2} = P_{i,2} - \rho(P_{i,2})g\Delta z - P_{loss,i,2} \quad (4.6)$$

- Step 5: Define $f_1 = P_{n,1} - P_{surface}$, $f_2 = P_{n,2} - P_{surface}$. If f_1 is less than tolerance, then the algorithm is terminated, else cut the interval $[P_{guess,1}, P_{guess,2}]$ into two halves and go back to Step 3.

The model's inputs and outputs are summarized below in Table 3 and Table 4 (See Appendix B).

4.3. Cuttings Transport Model

A critical model for the drilling operations is the cuttings transport. During drilling, the cuttings generated by the drill bit have to be transported out of the well to avoid cuttings accumulation. This accumulation may lead to a stuck pipe/tight hole or pack-off situation. For that reason, a sufficient flow rate is required for each hole section; moreover, special attention must be given to hole cleaning in deviated wells due to the build-up of cuttings beds.

Cuttings appearing over the shaker are of extreme importance in determining hole cleaning and wellbore instability issue. However, the rates required to maintain those issues at bay are often challenging to model and predict, considering many factors affect them.

In the interest of acquiring a proper transport of cuttings, the following parameters are necessary: significant flow rates which translate into sizeable fluid velocity, high drill pipe rotation, low ROP, heavy mud weight in order to create higher buoyancy of the particles, large hole size to have more space for the cuttings, follow a trajectory as vertical as possible to make it easier for the cuttings to be transported and the last but not least, high viscosity for vertical wells to create a laminar flow and low viscosity for inclined or horizontal wells to disturb the cutting beds (Kåre, 2020).

Keeping in mind the prevention of cutting beds, said model requires faster annular velocities. However, such may not be achieved due to pump pressures, flow rate limitations in the BHA equipment, ECD limitations due to narrow drilling margins, which may lead to losses, and unconsolidated nature of lithology (washout potential) or faulting (rubble zone). Therefore, a compromise between each limitation must be reached to ensure fast and safe drilling operations for all sections of the well.

A standard model for cuttings transport is Larsen's model, where the user is able to predict the average cuttings travel time velocity, the critical transport fluid velocity to avoid cuttings bed formation in highly inclined wellbores ranging from 50° to 90° (Larsen, 1997). Furthermore, the model predicts the critical velocity as well as the cuttings bed thickness providing that the flow rate be less than the one suggested. The model's inputs and outputs can be seen in Tables 5 and 6 (See Appendix B).

4.4. Buckling Model

Buckling can be defined as applying too much weight to the drill pipe from the surface when the weight on the bit to be used is higher than the buoyed weight of the drill collars and heavy-weight drill pipe (Belayneh, 2006).

The key is to have the drill pipe in compression but at a limit to avoid buckling. However, this condition is not always accomplished, so sinusoidal buckling (elastic buckling) and then helical buckling (severe buckling), if no actions are taken, may occur due to a continuous application of axial loads. Ultimately this axial compressive load may lead to lock-up or permanent deformations called corkscrewing, which is to be avoided (Kårstad, 2020).

One essential parameter introduced in the model presented in this thesis and not usually considered for buckling is friction. Friction redistributes the internal axial forces, making buckling less predictable; thus, making this effect relatively significant to analyze during well planning or drilling operations (Gulyayev, 2016).

On the other hand, this buckling effect is less visible in high-angled wells since the force of gravity drags the drill string across the low side of the hole. This stabilizes the string allowing the drill pipe to carry high axial loads without buckling happening (Masoomi & Moghadasi, 2014).

Models for the critical (sinusoidal) buckling force in vertical wells (Lubinski et al., 1962 and Wu et al., 1993) and inclined wells (Dawson and Paslay, 1984) are well accepted by the drilling industry. In addition, several models have also been proposed to predict the helical buckling load of tubular in vertical wells (Lubinski et al.,1962) and for inclined and horizontal wells (Mitchell, 1996).

The list of inputs and outputs is shown in Table 7 and Table 8 (See Appendix B).

4.5. Temperature Model

This model's objective is to develop an detailed temperature model that can calculate wellbore temperature distributions accurately. The model is derived based on the balance of energy between the well and the formation. Inside the drill pipe, the flow is directed downwards, and heat will enter the system at x and leave the system at x+dx distributions accurately (Sui et al., 2018).

In Figure 4.1 it is seen the transfer of heat from the formation to the cementation, annulus, and drill pipe.

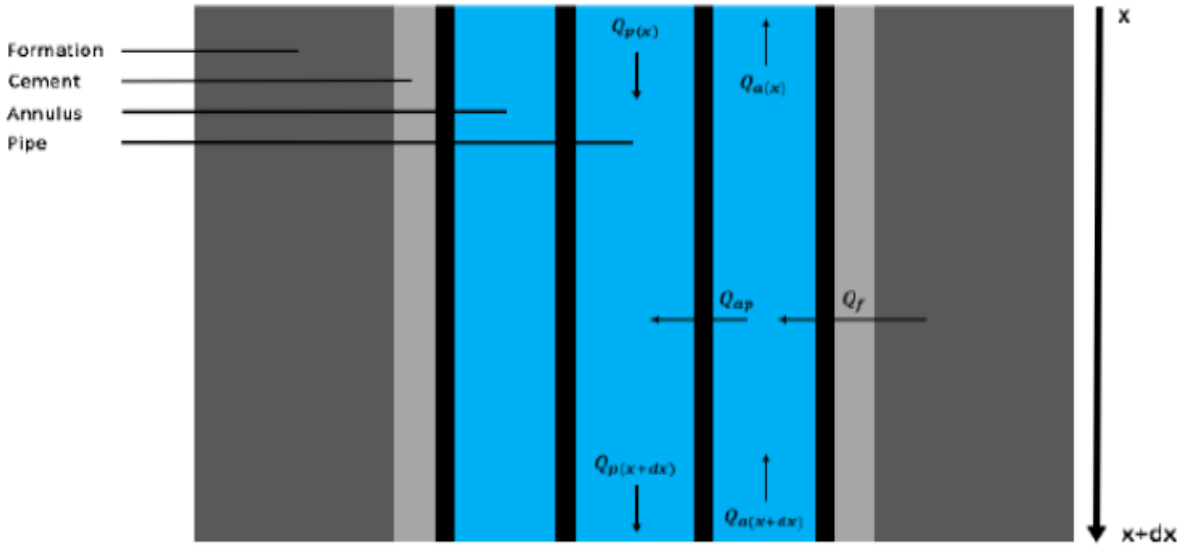

Figure 4.1: Heat Transfer in Annulus and Drill Pipe.
Source: (Sui et al., 2018).

The equation below shows the temperature distribution for the drill pipe:

$$\frac{dT_p}{dx} = A(T_a - T_p) \tag{4.7}$$

The temperature distribution for the annulus section is shown in the equation below:

$$\frac{dT_a}{dx} = C(T_a - T_p) - B(T_f - T_a) \tag{4.8}$$

The coefficients A (annulus), B, C are defined in Equations (4.9) to (4.11):

$$A = \frac{2\pi r_{pi} U_p}{m_p c_p} \tag{4.9}$$

$$B = \frac{2\pi r_{ci} U_a k_{fo}}{(k_{fo} + r_{ci} U_a T_D) m_a c_p} \tag{4.10}$$

$$C = \frac{2\pi r_{pi} U_p}{m_a c_p} \tag{4.11}$$

Where:

- T_a is fluids' temperature inside annulus [K];
- T_p is temperature of fluid in pipes [K];
- T_f is formation temperature [K];
- r_{pi} is the inner radius of pipe [m];
- U_p OHTC inside pipes;
- m_p is mass rate in pipes [kg/s];
- c_p is SHC of fluids [J/(kg.K)];
- r_{ci} is the inner radius of casing [m];

- U_a OHTC inside annulus;
- k_{fo} is TC of formation [W/(m.K)];
- T_D is dimensionless temperature;
- m_a mass rate in annulus [kg/s];

A numerical approach called the shooting method is implemented to obtain; thus, allowing the wellbore to be divided into a certain number of boxes. “For each box, all the parameters that vary throughout the wellbore are updated and treated as constants over the box length”, allowing the model to be solved by the undetermined coefficients method (Sui et al., 2018).

4.6. ROP Model

The oil and gas industry utilizes two approaches to predict the ROP in a specific field: physics-based or traditional models and data-driven models. Physics-based models are mathematical functions obtained during lab experiments, while the data-driven approach uses machine learning to create a model capable of predicting ROP. Traditional models are decisive and allow for easy optimization; however, they have limitations, such as low accuracy in ROP prediction, a strong dependency on empirical coefficients based on lithology that varied continuously, and the requirement of static parameters as inputs that are not always available.

On the other hand, there are data-driven models, and as the title suggests, they are purely dependent on data, thus only designed for a specific field. However, these models give more accurate ROP prediction than traditional models, as Hegde et al. (2017) show. Also, they have no bit or BHA specifications and are independent of the drilled layer since they have no empirical constants.

For the primary purpose of this section, accuracy in ROP prediction is not necessary and traditional models will be used. However, many models exist, and six of them will be briefly described below.

4.6.1. Bingham’s Model

Bingham’s (1965) is an empirical ROP model that considers the penetration rate as a function of WOB, RPM, and bit diameter. It is designed for any bit type. The equation used in this model is given as such:

$$\mathrm{ROP} = \mathrm{K}\left(\frac{\mathrm{WOB}}{\mathrm{D_b}}\right)^{\mathrm{a}} \mathrm{RPM} \tag{4.12}$$

Where:

- ROP is the penetration rate [m/s];
- WOB is the weight on bit [kg];
- RPM is the rotary speed [revolutions/min];
- D_b is the bit diameter [m];
- and ‘a’ and ‘K’ are rock formation constants obtained by linear regression.

As pointed by Soares et al. (2016), adjusting the coefficient bounds to fit the model with field data received is imperative.

4.6.2. Burgoyne et al.'s Model

The second model described in this section is Burgoyne et al. (1991); this ROP model includes more drilling parameters if compared to Bingham, such as pore pressure, WOB, sediments compaction, and is expressed as a function of eight components:

$$ROP = f_1 \, x \, f_2 x \, f_3 x \, f_4 x \, f_5 x \, f_6 x \, f_7 x \, f_8 \tag{4.13}$$

$$f_1 = e^{a_1} \tag{4.14}$$

$$f_2 = e^{a_2(13000-TVD)} \tag{4.15}$$

$$f_3 = e^{a_3 TVD^{0.69}(P_{pore}-10.5)} \tag{4.16}$$

$$f_4 = e^{a_4 TVD(P_{pore}-ECD)} \tag{4.17}$$

$$f_5 = \left(\frac{\left(\frac{w}{d_b}\right) - \left(\frac{w}{d_b}\right)_t}{4 - \left(\frac{w}{d_b}\right)_t} \right)^{a_5} \tag{4.18}$$

$$f_6 = \left(\frac{RPM}{60}\right)^{a_6} \tag{4.19}$$

$$f_7 = e^{-a_7 h} \tag{4.20}$$

$$f_8 = e^{a_8 \frac{\rho q}{350 \mu d_n}} \tag{4.21}$$

Where, f_i includes drilling parameters and a_i are the variable coefficients calculated using linear regression. Coefficients are described in the following way:

- f_1 represents the formation strength.
- f_2 and f_3 represent pore pressure influence, where TVD is true vertical depth and P_{pore} is the pore pressure [ppg].
- f_4 represents the differential pressure effect, where ECD is the equivalent circulating density.
- f_5 represents the variation of WOB and bit diameter and changes for bit type, where $\frac{w}{d_b}$ is the applied WOB per inch, d the bit diameter and $\left(\frac{w}{d_b}\right)_t$ the threshold WOB per inch.
- f_6 represents the influence of the RPM.
- f_7 represents the drill bit wear.
- f_8 represents the hydraulic effects, where d_n is a bit nozzle diameter and μ is the viscosity of the drilling fluid.

4.6.3. Winters, Warren, and Onyia Model

In 1987, Winters, Warren, and Onyia published a paper presenting their model for connecting roller bit penetration rates to bit design, the rock mechanics, and operational conditions. This process was done identifying rock ductility as having a large influence on bit performance and the cone offset as being the most crucial design parameter for drilling ductile rock. The ROP effects in this model are "bit indentation, bit teeth, bit hydraulics, and bit offset" (Winters et al., 1987). The WWO model is the first to approach a specific type of bit; by focusing on roller cone bits. The model equation is as follows:

$$\frac{1}{ROP} = \frac{\sigma * D^2}{N * W} * \left(\frac{a * \sigma * D * \epsilon}{W} + \frac{\Phi}{W}\right) + \frac{b}{N * D} + \frac{c * \rho * \mu * \epsilon}{I_m} \tag{4.22}$$

Where all parameters are in SI units and are presented below:

- σ is rock compressive strength [MPa];
- D is bit diameter [m];
- ϵ is rock ductility;
- N is rotary speed [m/s];
- W is weight on bit [kg];
- Φ is the cone offset coefficient;
- a, b, c are model coefficients;
- ρ is the equivalent mud density which is defined as the apparent mud density which results from adding annular friction to the actual fluid density in the well [kg/m²];
- μ is mud viscosity [Pa.s];
- I_m is the modified jet impact force [N].

The following equation defines the modified jet impact force:

$$I_m = \left[1 - {A_v}^{-0.122}\right] * F_j \tag{4.23}$$

Where:

- A_v is the ratio of jet velocity to return velocity;
- F_j is the jet impact force [N].

The ratio of jet velocity, A_v , can be found by assuming the bit possess three jets, and can be calculated from the equation:

$$A_v = \frac{\nu_n}{\nu_f} = \frac{0.15D^2}{3d_n^2} \tag{4.24}$$

Where:

- d_n is nozzle diameter [m];
- v_n is nozzle velocity [m/s];
- ν_f is returned fluid velocity [m/s].

Winters, Warren, and Onyia's papers are more advanced than its predecessor B&B because it provides accurate explanations for applying the model to field data. Their paper discusses how "one can predict and interpret roller bit performance in offset wells by generating a continuous rock strength log from interpreting field data and comparing the rock strength log to the triaxial compressive strength of the rock at a confining pressure equal to the differential bottom hole pressure" (Winters et al., 1987).

4.6.4. G. Hareland's Drag Bit Model

Hareland's (1994) model proposed a model to predict ROP for drag bits. This model improves on previous ones by adding equivalent bit radius, lithology coefficient, dynamic cutter action, and cutter wear. The model optimizing drilling parameters and aids in solids control (Barros L.M.L., 2015).

This model uses a correlation factor to account for the specific "theoretical properties that affect ROP, such as bit cleaning, imperfections in bit and cutter geometry, and microscopic variations in rock strength" (Barros L.M.L., 2015). For example, here is the equation for drag bits and the correlation factor:

$$\mathrm{ROP} = \frac{14.14 * \mathrm{N} * \mathrm{RPM}}{\mathrm{D}} * \left[\left(\frac{\mathrm{d_s}}{2}\right)^2 * \cos^{-1}\left(1 - \frac{4 * \mathrm{W_{mech}}}{\mathrm{N} * \mathrm{d_s^2} * \pi * \sigma_c}\right) - \left(\frac{2 * \mathrm{W_{mech}}}{\mathrm{N} * \pi * \sigma_c}\right) - \left(\frac{4 * \mathrm{W_{mech}^2}}{\mathrm{N} * \mathrm{d_s} * \pi * \sigma_c}\right)^{0.5} * \left(\frac{\mathrm{d_s}}{2} - \left(\frac{2 * \mathrm{W_{mech}}}{\mathrm{N} * \mathrm{d_s} * \pi * \sigma_c}\right)\right)\right] \quad (4.25)$$

$$\mathrm{COR} = \frac{\mathrm{a}}{\mathrm{RPM^b x W^c}} \quad (4.26)$$

Where:

- D is bit diameter [m];
- N is the number of cutters;
- RPM is the rotary speed [revolutions/min];
- d_s is diamond cutter diameter [m];
- W_{mech} is weight on bit per diamond cutter [kg];
- σ_c is uniaxial compressive strength [kg/m²]
- W is weight on bit [kg],
- a, b, c are cutter geometry correction factors.

4.6.5. G. Hareland's Roller Bit Model

G. Hareland's (2010) model proposes an approach to calculate ROP for roller cone bits. This model analyzed previous drilling models and improved on them by including bit-rock interaction. This complexity derives from a wedge relating the roller cone bit and rock interaction to rock failure (Barros L.M.L., 2015). The model is shown in Equation (4.27).

$$ROP = K * \left(\frac{80 * n * m * RPM^{a}}{D^2 * \tan^2 \Psi}\right) * \left(\frac{W}{100 * n * CCS}\right)^{b} * W_f \quad (4.27)$$

Where:

- K is the comprehensive coefficient,
- m is number of insert penetrations per revolution,
- n is the number of inserts in contact with rock at the bottom,
- RPM is rotary speed [revolutions/min],
- D is bit diameter [m],
- Ψ is chip formation angle [°],
- W is weight on bit [kg],
- CCS is confined compressive strength [kPa],
- W_f is bit wear,
- a and b are model coefficients.

4.6.6. Motahhari's PDC Bit

Motahhari's (2010) model predicts ROP for PDC bits and PDMs. This model is beneficial for directional and horizontal drilling operations with PDMs since it enhances planning, and reduces the drilling time with the ROP optimization (Barros L.M.L., 2015). According to Motahhari (2010), "PDM performance/selection in the drilling planning phase will help perform a safe and cost-effective operation by preventing motor stalls and maintaining highest average ROP for the section." Motahhari's PDC bit ROP model includes the effect of mud motors and considers perfect bit cleaning. Its equation is:

$$ROP = W_f \left(\frac{G * RPM_t^{\gamma} * WOB^{\alpha}}{D_b * S}\right) \quad (4.28)$$

Where:

- G is a model coefficient;
- RPM_t is the total bit rotary speed [revolutions/min];
- WOB is the applied weight-on-bit [kg];
- D_b is the bit diameter [m];
- S is the confined rock strength [kPa];
- α and γ are ROP model exponents.

The wear function, W_f, is given by:

$$W_f = k_{wf} \left(\frac{WOB}{N_c}\right)^{\rho} \frac{1}{S^{\tau} {A_w}^{\rho+1}} \quad (4.29)$$

Where:

- k_{wf} is a wear function constant,

- ρ and τ are the wear function exponents,
- N_c is the number of cutters on the bit face
- and A_w is the wear flat area underneath a cutter (m^2).

The G coefficient is calculated from offset well data accompanying the α and γ model exponents (Motahhari, 2010).

4.7. Models Integration

The integration of the models presented in this section was done in a web application designed by Hamed Sahebi; members of the Drillbotics Team A coded each model. Simulations performed by the application are key features to show a simple drilling operation and provide accuracy.

The Web-based Well Planning Software implements a user-friendly created to target drilling engineers concerning difficult well designs. The software is built encompassing the well-control framework, covering well trajectory control, pressure & temperature control, and bit position control.

The application provides its user with a well design simulator; this simulator presents 7 modules: Well Path Panel, Hole Section, Drill String, Fluid, Geotemperature, Operation, and Result, as shown in Figure 4.2.

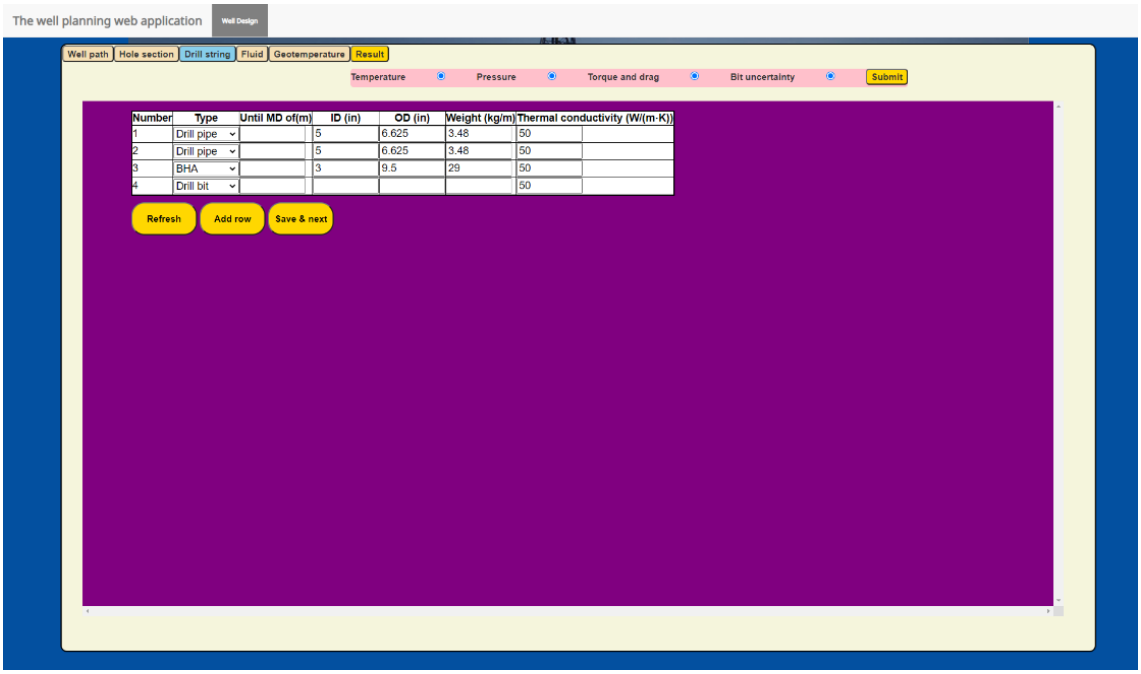

Figure 4.2: Layout of the Web-based Well Planning Simulator.

Each module has its own set of inputs that the user must implement to construct the well path; the application also provides some default values that can be changed if needed. For example, the first module is the Well Path Panel; in this module, the user must choose the type of well design dimension between 2D and 3D; once chosen, the user should specify the different parameters for the trajectory design, such as:

- Vertical length;
- North and East coordinates;
- I, A, BUR, KOP, and MD;
- The number of survey points.

Each input should be provided for the initial and final points of the well trajectory. Once the inputs have been feed, the trajectory will be calculated, and a table with the results will be provided. This table will be saved, and the user will go to the next section, the Hole module.

In this module, the user can add the sections of the well with its specific casings, diameters, and its measured depths. This data will be saved, and the page will be directed to the next section, the drill string module. In the drill string module, the user provides the system with inputs regarding the drill string, such as:

- The friction coefficient (used by the T&D model for its calculations);
- Type of string and its OD and ID;
- Measured depth;
- WOB and thermal conductivity.

Once these inputs are feed, the user may save them and go to the Fluid module next section. The fluid module requires information on the dynamic properties of the fluid, such as density, flow rate, mud temperature, specific heat capacity, among others. First, information on dynamic models is given in the web application; once calculated, the system provides a graph for fluid rheology. The next module is the geotemperature module, where the information of formation and the well layers lithology must be given.

In the final module, the operation module, the user must give the WOB and the RPM of the operation. Once all modules have been complete, the Results tab can be open, and the user may choose which parameters must be calculated, Temperature, Pressure, T&D, Bit Uncertainty. Then, the data shall be submitted, and these parameters will be calculated. The results will present 5 tabs; each grants the calculated parameters; the first one is the Trajectory tab, with values of DLS and ROP, the second tab is for Pressure, which allows the user to check the pressure profile of the well path.

The third tab is for Temperature, which provides the well, formation, and annulus temperature profile. The fourth tab is for T&D, which presents drag force tripping in/out of well, and the torque profile. The fifth and final tab is the bit uncertainty, which provides the user with the profile for bit errors.

Another function of the simulator is allowing the user to change some parameters after calculating the trajectory and comparing the differences between both trajectories and their profiles. It also provides an option to download the data in several formats. More information can be found in the video presentation made by Hamed Sahebi at the Drillbotics Youtube Channel[1], the web application can be found in the link on the footnotes.[2]

[1] https://www.youtube.com/watch?v=BhXTYXqc5Sc&t=2s
[2] https://wellplanning-api-ver12.herokuapp.com/design

5. In-House UiS Real-Time Drilling Simulator

This section will present the Real-Time Drilling Simulator developed by the Drillbotics UiS Team. Hamed Sahebi programmed the web application for this simulator. This chapter will present the models applied to it, optimizing the drilling and the models' integration.

5.1. Models

This section will go over the models applied in the Real-Time simulator. The current models are the Drill Bit model, the BHA model, the Drillstring model, and the RSS model.

5.1.1. Drill Bit Modeling

One of the models designed by the Drillbotics UiS Team is the drill bit model. The main parameters for this system are "mechanical specific energy input, drilling efficiency, and minimum specific energy equal to rock strength". The critical indexes in drilling performance with the primary role of making a proper bit selection are specific energy input, "bit-specific coefficient of sliding friction, and mechanical efficiency". The model that will be defined can analyze the effect of bit gauge, bit profile, walking tendency, and steerability (Pessier & Fear, 1992).

One of the main parameters of the MSE (Es) is defined as the measure of the required energy to depose of a unit volume of the formation:

$$(\mathrm{E_s}) = \frac{\mathrm{WOB}}{\mathrm{A_b}} + \frac{2\pi\ \mathrm{RPM\ T}}{\mathrm{A_b\ ROP}} \tag{5.1}$$

The Minimum specific energy ($\mathrm{E_{smn}}$) is equal to the compressive strength of rock (σ) and can be defined as:

$$\mathrm{EFF_m} = \frac{\mathrm{E_{smn}}}{\mathrm{E_s}} \tag{5.2}$$

The RSS model obtains the necessary torque in operation, as well as the necessary ROP. Base on specific energy, we can have a definition of depth of cutter:

$$\mathrm{DOC} = \frac{2\ \pi\ \mathrm{T}}{\mathrm{A_b\ E_s}} \tag{5.3}$$

Where:

- WOB is the weight on bit [N];
- RPM is rotations per minute [rpm];
- ROP is the penetration rate [m/s];
- $\mathrm{D_b}$ is the diameter of the bit [m];
- $\mathrm{A_b}$ is the area of bit [$\mathrm{m^2}$];
- T is the torque [Nm];
- μ is the bit-specific coefficient of sliding friction between bit and rock.

5.1.2. BHA Modeling

Directional control is one of the main problems found in directional drilling. The well path is mainly controlled by the DLS. However, considering that the dogleg severity and the index of curvature of a wellbore are defined by the turning angle of a drill direction over the length of the wellbore, a poor DLS design may cause the wellbore to deviate from its target.

In like manner, the drilling direction is influenced mainly by the direction of the drill bit and the side force applied on the drill bit. When the direction of the bit is inclined to the wellbore axis, the axis force or weight on bit will add an extra turning angle to the wellbore axis. The side force is also capable of causing an extra angle to the wellbore axis.

For the Drillbotics Team's model, the DLS is found by the RSS model, which will be explained later in this chapter. Therefore, the purpose of the BHA model is to calculate the walk angle and the walk rate. The models designed in this section try to provide the relationship between the deformation of the BHA, the side force, and the tilt angle. Therefore, the tilt angle and side force can calculate the walk angle and the walk rate. Some parameters applied in this calculation are defined below:

- Walk angle (θw): is the result movement direction of the drill bit, the angle between the axis of the wellbore and its baseline.
- Tilt angle (θt): is the inclination direction of the drill bit, the angle between the axis of the bit and the baseline.
- Push angle (θs): is the angle caused by the side cutting and can be defined by the formula below:

$$\theta s = \tan^{-1}\left(\frac{\mathrm{ROS}}{\mathrm{ROP}}\right) \tag{5.4}$$

Where ROS is the side cutting rate. The side cutting rate depicts how much formation is removed during the time of the operation and its direction from the cutting face towards the wall. As seen in Figure 5.1, the direction of the ROP is perpendicular to the side cutting rate and the bit face.

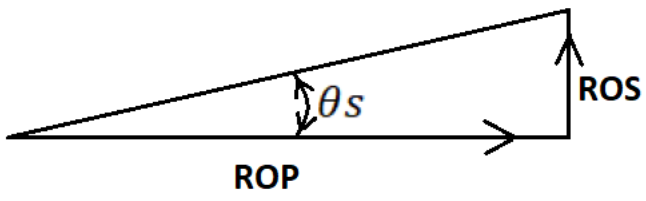

Figure 5.1: Push angle.

The tilt angle and the push angle create a deviation of the drilling direction due to their relationship between them and the walk angle, as shown in Figure 5.2.

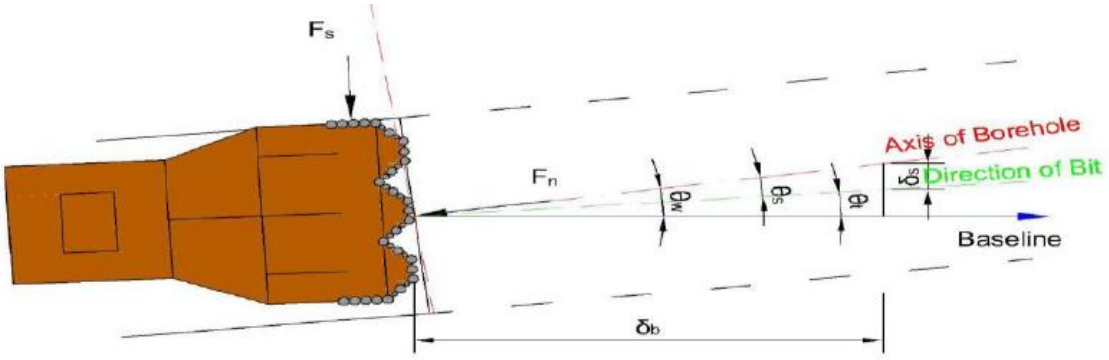

Figure 5.2: Walk angle, tilt angle, and push angle relationship.
Source: (Zhang Y., 2013).

Furthermore, the walk angle is the result of total tilt angle and push angle:

$$\theta w = \theta t + \theta s \tag{5.5}$$

The primary reason concerning the existence of the push angle is the side force. To apply this force on the bit, the BHA is deformed; when the wellbore stops the deformation of the drill string, the deformed BHA will apply a side force on the wall of the wellbore. Thus, there are two types of bit side forces the positive side force (build force) and the negative side force (pendulum force). These are shown in Figure 5.3.

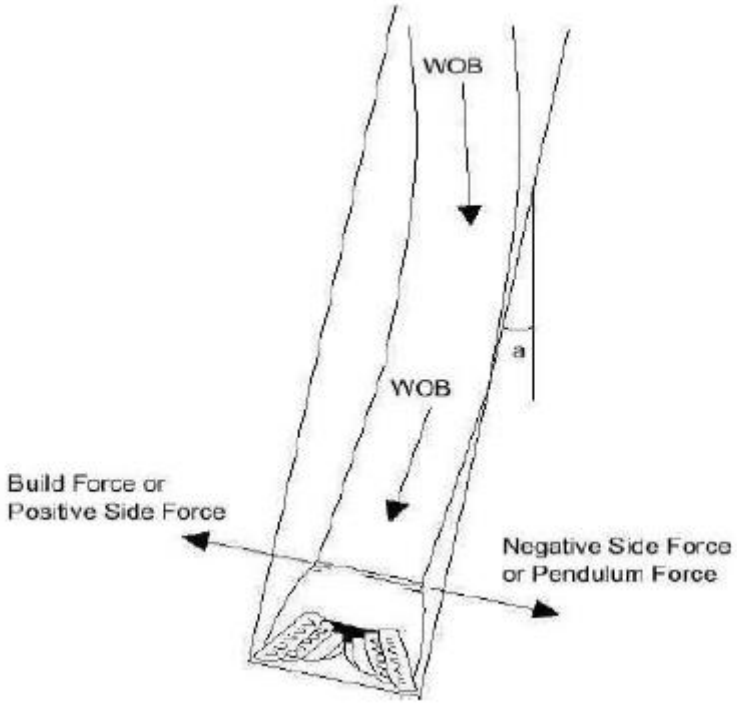

Figure 5.3: Types of bit side force.
Source: (Zhang Y., 2013).

A model for the calculation of the side cutting rate is propped by Brett et al. (1986):

$$ROS = \frac{A\,(Fs1)^2}{Sr} \qquad (5.6)$$

Where:

- ROS is the side cutting rate [ft/hr];
- Fs1 is the total side force at bit [lbf];
- Sr is the dimensionless rock strength
- A is an empirical constant equal to $5*10^{-6}$

It is imperative to mention that when applying the same side force on the bit, the cutting rate will be higher if the gauge of the bit is shorter, as shown in Figure 5.4.

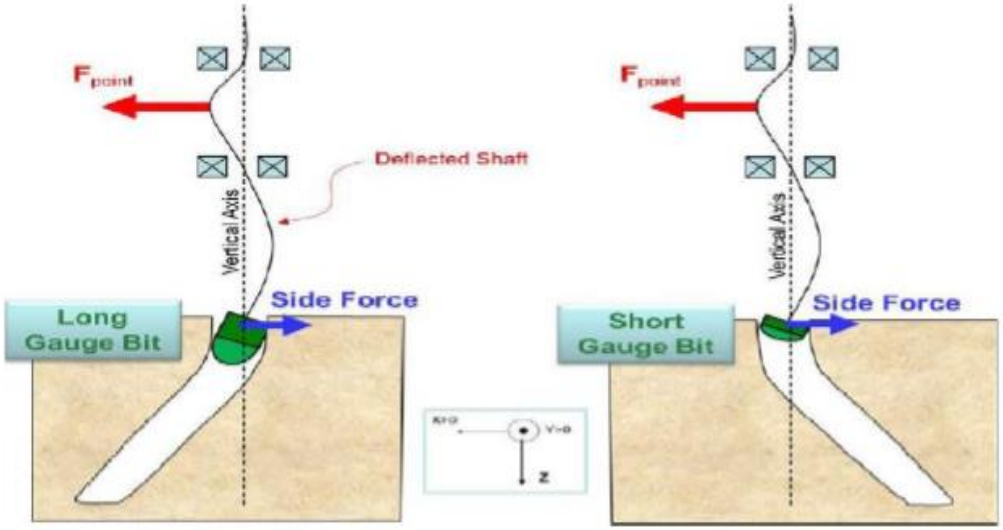

Figure 5.4: Effect of the gauge length on the cutting rate.
Source: (Ali A.M.B et al., 2017).

The rotary steerable system has two methods of drilling, push the bit and point the bit. In point the bit, there are two main driving mechanisms which include applying dynamic force from a rotating housing and applying static side force from a none rotating house, as seen in Figure 5.5.

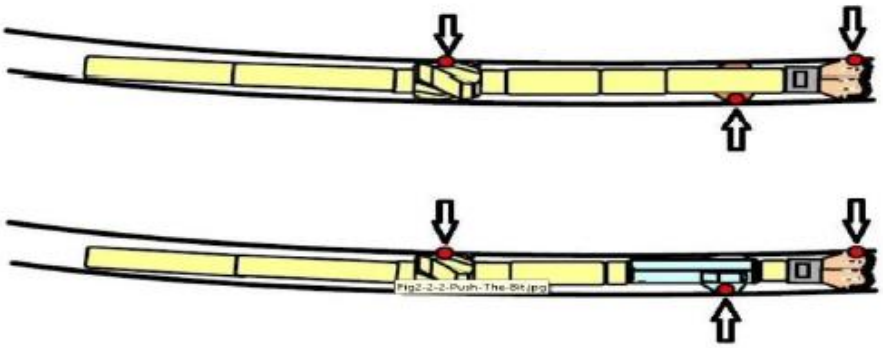

Figure 5.5: Rotating and non-rotating housing.
Source: (Ali A.M.B. et al., 2017).

To make a simplified model of the BHA regarding the side force, we consider some assumptions such as:

- No deformations in the rock (rigid body);
- Non-rotating pad and bit, pipe, and stabilizer are a rigid body;
- The effect of the BHA weight is ignored;
- The stiffness of the drill pipe beyond the BHA is not considered.

Having those in consideration, the force model of push-the-bit can be simplified to be a 3-support-continued-string model, as demonstrated in Figure 5.6.

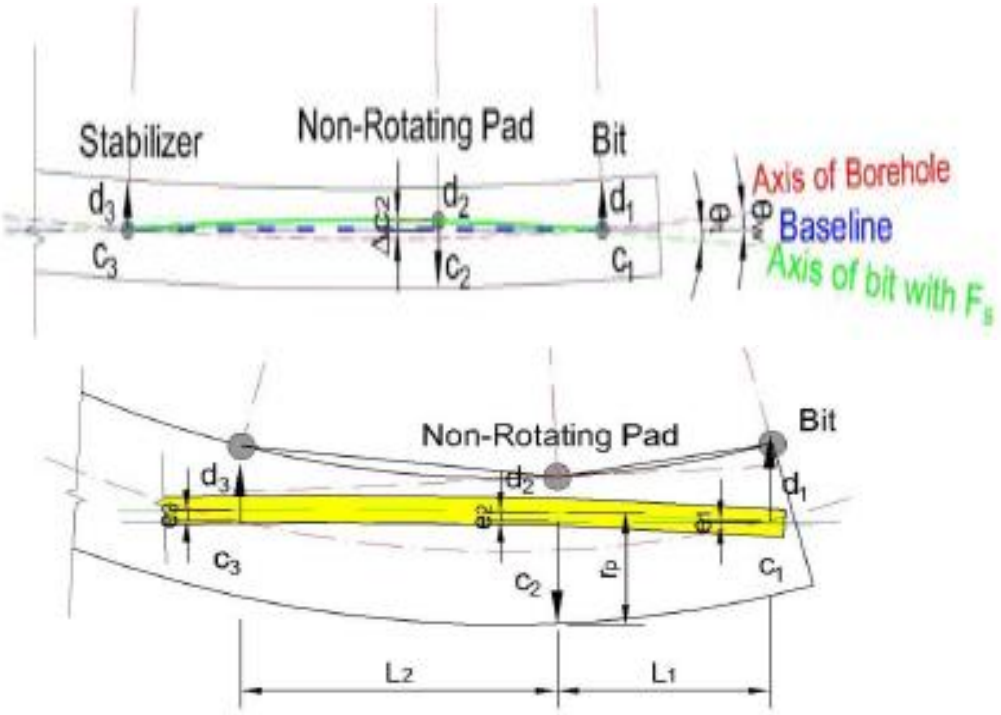

Figure 5.6: Deformation Model for Elastic BHA Push-The-Bit.
Source: (Ali A.M.B. et al., 2017).

The following equations express the position of the axis of the BHA:

$$e1 = -(rw - rb) \tag{5.7}$$

$$e2 = -(rw - rp) \tag{5.8}$$

$$e3 = -(rw - rs) \tag{5.9}$$

Where:

- rw is the radius of wellbore [ft];
- rb is the radius of drill bit [ft];
- rp is the radius of BHA [ft];
- rs is the radius of stabilizer [ft];

Combining the Equations (5.4) and (5.6), push angle (θs) and side cutting rate, the following equation is formed:

$$\theta s = \frac{A\,(Fs1)^2}{Sr\ ROP} \tag{5.10}$$

Then the tilt angle of the drilling pipe is calculated by:

$$\theta t = \frac{e1 - e3}{L1 + L2} \tag{5.11}$$

Walk angle is defined regarding θs and θt:

$$\theta w = \theta s + \theta t = \frac{A\,(Fs1)^2}{Sr\ ROP} + \frac{e1 - e3}{L1 + L2} \tag{5.12}$$

Apart from the walk angle, the walk force and the walk rate are important parameters to be found. The walk angle can be used to define the bit walk tendency. Once the walk force, Fw, is calculated from Chen's (2007) model seen in Figure 5.7 and the walk rate is calculated from the equation below:

$$\text{Walk rate} = DLS * \frac{Fw}{Fs} \tag{5.13}$$

Where:

- DLS is dogleg severity [°/30m];
- Fw is the walk force [N];
- Fs is the side force [N];

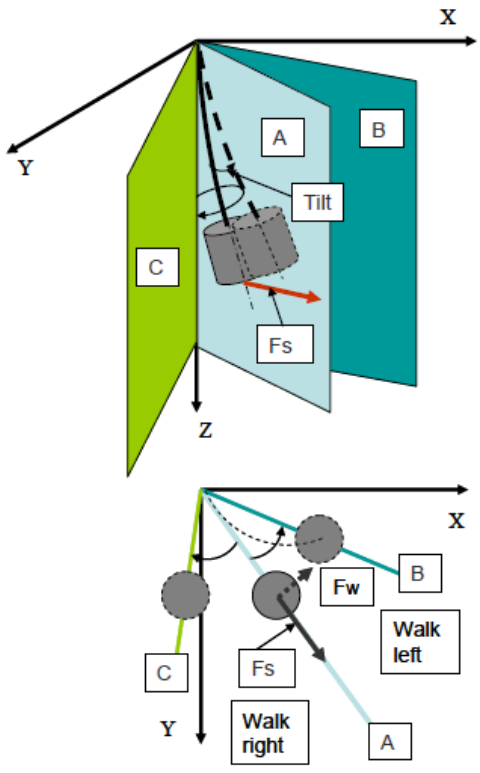

Figure 5.7: Steer forces and walk force of a bit in directional drilling.
Source: (Chen et al., 2007).

From Figure 5.7, it is possible to conclude that:

$$Fw = \tan \theta w * Fs \quad (5.14)$$

5.1.3. Drill String Modeling

The drill string model is mainly used to calculate buckling conditions. Drilling ahead in a simulation will not be allowed if the drill string is buckling at any point along the drill string. This model must simulate the torsional oscillations, like stick-slip; it should be made of multiple torsional spring elements and have friction damping from wellbore contact.

Stick-slip tends to occur in different bit behaviors when combined with different rocks and WOB/RPM settings. Therefore, the control system for the top drive must counteract the stick-slip when it appears and model the lateral vibrations of the drill string or BHA if necessary.

Drilling operations are often impeded by excessive downhole friction, which causes high T&D and axial, torsional, and lateral drill string vibrations. Drill string dynamics can be fully described by six DOFs per node: axial and lateral translation, bending in two planes, and angular rotation around the longitudinal axis.

The drill string exhibits severe stick-slip vibration induced by the contact between the drill bit and the formation and usually appears as periodic alternations of stick and slip phases; the transition between static and kinetic energy creates these phases. The stick phase initiates when friction between drill string/bit and rock exceeds the torque provided by the top drive, causing the top of the drill string to continue rotating, storing potential torsional energy within the string. The stored energy becomes higher than the friction torque, and BHA/drill bit rotates several times faster than at the surface. The period of oscillations is determined by BHA and drill string weights and somewhat by rotational velocity.

At the surface, stick-slip is observed by periodic oscillations in RPM. A combination of deep deviated well and hard formation increases the risk of stick-slip occurrences. At the same time, the high downhole rotational velocity of the slip phase can cause strong axial and lateral vibrations. In the worst case, bit bouncing and axial vibrations typically occur in a hard rock environment when the dominant frequency of external forces corresponds to the natural frequency of drill string; this condition is called resonance. Such vibrations result in impaired drill bit cutters and other drill bit elements and typically happen in vertical wells.

The main focus of the designed model by Rishyank C. (2021) for the Drillbotics 2021 Competition is the investigation of combined axial and torsional drill string motion for directional drilling with 4 DOFs. The evaluated parameters include downhole axial and rotational velocities, downhole WOB, and downhole TOB.

An important model used as a base for developing the drill string dynamics model was presented by Ren & Wang et al. (2017); it uses two DOF lumped parameter models to study the coupling between stick-slip and bit-bounce through bit-rock interaction. It is assumed that WOB varies sinusoidal with drill bit rotation and depends on rock stiffness constant. The

Heaviside function was used in frictional torque calculation to discriminate between sticking and slipping phases.

The resulting torque on bit was expressed the following way:

$$T_b = \left[\frac{a^2 \varepsilon d}{2} H(\varphi) + \frac{\mu \gamma a \omega_f}{2} \text{sign}(\varphi) H(\dot{x})\right] H(d) \tag{5.15}$$

Where:

- a is bit radius [m];
- ε is the intrinsic specific energy of rock [J.cm^{-3}];
- ω_f is normal contact force [N],
- g is a bit parameter,
- γ is a bit-rock interaction parameter,
- H is the Heaviside function.

It was concluded that to reduce stick-slip and bit-bounce, both WOB and angular velocity must be increased. It was also determined that as drill string length increases, the frequency of stick-slip vibrations reduces.

The main features for developing a two-dimensional 4 DOFs axial-torsional vibrations model in directional drilling developed by Rishyank C. (2021). The model combines mathematical models (models for axial, torsional, traverse, and bending motion of drill string and a friction model) with appropriate boundary conditions adapted for dynamic drill string position. A numerical procedure is based on the finite element method. A parameter to evaluate the presence and intensity of stick-slip is stick-slip severity, which was defined by Wiktorski et al. (2020) and is presented below:

$$SS = \frac{\bar{\dot{\theta}}\_max - \bar{\dot{\theta}}\_min}{2\dot{\theta}_s} \tag{5.16}$$

Where:

- $\bar{\dot{\theta}}$ is peaks average of downhole rotational velocity;
- $\bar{\dot{\theta}}_s$ is average surface rotational velocity.

When this parameter is below 0.5, the system is considered stable; when it exceeds 1 - stick-slip occurs; when it is between these two values, the system is considered unstable.

The method chosen by Rishyank C. (2021) is finite element modeling; this method is based on the discretization of a structure into elements; the approximation of unknown variables is used to transform partial differential equations towards a system of algebraic equations that are solved simultaneously by applying numerical methods.

This method can be understood by analyzing the drill string element presented in Figure 5.8, which has two nodes at its ends, Δθ, and ΔθX are respectively, relative torsional displacement and relative axial displacement. The problem presented below has a dynamic nature; that

involves variation in time, meaning a second-order ODE represents the EOM. Note that the Z-axis is represented with x, and X-axis is represented in y for easy interpretation.

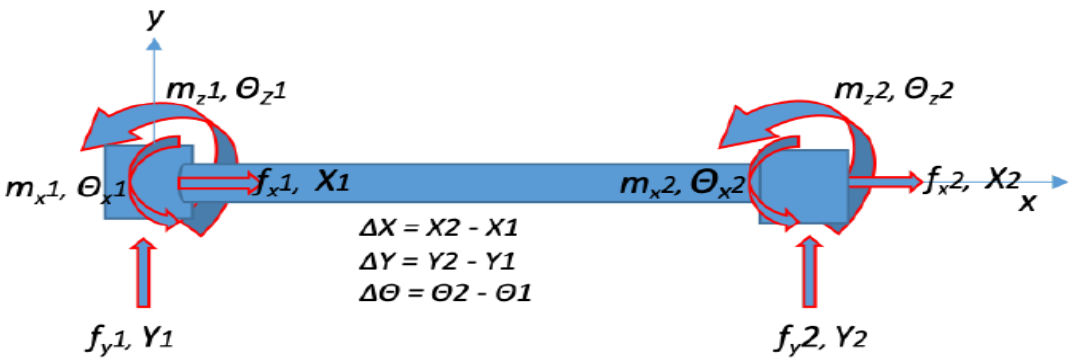

Figure 5.8: 4-DOF System: Axial and Lateral Translation, Axial Rotation and Bending in Plane.

Equation (5.17) demonstrates the calculation of forces in this drill string:

$$M\ddot{U}(t) + C\dot{U}(t) + KU(t) = F_{ext}(t) + F_g \tag{5.17}$$

Where:

- M is mass matrix;
- C is damping matrix;
- K is stiffness matrix;
- F_{ext} is sum of all external forces;
- U is vector matrix of displacements;
- $\dot{U}$ is vector matrix of velocities;
- $\ddot{U}$ is vector matrix of accelerations.

This model considers that f_{x1} and f_{x2} are axial displacements f_{y1} and f_{y2} lateral displacements θ_{x1} and θ_{x2} are torsional moments θ_{y1} and θ_{y2} are bending moments.

“Mass matrix is related to the concept of center of mass. Generally, lumped mass assumes that all mass is concentrated at the center of one rigid object. This means only the center of the object has mass while other parts of the object are massless. To achieve a more accurate analysis, we must equally distribute the mass to different parts of the object” (Lei et al., 2014). The equations for a beam element consist of the contribution of translation and rotation by applying the following to the matrix layout.

$$a = \rho \frac{I_z}{l} \tag{5.18}$$

$$b = \frac{\rho A l}{420} \tag{5.19}$$

$$I_z = \frac{\pi(d_0^4 - d_i^4)}{32} \tag{5.20}$$

$$M = \begin{bmatrix} 160a & 0 & 0 & 0 & 80a & 0 & 0 & 0 \\ 0 & \frac{6}{5}a + 156b & 0 & a\frac{l}{10} + 22lb & 0 & -\frac{6}{5}a + 54b & 0 & a\frac{l}{10} - 13lb \\ 0 & 0 & \frac{J}{3A} & 0 & 0 & 0 & \frac{J}{6A} & 0 \\ 0 & a\frac{l}{10} + 22lb & 0 & 2l^2a + 4l^2b & 0 & a\frac{l}{10} + 13lb & 0 & -l^2\frac{a}{30} - 3l^2b \\ 80a & 0 & 0 & 0 & 160a & 0 & 0 & 0 \\ 0 & -\frac{6}{5}a + 54b & 0 & -a\frac{l}{10} + 13lb & 0 & \frac{6}{5}a + 156b & 0 & -a\frac{l}{10} - 22lb \\ 0 & 0 & \frac{J}{6A} & 0 & 0 & 0 & \frac{J}{3A} & 0 \\ 0 & a\frac{l}{10} - 13lb & 0 & -\frac{l^2}{30}a - 3l^2b & 0 & -a\frac{l}{10} + 22lb & 0 & 2\frac{l^2}{15}a + 4l^2 \end{bmatrix} \quad (5.21)$$

Where:

- ρ is the density [kg/m^3];
- I_z is the radial moment of inertia;
- J_z is the mass moment of inertia;
- A is the cross-sectional area [m^2]
- d_o is the outer diameter of pipe [m];
- d_i is the inner diameter of pipe [m];
- l is the length of element.

For the finite element method of the numerical solution of an elliptic partial differential equation, the system linear equations that ought to be solved to accomplish an approximation to the differential equation that is represented by the stiffness matrix. Generally, it defines the geometric and material properties of the element in the system. Therefore, the stiffness matrix is a central part of FEM (Lei et al., 2014).

$$K = \begin{bmatrix} k_1 & 0 & 0 & 0 & -k_1 & 0 & 0 & 0 \\ 0 & k_2 & 0 & \frac{1}{2k_2l} & 0 & -k_2 & 0 & \frac{1}{2k_2l} \\ 0 & 0 & k_3 & 0 & 0 & 0 & -k_3 & 0 \\ 0 & \frac{1}{2k_2l} & 0 & \frac{1}{3k_2l^2} & 0 & -\frac{1}{2k_2l} & 0 & \frac{1}{6k_2l} \\ -k_1 & 0 & 0 & 0 & k_1 & 0 & 0 & 0 \\ 0 & -k_2 & 0 & -\frac{1}{2k_2l} & 0 & k_2 & 0 & -\frac{1}{2k_2l} \\ 0 & 0 & -k_3 & 0 & 0 & 0 & k_3 & 0 \\ 0 & \frac{1}{2k_2l} & 0 & \frac{1}{6k_2l} & 0 & -\frac{1}{2k_2l} & 0 & \frac{1}{2k_2l^2} \end{bmatrix} \quad (5.22)$$

$$k_1 = \frac{EA}{l} \quad (5.23)$$

$$k_2 = \frac{EI_z}{l^2} \quad (5.24)$$

$$k_3 = \frac{GJ}{l} \quad (5.25)$$

Where:

- E is Young's modulus [N/m^2];
- G is the shear modulus [N/m^2].

The characterization of damping is important in accurately predicting the true response and the frequency response of any apparatus or arrangement dominated by energy dissipation. "The process of modeling damping matrixes and experimental verification is challenging because damping cannot be determined via static tests in the same way as mass and stiffness. Furthermore, damping is more difficult to determine from dynamic measurements than natural frequency" (Lei et al., 2014).

$$[C_D] = \alpha[M] + \beta[K] \tag{5.26}$$

The equation above presents two coefficients, α, and β, that represent the weighting parameters that permit the system damping to be accustom. Admitting that the gravity is uniformly distributed on the beam element, the equivalent force is used on both nodes of one element to substitute the distributed gravity during the simulation (Lei et al., 2014).

$$F_g = [\frac{w}{2} \quad \frac{w}{2} \quad 0 \quad \frac{wl^2}{12} \quad \frac{w}{2} \quad \frac{w}{2} \quad 0 \quad -\frac{wl^2}{12}]^T \tag{5.27}$$

The external force is:

$$F_{ext} = [0 \quad 0 \quad 0 \quad 0 \quad -WOB \quad 0 \quad -TOB \quad 0]^T \tag{5.28}$$

Where:

- WOB is weight on bit [kg];
- TOB is torque on bit [N m].

The model is then applied with necessary boundary conditions. Many methods aim to analyze dynamic vibration equations, and the one chosen by the Team uses a central difference method as a solution method.

Solving for displacements using the central difference method acceleration and velocity is computed by differentiating the displacement with first-order and second-order time derivatives. With this, stick-slip is calculated using Equation (5.16) and defining a range of input parameters within a physical limit. Based on these values, we will determine the setpoints for the input parameters in the chosen model.

Furthermore, based on the stick-slip values, a regression function is formed to predict the value of stick-slip for given input parameters. Finally, a suitable control algorithm is made to find the best set points to mitigate the stick-slip values stick-slip based on the threshold setting.

5.1.4. RSS Modeling

The original RSS model for the Drillbotics UiS Team was developed by Saramago (2020) to simulate the movement and positioning of the bit while drilling. The model derives the forces on the bit caused by WOB and bending of the RSS system; with these forces, the model

decomposes the traditional ROP definition into 2 or 3 ROPs values, analogous to 2D or 3D modeling (Saramago, 2020).

The process of calculation of the RSS 2D/3D model is presented by functions or operations used for foretelling the bit position and the tool's displacement, expressed through TVD, HD, DLS, and I, which are the main output parameters for the development of a 2D/3D directional drilling.

This new model was designed by Saavedra L.A.J. (2021) for the Drillbotics 2021 Competition and is described in full in his MSc Thesis.

The first step in the RSS modeling is to present the well plan design with the data needed (see Appendix B.5) for starting the simulation or calculation. Apart from that data, one more parameter must be given, the target inclination; this is the main parameter to monitor in the next process.

In the next step, the offset controller maneuvers the bit towards the target inclination using some conditional statements. These allow increasing the offset if the bit has yet to reach the target inclination or inverting the offset if the bit has overpassed the target inclination. Finally, when the target inclination is reached, the offset is reduced to 0.

Afterward, the geometry function calculates the natural displacement (H_{normal}) created by the formation. In order to achieve H some coordinates are required; these come from the HD and the TVD of the bit, actuator, and stabilizer; thus, being possible to generate two straight-line equations that can be used to determine the distance between ends.

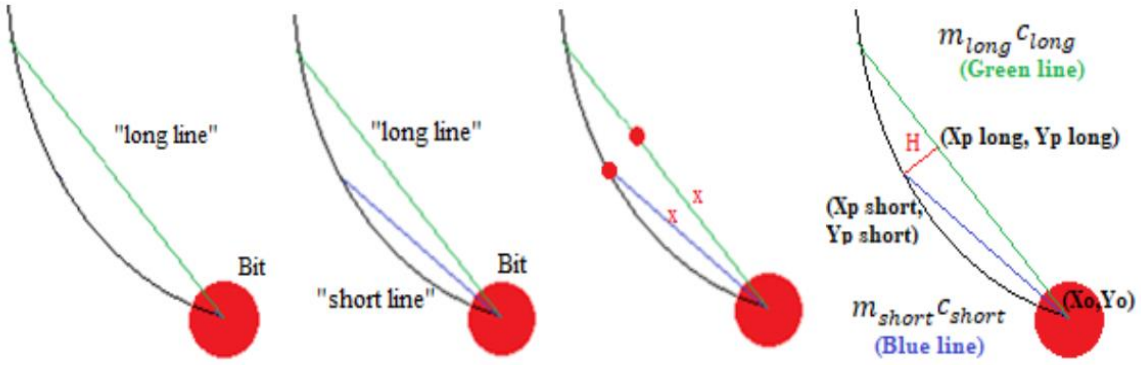

Figure 5.9: Natural Displacement (H) Calculation Process.
Source:(Saramago, 2020).

In Figure 5.9, the "short line" represents the linear distance between the actuator and the bit, while the "long line" is the linear distance between the bit and the stabilizer. A new coordinate is created by superposing the length of the "short line" with the "long line," these coordinates are (Xp_{long}, Yp_{long}). The natural displacement (H_{normal}), is then defined as the distance between the coordinate of the actuator (Xp_{short}, Yp_{short}) and the new coordinate.

The determined offset and the natural displacement calculated must be converted to force magnitude using the beam bending model scenario. The distance from the bit to the actuator is defined as 0.5 m, and the distance from the actuator to the upper stabilizer is defined as 2.7 m.

The model's next step is to execute the ROP axial process; this process is in function of some parameters that shall be explained later. Finally, the ROP normal process is also executed along with the axial process. First, however, the normal process considers the value obtained from the bit force process; this can be seen in the following equations (Saramago, 2020):

$$\mathrm{ROP_{axial}} = \frac{13.33 \cdot \mu \cdot \mathrm{N}}{\mathrm{D} \cdot \left(\frac{\mathrm{Es}}{\mathrm{WOB}} - \frac{1}{\mathrm{A_b}}\right)} \tag{5.29}$$

$$\mathrm{ROP_{normal}} = \frac{13.33 \cdot \mu \cdot \mathrm{N}}{\mathrm{D} \cdot \left(\frac{\mathrm{Es}}{\mathrm{F_{bit}}} \pm \frac{1}{\mathrm{A_b}}\right)} \cdot \alpha \tag{5.30}$$

Teale proposes Equation (5.42) in 1965, where the dependency on the rock mechanisms is represented in the value of the rock energy (Teale, 1965). Nevertheless, Saramago (2020) adapted this equation by transforming the WOB to $\mathrm{F_{bit}}$ and decomposing the common ROP into axial and normal. Both ROPs are used in the following equations; these are adopted to simulate the position of the bit and inclination after a determined delta time (Δt) (Saramago, 2020):

$$\mathrm{Inc_{(t)}} = \mathrm{Inc_{(t-1)}} + \tan^{-1}\left(\frac{\mathrm{ROP_{norm(t)}}}{\mathrm{ROP_{axial(t)}}}\right) \cdot \frac{\Delta t}{3600} \tag{5.31}$$

$$\mathrm{MD_{(t)}} = \mathrm{MD_{(t-1)}} + \sqrt{\mathrm{ROP_{norm(t)}}^2 + \mathrm{ROP_{axial(t)}}^2} \cdot \frac{\Delta t}{3600} \tag{5.32}$$

$$\mathrm{TVD_{(t)}} = \mathrm{TVD_{(t-1)}} + \cos\left(\mathrm{Inc_{(t)}}\right) \cdot \sqrt{\mathrm{ROP_{norm(t)}}^2 + \mathrm{ROP_{axial(t)}}^2} \cdot \frac{\Delta t}{3600} \tag{5.33}$$

$$\mathrm{HD_{(t)}} = \mathrm{HD_{(t-1)}} + \sin\left(\mathrm{Inc_{(t)}}\right) \cdot \sqrt{\mathrm{ROP_{norm(t)}}^2 + \mathrm{ROP_{axial(t)}}^2} \cdot \frac{\Delta t}{3600} \tag{5.34}$$

$$\mathrm{DLS} = \frac{\left(\mathrm{Inc_{(t)}} - \mathrm{Inc_{(t-1)}}\right) \cdot 180}{\left(\mathrm{MD_{(t)}} - \mathrm{MD_{(t-1)}}\right) \cdot \pi} \cdot 100 \tag{5.35}$$

The reaction force on the bit ($\mathrm{F_{bit}}$) is the force that the bit feels acting against its surface. For instance, if the actuator applies a force in some direction, as seen in Figure 5.10, it will generate a reaction force that will push the bit against the opposite formation face. Thus, contact with the bit will implement a force composed of the force due to the horizontal displacement and the force due to the offset displacement.

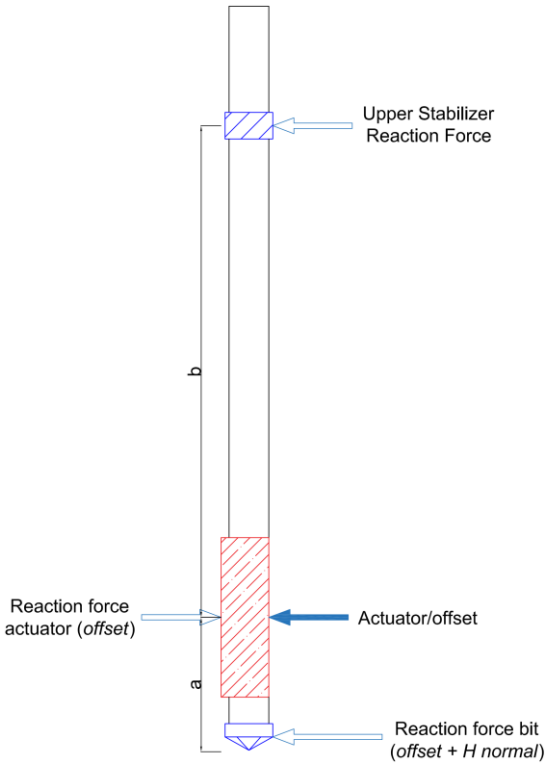

Figure 5.10: Acting Forces on the RSS.
Source: (Saavedra L.A.J., 2021).

All the procedure showed before is implemented in a Python coded simulator, that allows iterating thousands of times. Consequently, the algorithm of the current simulator is expressed through the flowchart shown in Figure 5.11, which has two groups: the group in red represents the main algorithm function. In contrast, the group in purple represents the simulations. Where the PWP represents the Planned Well Path and CP is the Correction Path.

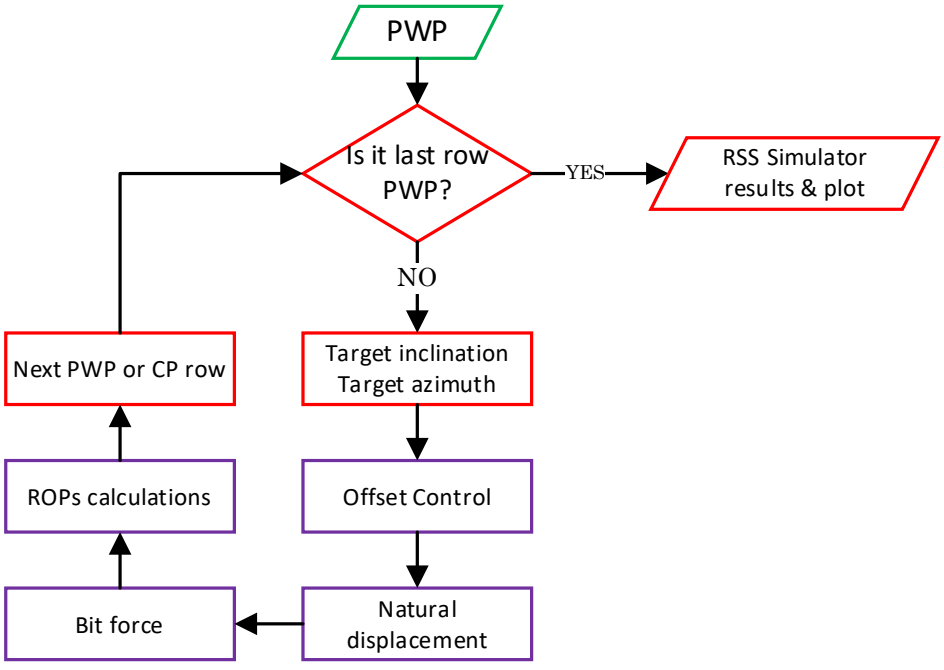

Figure 5.11: Simple flowchart of the RSS model simulator.
Source: (Saavedra L.A.J, 2021).

The principle for the RSS 3D model has an extra dimension represented by the azimuth prediction. As a result, some small differences can be seen in the simulation. The operations remain the same as discussed before, except one more input data is required, the target azimuth. Moreover, there are two returns for the functions of the 3D offset controller, the geometry function and bit force.

5.2. Drilling Optimization and Real-Time Control

According to the Drillbotics® 2021 Guidelines, it is needed to optimize setpoint commands for drilling parameters such as WOB, RPM, and so on, such that drilling performance and steering are optimized. Such real-time optimization should be done automatically. This chapter will discuss some parameters for drilling optimization, such as the optimization of the ROP/MSE, the safety windows, and the trajectory control.

5.2.1. ROP/MSE Optimization

The maximum ROP technic is one of the most popular techniques to reduce drilling costs; this technic is affected by several parameters, such as hole cleaning and WOB. In addition, ROP optimization in a real-time simulator is affected by dynamic and static parameters. Te dynamic parameters, such as WOB, RPM, flow rate, and so forth, can be controllable or uncontrollable depending if the driller can alter these manually during operations or not. On the other hand, static parameters include fixed properties such as compressive strength and drilling mud density.

The word optimization is defined as the maximum or minimum value in a real function. Ruiz R. (2021) chose a differential evolution algorithm to find the maximum ROP for each machine learning model implemented for this simulator. This algorithm is established on Darwin's theory of natural selection, where the fittest individual survives.

The ML model serves as a cost function based on the cost value; in this case, the ROP values, the best members of this population are selected. The fittest member generates the new individuals with better cost values for each generation, known as the evolution process. For this purpose, the Python SciPy library contains simple algorithms used to modify certain parameters. Since the algorithms calculate the minimum values, it must be modified to detect the maximum ROP and its respective WOB, RPM, and flow rate values given its boundaries. It is important to recall that the boundaries are set up with no specific requirements in the first instance. Optimization is strongly linked to modeling since a good ROP prediction will optimize other parameters.

MSE is a parameter to measure efficiency in drilling, and it is defined as the energy required by a drill bit to dislocate a unit of volume of rocks. Thus, the concept indicates how effective the process will be. For example, if the rock is crushed into smaller fragments than necessary, this leads to extra energy usage. In contrast, with the rock fragments being too big, this will also lead to extra energy usage, making necessary the breakage of these fragments into smaller pieces (Khadisov et al., 2020).

The equations for MSE are displayed below:

$$\mathrm{MSE} = \frac{\text{Total Energy Input}}{\text{Volume Removed}} \tag{5.36}$$

The above equation can remodel to a more functional equation as:

$$\mathrm{MSE} = \frac{\text{Vol Energy Input}}{\text{Vol Removed}} + \frac{\text{Rotational Energy Input}}{\text{Vol Removed}} \tag{5.37}$$

or

$$\mathrm{MSE} = \frac{\mathrm{WOB}}{\mathrm{Area}} + \frac{2\pi * \mathrm{RPM} * \mathrm{T}}{\mathrm{Area} * \mathrm{ROP}} \tag{5.38}$$

Where:

- WOB is weight on bit [kg];
- Area is the area of the drill string [m²];
- RPM is the drill string rotation [revoltutions/min];
- ROP is the rate of penetration [m²/30m];
- T is the torque [N].

In order to achieve optimal drilling efficiency, the main objective is to minimize the MSE or maximize the ROP. The MSE minimization can be performed by adjusting the set-points for the WOB, the RPM, and the ROP, being aware of other factors, such as wellbore stability, drilling safety, and cutting transport (Khadisov et al., 2020).

Furthermore, more optimization algorithms could be implemented and show better accuracy than the evolutionary algorithm. Boundaries for this model must be more realistic, and models like cutting transports or the bit model must be used to adjust these constraints.

Another method for MSE optimization is the HMSE method, which considers the amount of energy used for drilling one unit of length. This concept takes into account the effect of hydraulic power and is expressed by the following equations:

$$\mathrm{HMSE} = \frac{\mathrm{W_{hyd}} + \mathrm{W_{axi}} + \mathrm{W_{rot}}}{\text{Volume of rock removed}} \tag{5.39}$$

$$\mathrm{HMSE} = \frac{\mathrm{WOB_e}}{\mathrm{A_b}} + \frac{120\pi\mathrm{NT} + \mathrm{C_\eta}\Delta\mathrm{P_b}\mathrm{Q}}{\mathrm{A_b} * \mathrm{ROP}} \tag{5.40}$$

Where:

- $\mathrm{W_{hyd}}$, $\mathrm{W_{axi}}$, $\mathrm{W_{rot}}$ are the hydraulic, axial, and rotational power [kW];
- N is rpm [l/s];
- $\Delta\mathrm{P_b}$ is the pressure loss across the bit [Pa];
- T is torque on bit [N.m];
- $\mathrm{A_b}$ hole section area [m²].

5.2.2. Safe Operation Window

In order to perform a safe drilling operation, some parameters must be kept in the same operational window to prevent accidents such as kicks, blowouts, and well collapse. Some of these parameters are the buckling limit, the maximum torque, and the control of the limits of the ROP-related parameters.

a) Buckling Limit

For the buckling limit, the parameters of slenderness is of critical importance. This parameter is defined as the tendency of the drill pipe to buckle; if it is greater than the critical ratio, it is empirically found that Euler's Critical Load formula shown in Equation (5.41) is applicable.

$$\text{slenderness} = \frac{l}{k} \tag{5.41}$$

Where:

- l is the length of drill pipe [m];
- k is the gyradius.

Furthermore, the gyradius k, is defined by:

$$k = \sqrt{\frac{I}{A}} \tag{5.42}$$

Where:

- I is the minimum moment area of the cross-section [m²];
- A is the cross-sectional area calculated with the following equations respectively [m²]:

$$I = \frac{\pi}{64}(OD^4 - ID^4) \tag{5.43}$$

$$I = \frac{\pi}{4}(OD^2 - ID^2) \tag{5.44}$$

Where:

- OD is the outer diameter [m];
- ID is the inner diameter [m].

The critical slenderness ratio is presented below:

$$\frac{1}{k} = \sqrt{\frac{2 \cdot \pi^2 \cdot E}{\sigma_y}} \tag{5.45}$$

Where:

- E is the modulus of elasticity [MPa];
- σ_y is the tensile yield strength [MPa].

The buckling of a drill pipe is the key limiting factor in selecting a maximum WOB. Buckling happens when a structure is exposed to compressive stress and starts to deflect sideways. This deflection causes the drill pipe to wear due to abrasion on the wellbore wall. On the other hand, if the deflection is too great, the drill pipe will start to deform plastically and ultimately lose its load-bearing capacity. For preventing the buckling effect, it is crucial to know the strength of the drill pipe by using Euler's Critical Load equation given below:

$$F_{cr} = \frac{\pi^2 \cdot E \cdot I}{(K \cdot L)^2} \tag{5.46}$$

Where:

- K is column effective length factor;
- L is unsupported length of the column [m];
- F_{cr} is the critical load [N].

b) Maximum Torque

The torsional vibrations are typically represented as stick-slips for the maximum torque limit, meaning the drill bit stops rotating and the drill string accelerates and decelerates periodically. It is vital, for this purpose, to know how much torque the drill pipe can endure to prevent it from failure. The maximum torque can, therefore, be calculated using the equation below:

$$T = \tau * \frac{J}{\rho_r} \tag{5.47}$$

Where:

- T is the torque [N.m];
- τ is the shear stress [Pa];
- J is the polar moment of inertia [m^4];
- ρ_r is the radial distance until the center of the pipe [m].

From Equation (5.57), the maximum torque is calculated as:

$$T_{max} = \frac{\pi}{16} \cdot \frac{(OD^4 - ID^4)}{OD} \tag{5.48}$$

Where:

- τ_{max} is the maximum shear stress [Pa].

The shear strength is dependent on the type of material used to construct the drill pipe. In order to achieve safe drilling, one must know the shear yield strength τ_y. By using the Euler-Mascheroni constant of 0.577, one can convert tensile yield strength, σ_y to the shear yield strength, τ_y, as shown in the equation below:

$$\tau_y = 0.577 * \sigma_y \tag{5.49}$$

The maximum torque before the drill pipe yields is calculated as:

$$T_y = \tau_y \cdot \frac{\pi}{16} \cdot \frac{(OD^4 - ID^4)}{OD} \tag{5.50}$$

Where:

- OD is outer diameter [m];
- ID is inner diameter [m];
- τ_y is shear yield strength [N.m^{-2}];
- T_y is the maximum torque [N.m].

c) ROP Control

Drilling operations are usually associated with severe vibrations from the drill string, which leads to an onerous and inefficient process. To avoid or diminish the impact of vibrations on the operational conditions, it is essential to perform a deep investigation that allows a proper understanding of the system dynamics. From Equation (5.16), the stick-slip severity is calculated from the drill string model for input variables such as WOB and RPM.

By constraining the maximum WOB, Torque is applied on drill string as shown in Equations (5.46) and (5.50), and the maximum limit to the RPM is constrained by Equation (5.16). With these boundary limits, a safe drilling operation can establish which parameter can mitigate the vibrations and ensure safe working limits for the drill pipe; these limit boundaries can be plotted by regression models as presented in Figure 5.12.

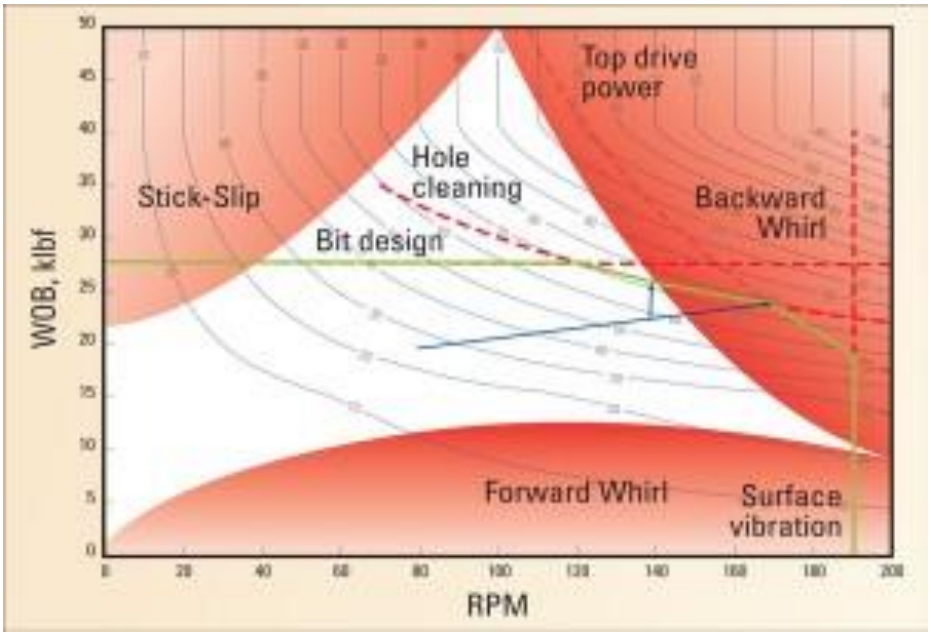

Figure 5.12: Safe Working Limits for WOB and RPM.
Source: (Hsieh, 2011).

5.2.3. Trajectory Control

The control of trajectory in its initial phase is given by modifying the direction of the inclination and the azimuth; these can be modified through the change in the percentage of the opening of the actuator or offset of the RSS tool in a certain direction.

As a result, the trajectory control is based on the full or partial opening of the offset if specific conditions are met. For the 2D RSS model, the offset can be expressed when the difference between the target inclination and the current inclination is less than 0.65 radians. A positive sign means build-up rate, and the negative sign means a decrease of well deviation angle (Saramago, 2020).

For this purpose, there is a precondition to working with a planned well trajectory (or ideal well path) that compares the target inclination from the planned trajectory and the current inclination calculated from the last result of the RSS simulation.

For example, in Figure 5.13, there are two lines: the black line representing the planned trajectory and the blue-dash line representing the simulated well trajectory. The blue line at some point deviates from the black line. When the simulator detects that this deviation is more than the 0.65 radians between the planned and the current inclination, it opens the offset 100% in the opposite direction to reduce the difference. Once the difference is less than 0.65 radians, the offset is reduced gradually until the current inclination is near the planned inclination when the offset is closed completely.

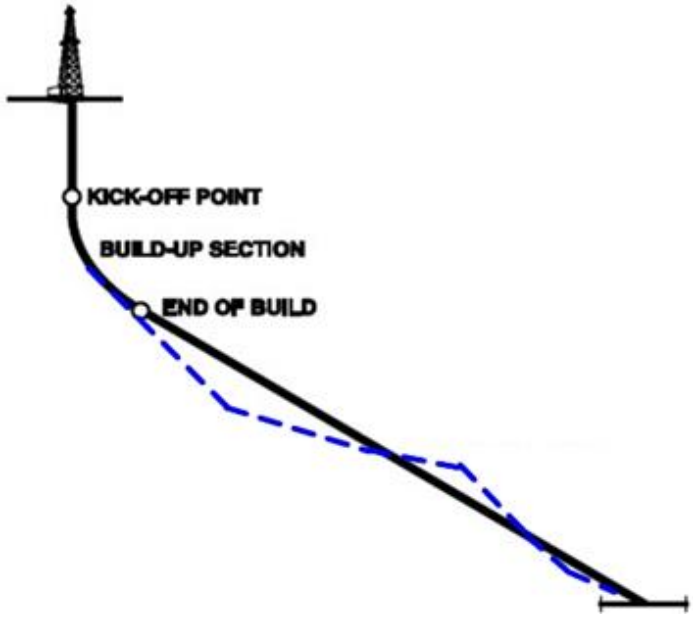

Figure 5.13: Trajectory Control of the RSS 2D Model.

For the 3D case, there is still some work to do, but in this case, the deviation now has two dimensions, one for the azimuth and the other for the inclination. Therefore, the Deviation Control is based on a resultant offset from both dimensions.

5.3. Model Coupled and Interacted in Simulator

Every parameter in automated drilling is dependent on other variables. Hence, the models should be coupled in order to ensure the proper working of the simulator. The bit selection first and foremost important factor, which is later in other sections. The selection of the bit is influenced by WOB and RPM as inputs and provides the required diameter of the drill bit.

For torque and drag analysis, the inputs of WOB and RPM ensure the drill string will withstand buckling and vibration to ensure proper drilling. The trajectory plan is set by using the inclination angle and the azimuth. When drilling starts, the BHA inclination is updated so that RSS Simulator can follow the designed trajectory path.

The ROP shall be considered by WOB, RPM, buckling, and an optimized ROP used in the simulator. The ROP shall be input for the cutting transport equation to maintain the required flow density, and this density will be the input to the bottom hole pressure calculation to ensure proper pressure.

An example of a coupled and interreacted model can be seen in Figure 5.14. This figure shows how a vertical section of a drilling model can be generated. In this example, we have a rig model, and the main controller is the driller. The controller gives the global inputs such as ROP and RPM to the RSS simulator and checks the results of inclination and azimuth calculated; if these are not comparable to the originally wanted trajectory, they are sent to the trajectory optimization model. Finally, a new target and offset are generated and sent to the RSS simulator with the fixed values of input given by the controller.

If the values are compatible, we send them to the hydraulics/cuttings transport model, combining with some input values from the controller and the outputs from the RSS model; this model will calculate the values pressure and minimum flow velocity. On the other hand, if those parameters are not satisfactory, the controller chose new input values for the RSS model until we get a fair value of pressure and minimum flow velocity.

From the hydraulics/cuttings model, the parameters of RPM and inclination are achieved and send to the drill string design system, which includes models such as T&D, bit model, BHA model, stick-slip, among others. Each one will receive inputs from the drill string design system and the controller. For instance, the T&D model will receive the inclination, RPM, and azimuth information, and the values of the model's calculation will be verified against the necessary/wanted T&D values.

For the Bit model, the parameters received from the drill string design system are the RPM at the bit, surface torque, and WOB at the bit. The output parameter values are DOC, MSE, axial and lateral displacement, and bit depth are checked as acceptable or not. In the stick-slip case, RPM, WOB, and inclination values are applied to the model and checked against the values of the safety window designed by the controller.

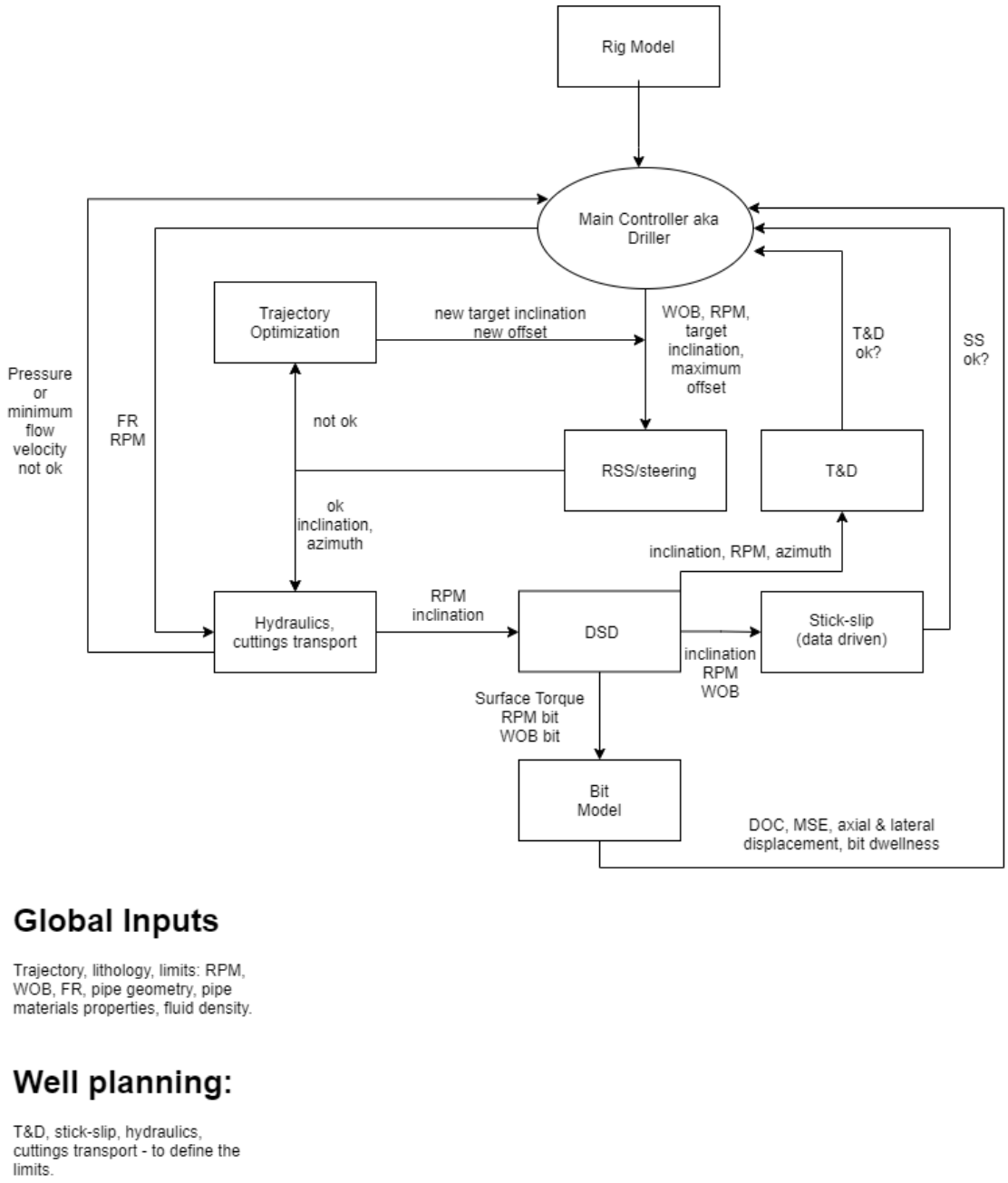

Figure 5.14: Simple Trajectory Proposed Model Diagram for Drillbotics Team.

As for integrating the ROP, BHA, and drill string models into the RSS Simulator, the concept can be seen in Figure 5.15. The ROP model should provide the value of penetration rate, the drill string model will calculate the values of WOB, and the BHA model is in charge of the sliding factor and the steerability values. These parameters are sent to the RSS Simulator; a simulation is performed; if the values are valid, they are sent to the GUI. Otherwise, the sensors should pick up the issues and provide them to the BHA model, which will then modify the parameters to new values.

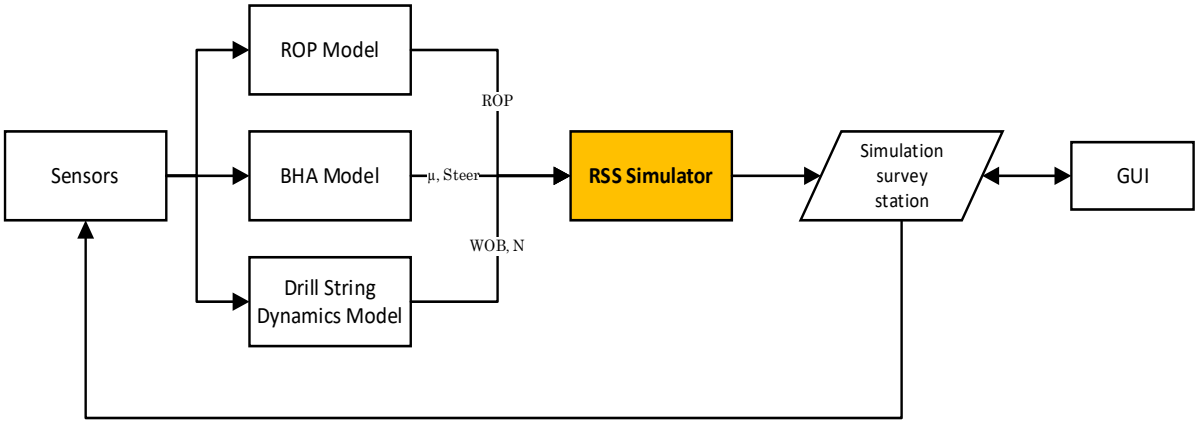

Figure 5.15: Real-Time Drilling Simulator Concept.
Source: (Saavedra L.A.J, 2021).

6. Study Cases on Drilling Inclined Wells via UiS Simulator

This thesis will provide a case study on the trajectory design of two 3D wells simulated with the RSS Simulator created by Luis Saavedra for the Drillbotics UiS Team A. The simulator is run for two different cases, one with a simple J-Shaped well and another for a more complex 3D shape.

It is imperative to mention that the data used for both cases was removed from the ISCWSA Excel example uploaded on their official web page to evaluate clearance scenarios (ISCWSA, 2017a). The file provides many different trajectories, and the ones chosen for this thesis are wells 01 and 04.

6.1. J-Shaped 3D Well Trajectory

The J-shaped well is built with a KOP at 500 m; the build-up curvature displays changes in the walk rate and displays a well path with a target inclination of 50° and azimuth of 137°. The trajectory starts at the origin point for TVD, North, and East coordinates (0 m, 0 m, 0 m). Finally, its target is reached at coordinates (3104.94 m, -2084.04 m, 1864.5 m), and the parameters used for such simulation can be found in Saavedra L.A.J. (2021) and Table 6.1. The results that can be found are plotted against MD and are presented below:

- Inclination;
- Azimuth;
- Total Azimuth Force;
- Total Inclination Force;
- DLS;
- ROP_{axial};
- ROP_{inc};
- ROP_{az}.

Table 6.1: General Inputs for correction parameters and PWP generator.

Variable	Value	Unit
WOB	69 866.664	N
RPM	143.44375	rpm
μ (sliding factor)	0.23	
Max DLS value	6	°/30m
Max Tortuosity Value	3	°/30m

6.1.1. J-Shape 3D Well TCO Results

The trajectory control optimizer results are express in an Excel sheet as PWP and Deviation Control tables; these results can be visualized by the plots in Figures 6.1 and 6.2 and are interpreted as follows: the red line represents the PWP that is based on the blue spaced lines with dots that represent the survey points from the original trajectory that will be optimized, and the black line represents the trajectory simulation run by the code.

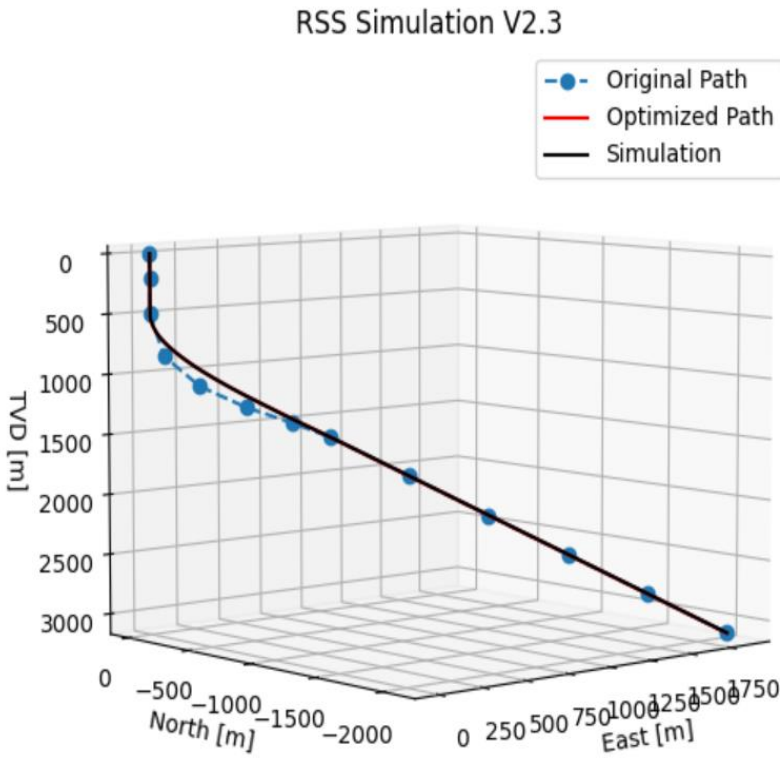

Figure 6.1: RSS Simulation for the J-Shaped 3D Well Trajectory.

As seen in Figure 6.2, the original trajectory was optimized by the simulator on the curved section of the well; such a result can be important when working on real projects since it might allow the team to save time and money.

Furthermore, the maximum distance between the optimized path and the simulation found in this case is 4.282615 m, a very small difference providing a very successful optimization.

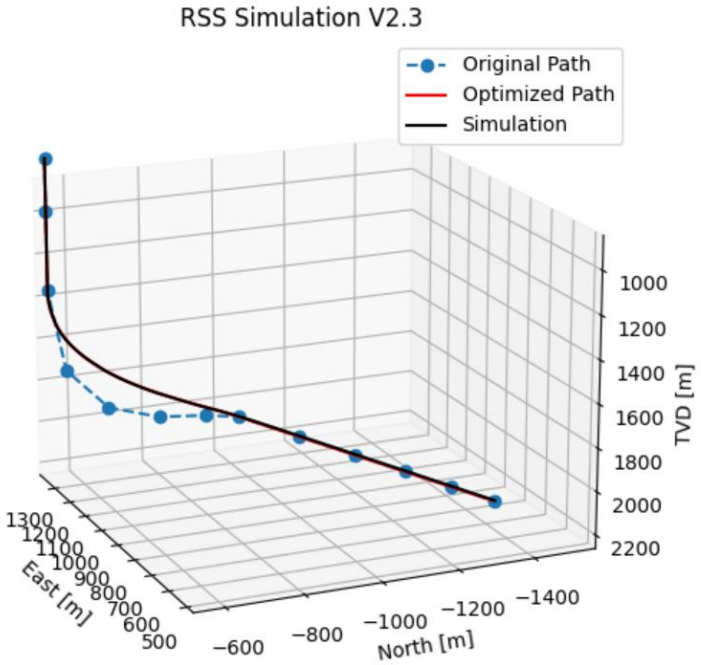

Figure 6.2: RSS Simulation for J-Shaped 3D Well Trajectory zoomed-in view.

6.1.2. J-Shaped 3D Well Simulation Results

The simulation results are presented in the same Excel sheet file as the PWP and Deviation Control. Because the simulator runs at a time step of 60 s, the amount of data acquired is too large to be provided in this thesis. Therefore, a more dynamic reading of the results is provided by designing several RSS-Simulator and Excel plots. In this section, some simulation results will be presented for the J-shaped well trajectory.

The first analysis is done in Figure 6.3, which shows the changes in azimuth where a drastic change occurs around 500 m (MD); this change seems to be kept somewhat stable after that interval with only a few small variations throughout its course. Figure 6.4. displays changes in the inclination, where there is a stable and gradual increment from vertical to the horizontal direction. These increments also start at a depth of 500 m; this happens due to the start of the build-up section.

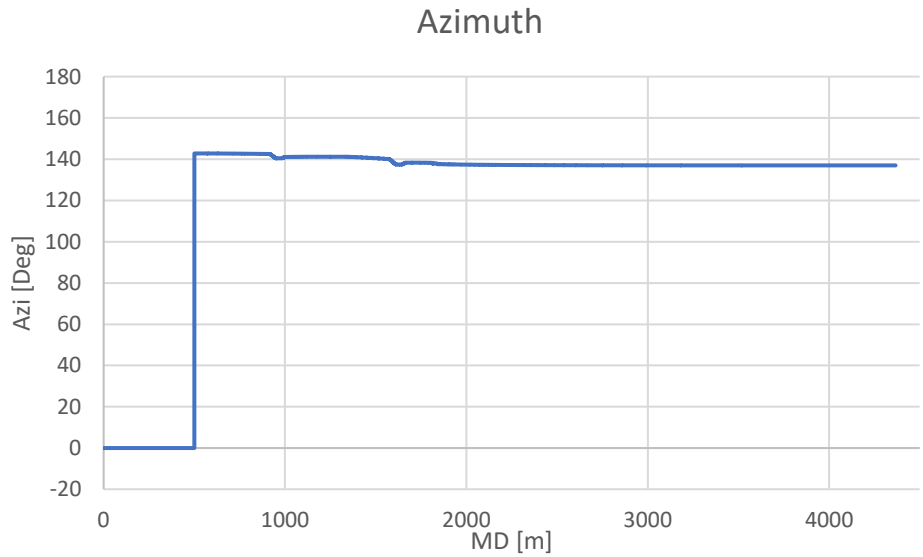

Figure 6.3: Azimuth for J-Shaped 3D Well Trajectory.

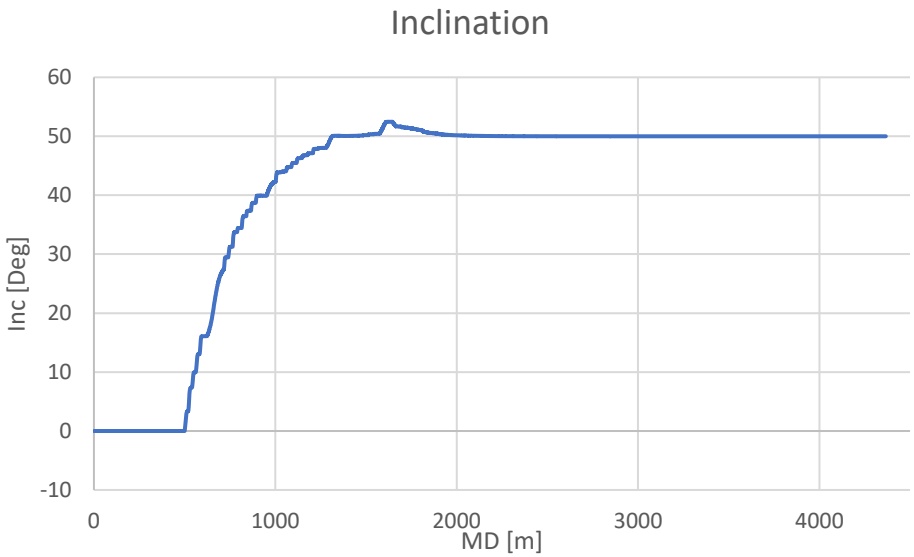

Figure 6.4: Inclination for J-Shaped 3D Well Trajectory.

One important parameter to be analyzed is the DLS of the well; as seen in Figure 6.5, the values for DLS in this well tend to remain below 15°/30m with three different peeks where this value goes above this margin, this happens in the curved section of the well at 500 m, 800 m, and 1000 m.

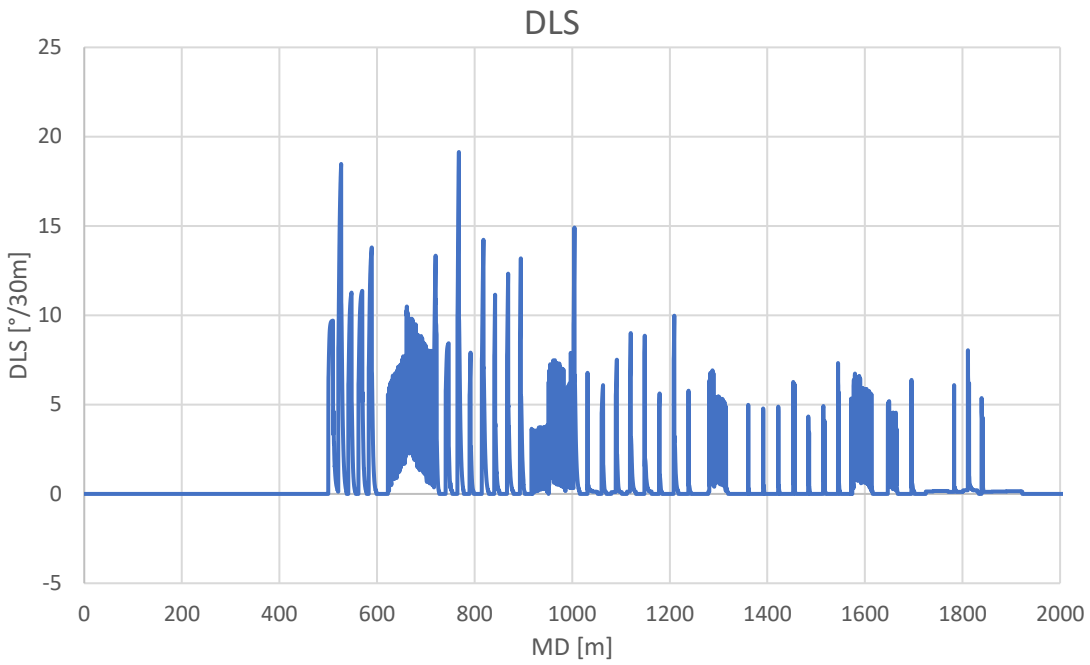

Figure 6.5: DLS in J-Shaped 3D Well.

The succeeding plots from Figures 6.6 and 6.7 demonstrate the total forces applied towards the azimuth direction and the inclination direction, respectively. This parameter provides information on the force needed to drop or buil-up the inclination and the azimuth regarding its negative and positive values.

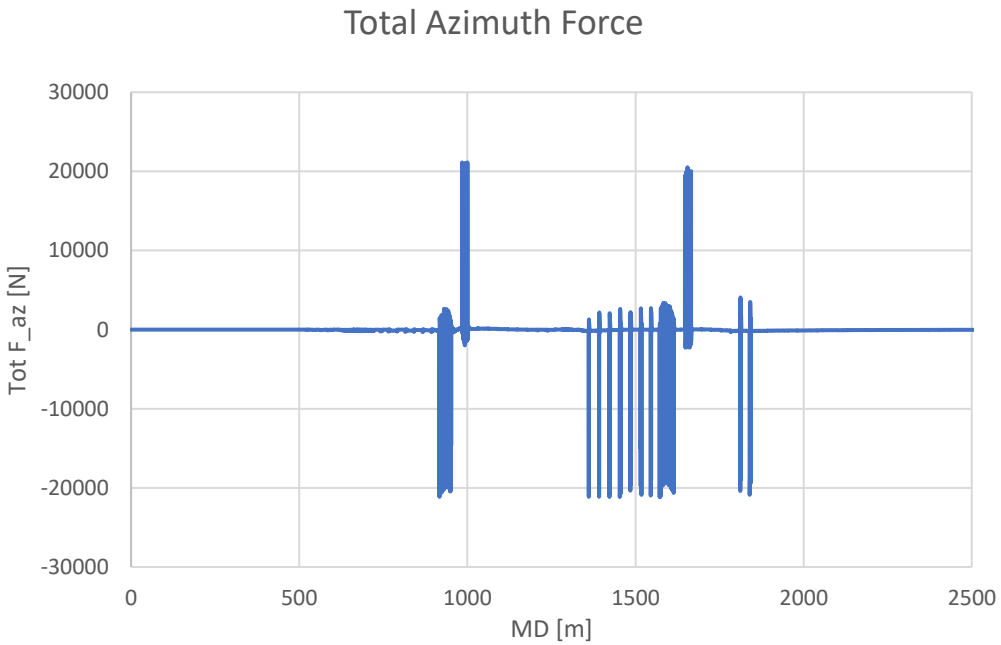

Figure 6.6: Total Azimuth Force for J-Shaped 3D Well.

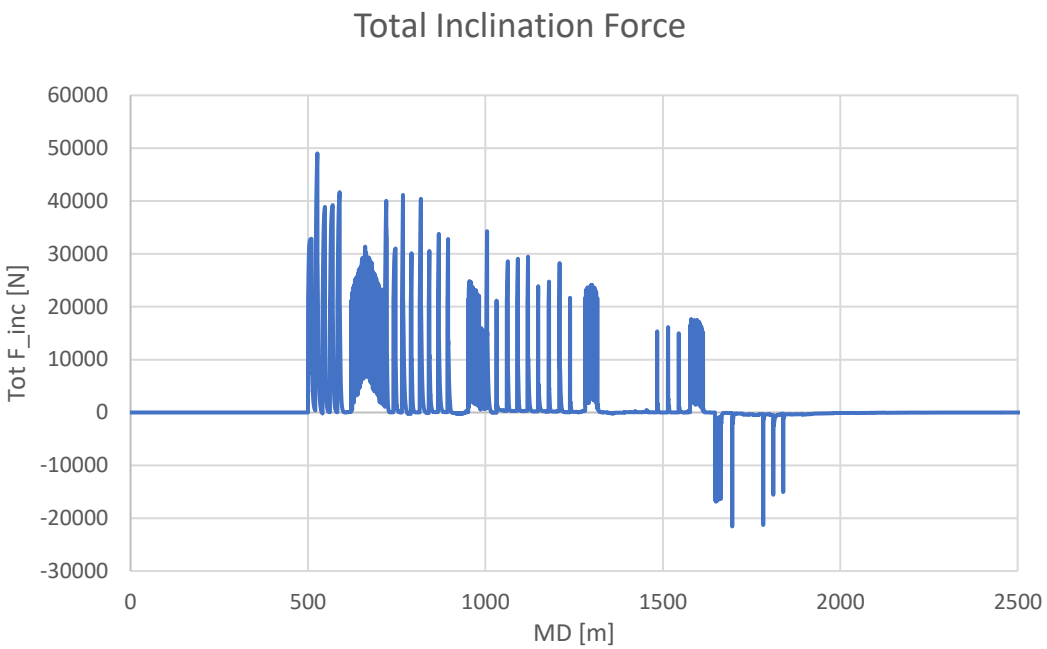

Figure 6.7: Total Inclination Force for J-Shaped 3D Well.

As seen in these plots, the values of force for both parameters appear to remain constant and close to 0 newtons for the begging and end section of the well trajectory, presenting major fluctuations in the inclined section of the well between 500 m and 2000 m.

Lastly, the ROP parameters are illustrated in Figures 6.8, 6.9, and 6.10; these parameters show alterations in penetration rate, impacting the bit position calculations. As explained by Saavedra L.A.J. (2021), the ROP_{axial} presents many fluctuations caused by noises added to external inputs from the model; the frequency of these oscillations equals the space in between the original points from the trajectory design.

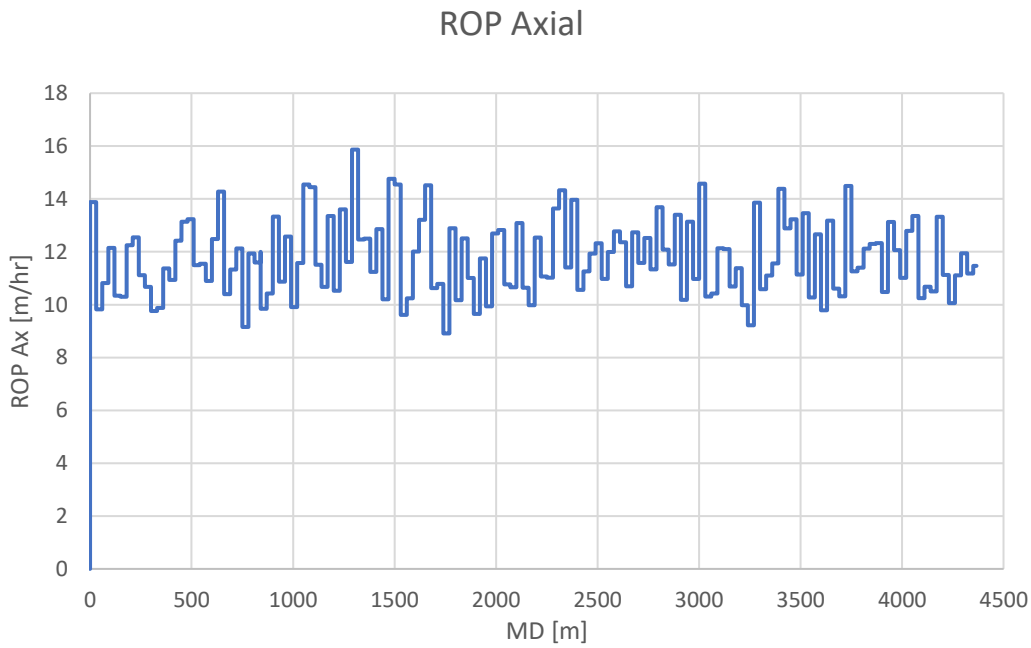

Figure 6.8: Axial ROP for J-Shaped 3D Well Trajectory.

The ROP_{az} and the ROP_{inc} are influenced by the forces on the bit and the wells offset. Both indicate the direction in which the bit is moving, either for the azimuth or the inclination plane. As seen in Figure 6.9 the major changes in the azimuth direction occur between 800 m and 1000 m and between 1400 m and 1800 m. As for the changes in inclination, they occur throughout the entire interval between 500 m and 1800 m and tend to have a higher intensity than the azimuth ROP.

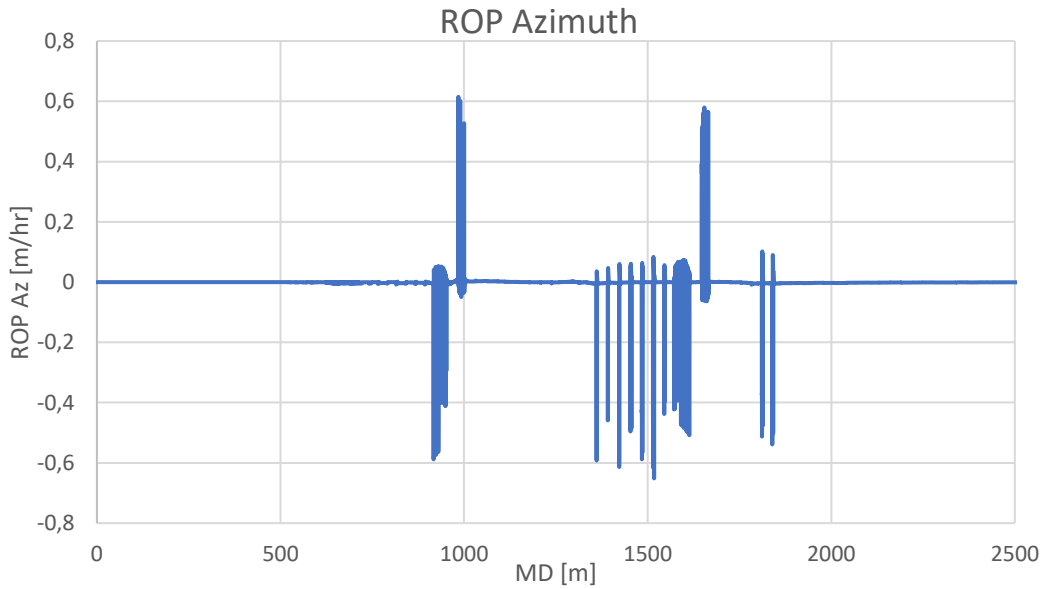

Figure 6.9: Azimuth ROP for J-Shaped 3D Well Trajectory.

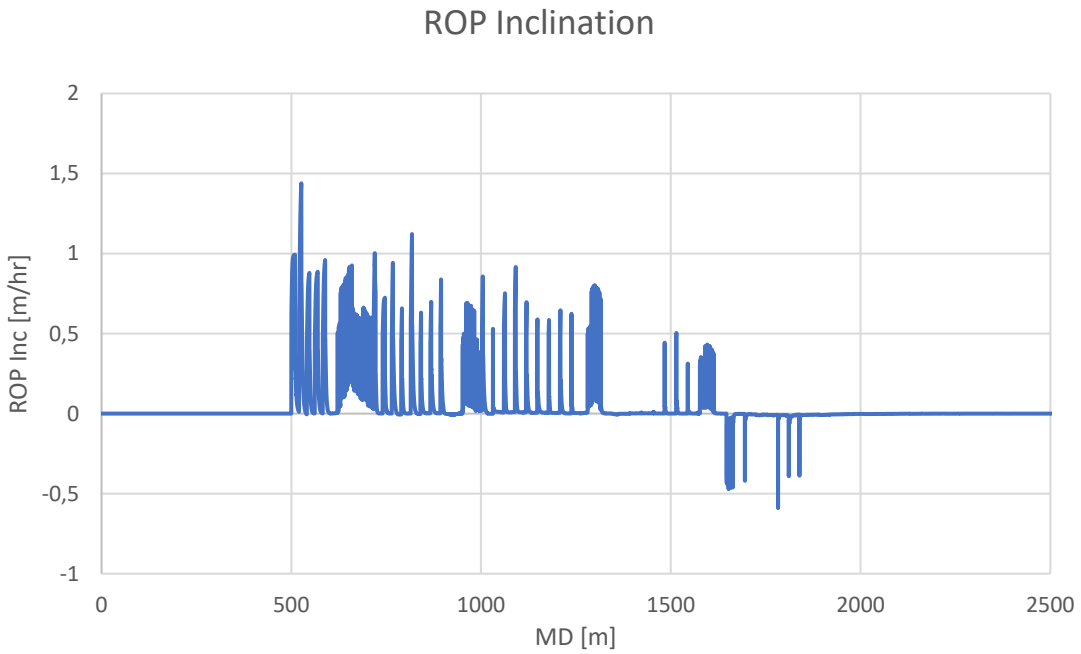

Figure 6.10: Inclination ROP for J-Shaped 3D Well Trajectory.

6.2. S-Shaped 3D Well Trajectory

The complex 3D well its first KOP at 753 m; it follows a slightly inclined trajectory and has its second build-up section at around 1350 m. The well path ends with a target inclination of approximately 0° (vertical well) and an azimuth of 141.4°. The trajectory starts at the origin point for TVD, North, and East coordinates (0 m, 0 m, 0 m), reaching its target at coordinates (3402.92 m, -3100.016 m, -1200.2 m), and the parameters used for such simulation are the same found in the Saavedra L.A.J. (2021) and Table 6.1, being the same as the J-Shaped 3D Well Trajectory.

6.2.1. S-Shaped 3D Well TCO Results

As the J-shaped Well plot, for these graphs, the red line represents the PWP based on the blue spaced lines with dots representing the survey points from the original trajectory that will be optimized. The black line represents the trajectory simulation run by the code.

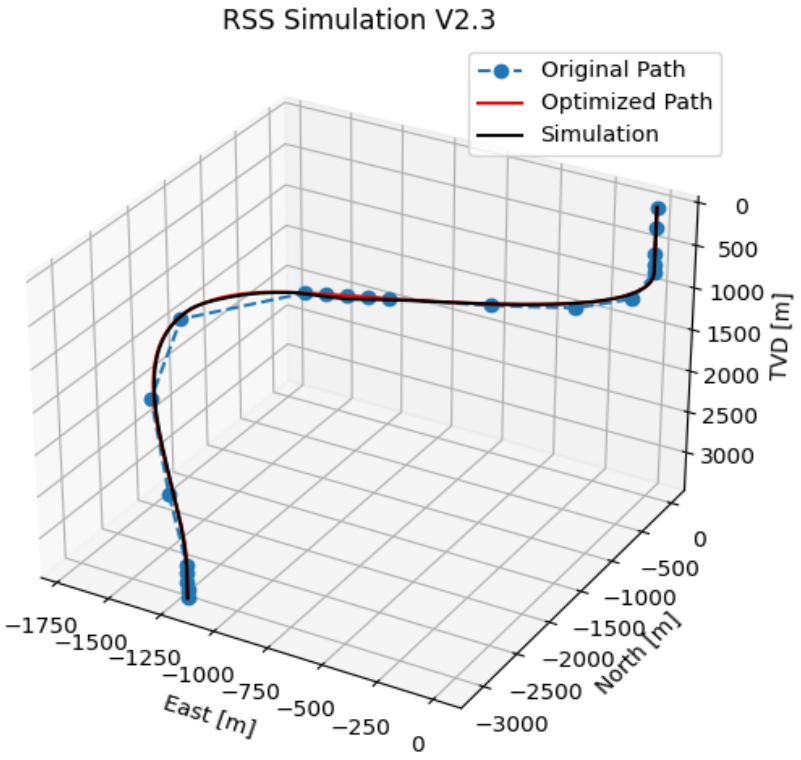

Figure 6.11: View from S-Shaped 3D Well Trajectory.

As seen in Figure 6.11, the original trajectory was optimized by the simulator throughout the well, with a small gap in the curve section. The maximum distance between the optimized path and the simulation found in this case is 29.76865 m, a small distance but larger than the J-Shaped 3D Well Trajectory, resulting from fewer survey points in the curved section seen in Figure 6.12.

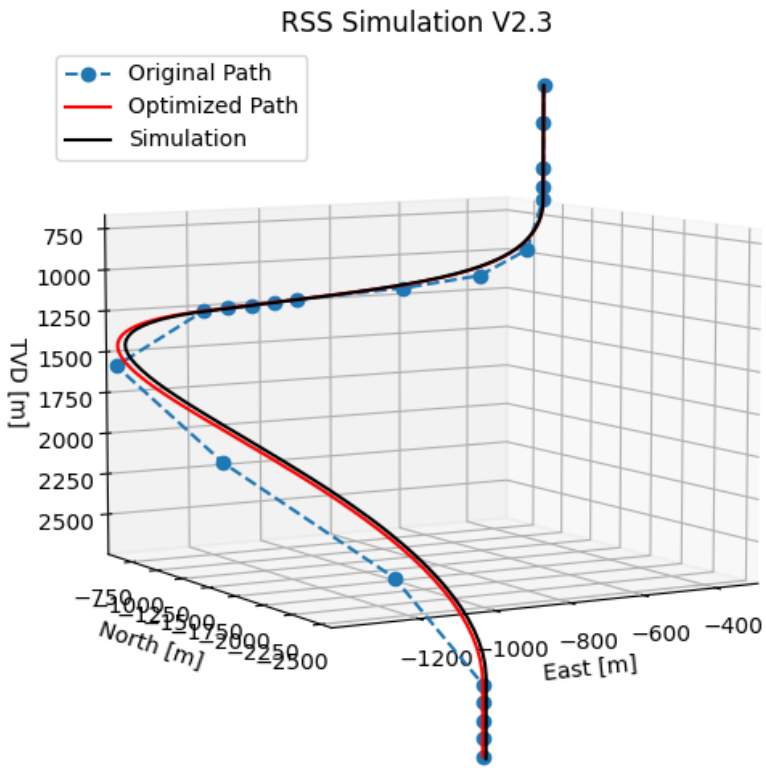

Figure 6.12: View from S-Shaped 3dWell Trajectory zoomed-in.

6.2.2. S-Shaped 3D Well Simulation Results

The first analysis in this section is done in Figure 6.13, which shows the changes in azimuth where a drastic change occurs around 753 m (MD); this change seems to be kept somewhat stable for a short interval before it begins to oscillate and then gradually decline. These changes seem to occur throughout the curved sections of the well trajectory.

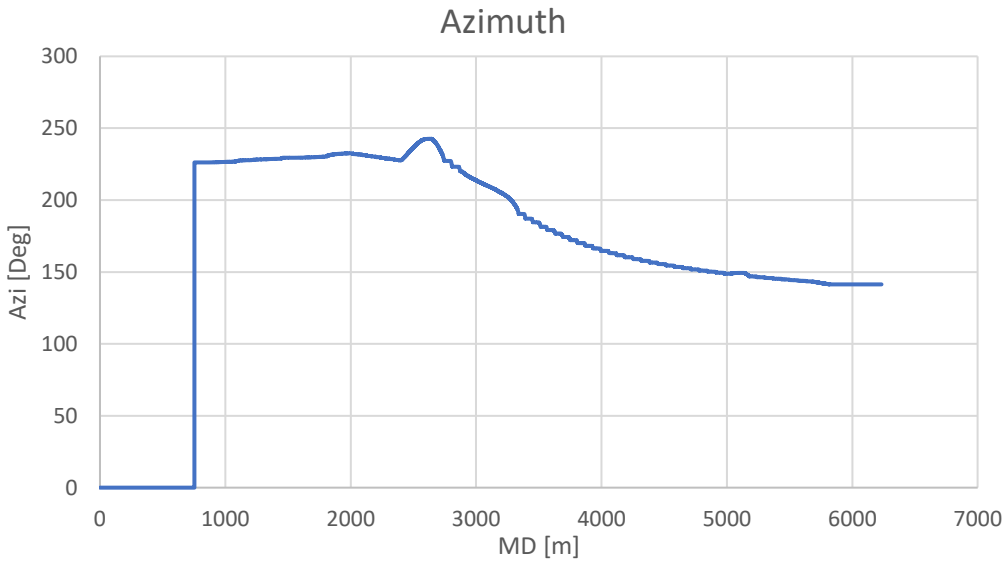

Figure 6.13: Azimuth of S-Shaped 3D Well Trajectory.

Figure 6.14 displays the changes in the inclination, where there is a gradual increment from in the inclination towards the mark of 90°, the well suffers a small oscillation up at the second build-up section. It then starts to decline towards an inclination of 0° with small oscillations throughout the trajectory.

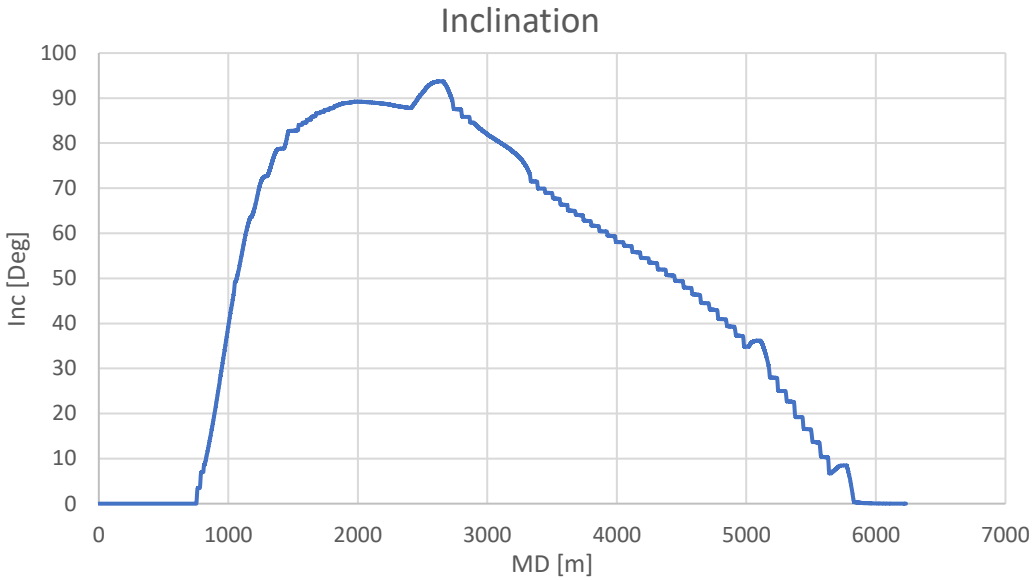

Figure 6.14: Inclination for S-Shaped 3D Well Trajectory.

Another important parameter, the DLS of the well; can be seen in Figure 6.15; the values for DLS in this well tend to remain below 16°/30m with one peek surpassing said value. Most peeks remain in the interval between 753 m and 5800 m, which are the curved section areas, as seen in Figure 6.12, and tend to stay below the intensity of 10°/30m.

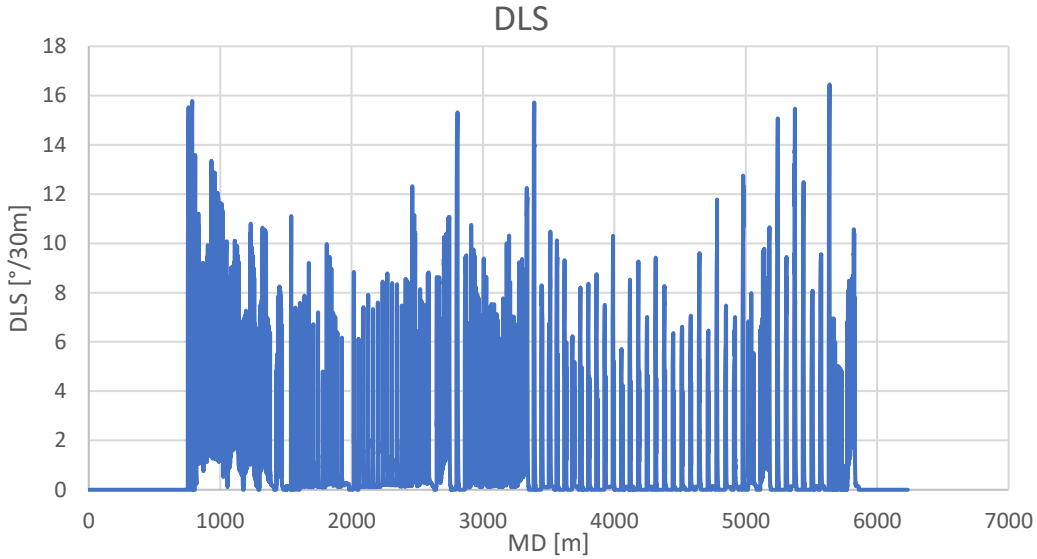

Figure 6.15: DLS of S-Shaped 3D Well Trajectory.

The succeeding plots from Figures 6.16 and 6.17 demonstrate the total forces applied towards the azimuth direction and the inclination direction, respectively. As mentioned prior, this

parameter provides information on the force needed to drop or build-up the inclination and the azimuth regarding its negative and positive values.

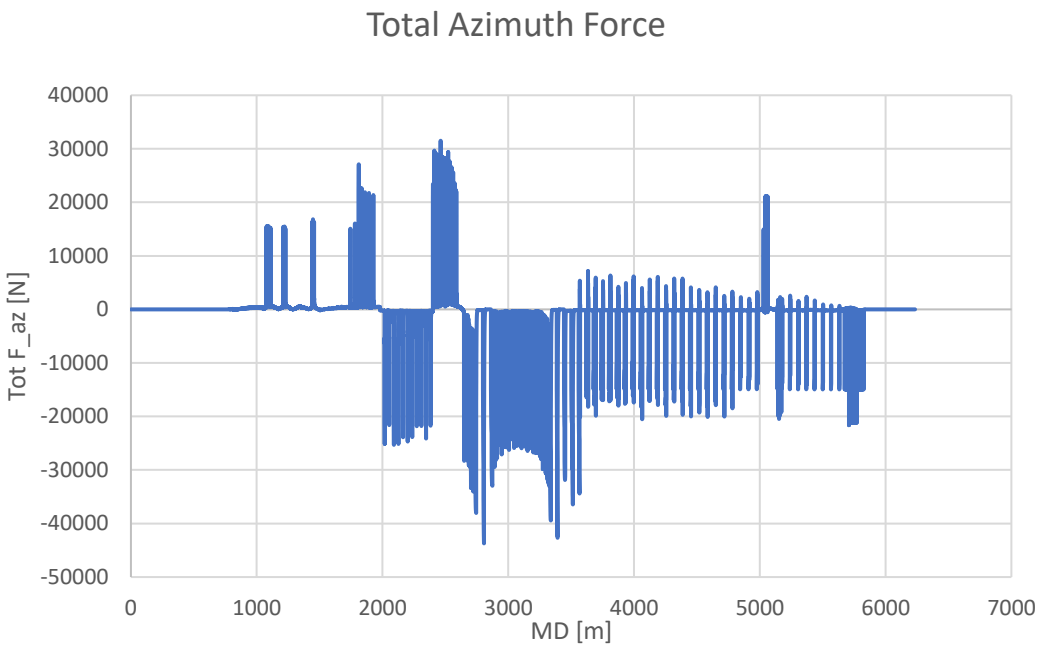

Figure 6.16: Total Azimuth Force for S-Shaped 3D Well Trajectory.

As seen in these plots, the values of force for both parameters appear to oscillate throughout most of the trajectory and close to 0 newtons for the trajectory's beginning and end. For the azimuth force (Figure 6.16), these forces seem to vary between positive and negative along the entire well, reaching its maximum values at the interval of 2000 m and 3500 m.

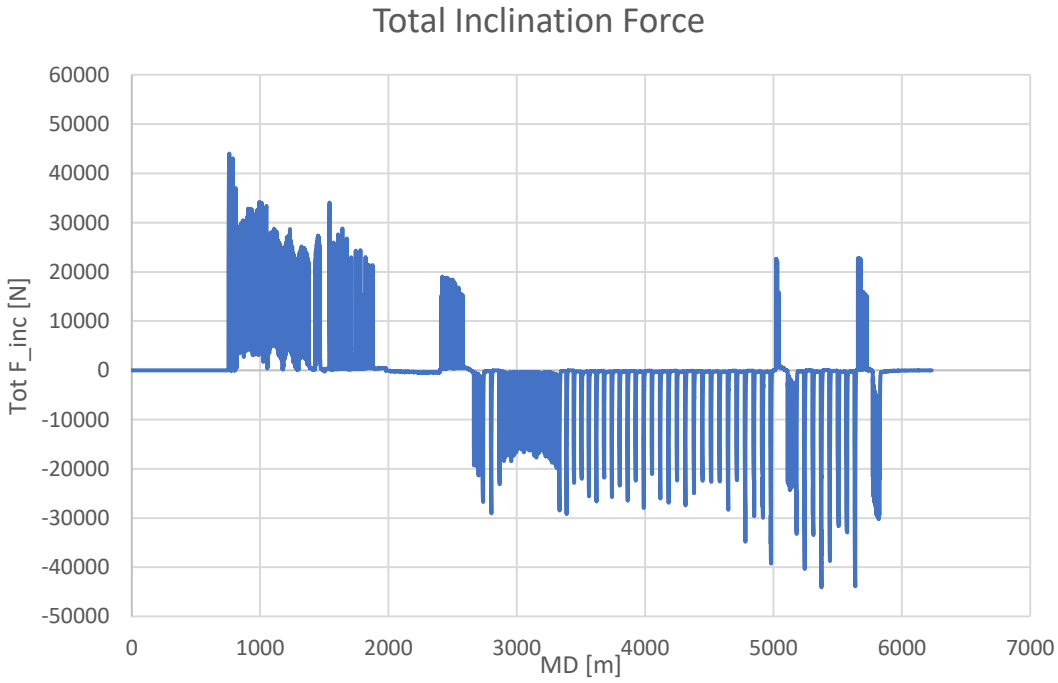

Figure 6.17: Total Inclination Force for S-Shaped 3D Well Trajectory.

In contrast, the inclination force appears to maintain positive values for the initial section of the well, between 750 m and 2000 m, and present negative values for the second part of the trajectory, between 2500 m and 6000 m. Such analysis can be made because the first section of the well increases its inclination as the second part decreases it, as shown in Figure 6.14.

Lastly, the ROP parameters are illustrated in Figures 6.18, 6.19, and 6.20. As mentioned before, the ROP_{axial} presents fluctuations caused by noises, and the frequency of these oscillations equals the space between the original survey points from the trajectory. Compared to the J-Shaped 3D Well Trajectory, the S-Shaped well appears to have more oscillations, a phenomenon explained by the fact that the survey points of this well are further apart from each other than those from the J-Shaped well.

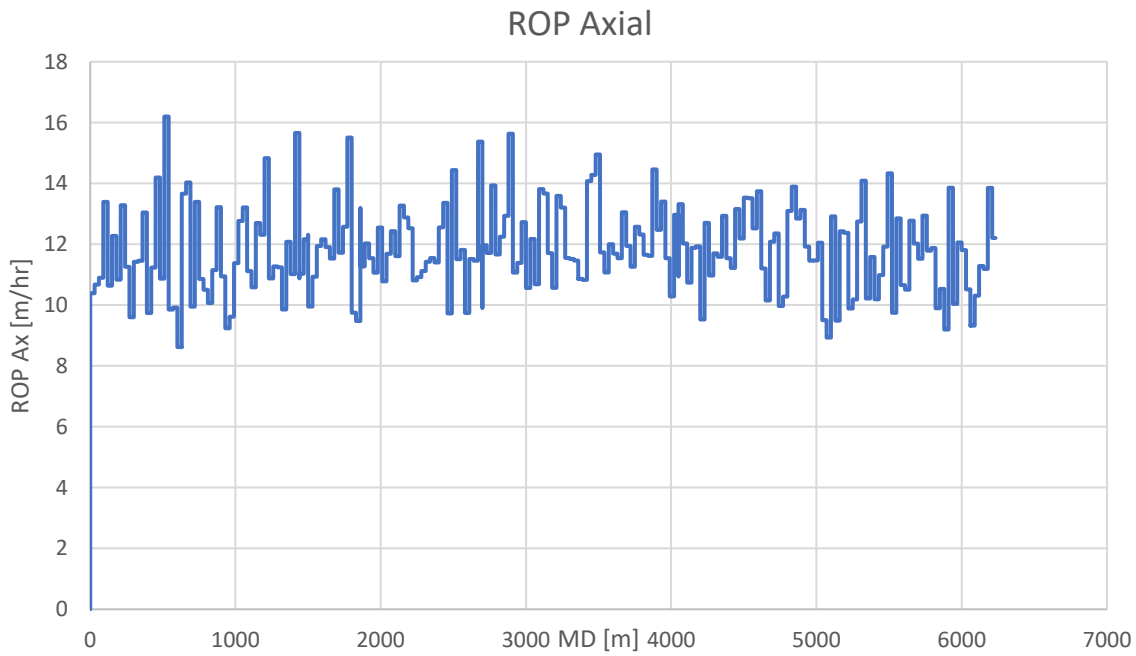

Figure 6.18: Axial ROP for S-Shaped 3D Well Trajectory.

As mentioned, the ROP_{az} and the ROP_{inc} are influenced by the forces on the bit, and the wells offset, indicating the bit's direction. As seen in Figure 6.19, the major changes in the azimuth direction occur between 2000 m and 6000 m. These changes tend to oscillate between positive and negative in the first section of this trajectory until it reaches the MD of 2800 m, where they being to be mostly negative.

As for the changes in inclination, they occur throughout the entire interval between 750 m and 6000 m being all of them positive throughout the first section of the well until reaching the MD of 2800 m, when they begin to become mostly negative with a few peeks of positive ROP between 5000 m and 6000 m, as seen in Figure 6.20.

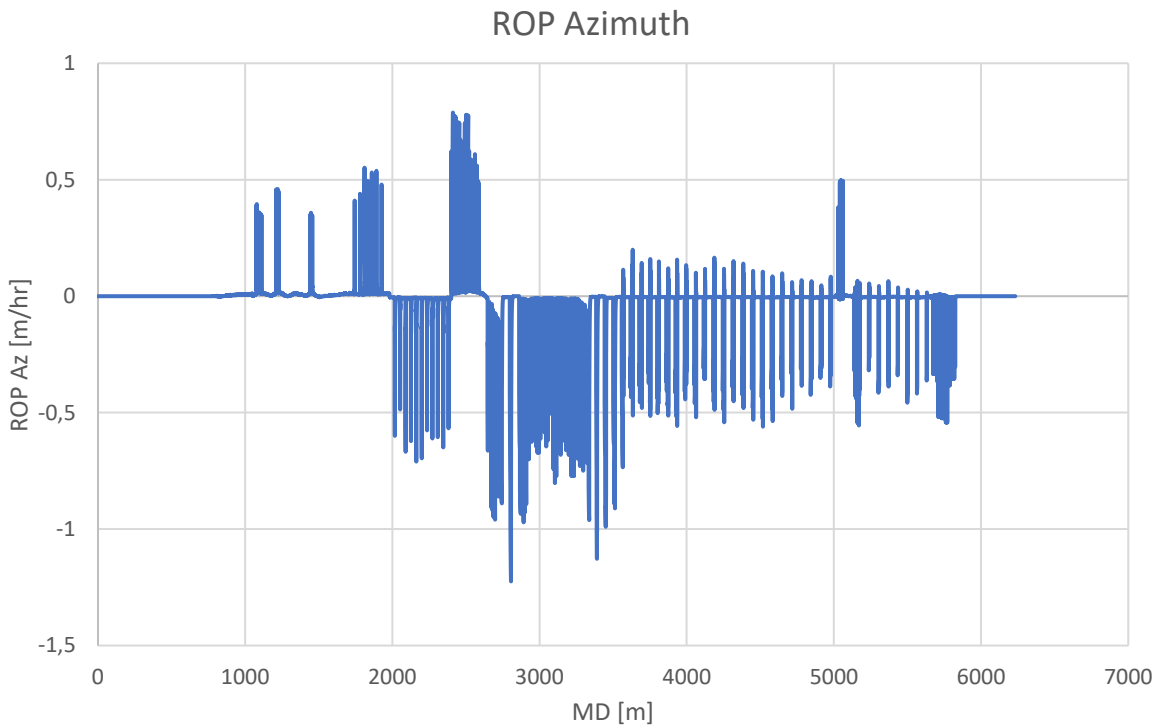

Figure 6.19: Azimuth ROP for S-Shaped 3D Well Trajectory.

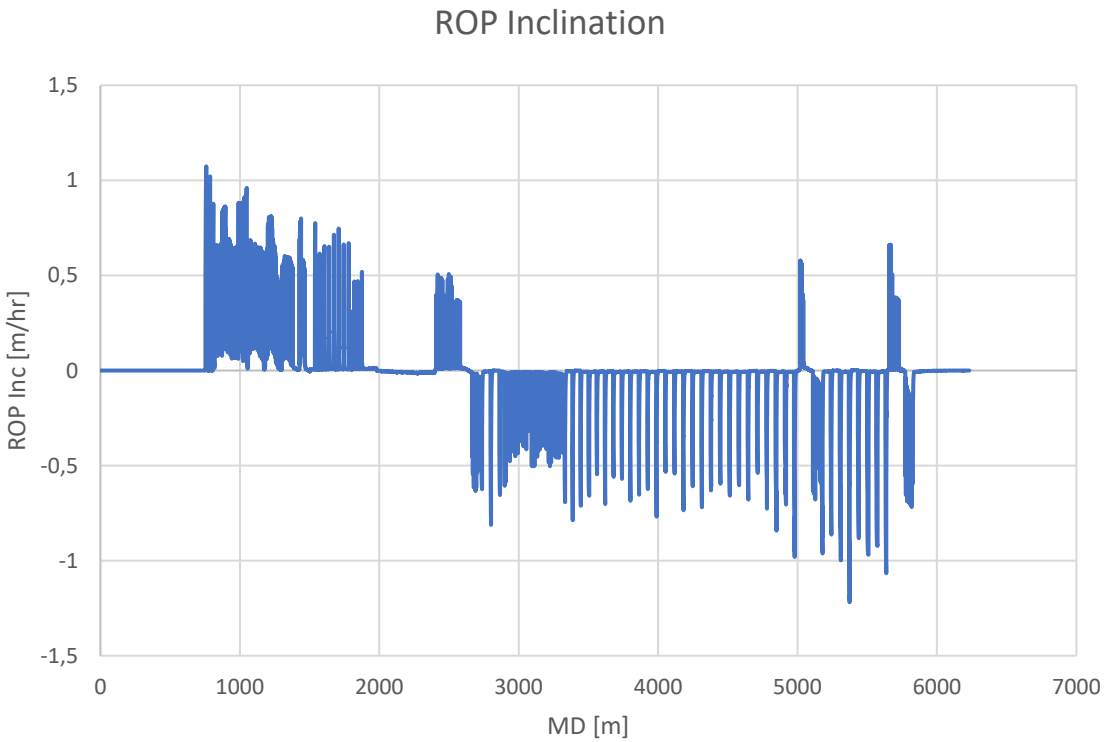

Figure 6.20: Inclination ROP for S-Shaped 3D Well Trajectory.

7. Discussion

The study of the RSS Simulator designed by Saavedra L.A.J (2021) was done in the examples presented in the previous chapter. The analysis of the results will focus on the performance of this simulator regarding its trajectory control optimizer and its correction parameters for both 3D wells.

This analysis will be done by comparing the results of trajectory with the TCO switched off. The initial data shown in Table 6.1 is kept as well as the original survey stations. The differences in simulation path caused by the kill of this asset cause a different error magnitude in respect to the PWP.

Moreover, a sensitivity analysis of the correction parameters of DLS and tortuosity will be performed by changing values of WOB, RPM, and μ in the simulator. The change in trajectory regarding these factors can be evaluated, and the maximum and minimum limits for the simulator to operate the TOC. Finally, some future recommendations for improving the performance of the RSS Simulator will be presented in this chapter.

7.1. TCO Performance on 3D Trajectories

The TCO is a new model presented by Saavedra L.A.J. (2021) for the RSS Simulator. It was developed as an automated tool capable of reaching a target coordinate without human intervention. However, it must be tested with different trajectories and survey points to review this asset and investigate its results.

The path generated by this tool should follow some constraints and be excluded from any integrity problems. This analysis will be done first in the trajectories with the original values of WOB, RPM, and μ and will be further applied in the sensitivity analysis.

It is crucial to notice that the terms for TOC on and off indicate the activation and deactivation of the real-time Deviation Control asset, involving the Deviation Control and the path correction functions, as mentioned by Saavedra L.A.J (2021).

7.1.1. TCO Performance for J-Shaped Well

In this section, the 3D example for J-Shaped Well Trajectory was simulated without corrections on the survey points to see the differences in the trajectory and the target coordinates reached in both cases.

Figure 7.1 presents the trajectories for both cases; in the left well, the Deviation Control is active, while in the right well, it is inactive. While analyzing this Figure, it is possible to conclude that when inactive, the bit performs without problems in the vertical section, only displaying a small variation on the curved part of the well.

However, the simulator seems to perform well even without those corrections; the difference in the PWP path and the simulation paths is quite small being 11.20599 m, only a meager increase compared to the difference of 4.282615 m given by the trajectory with the TOC On,

being both differences found in the bottom of the well trajectory in the last survey point, shown in Figure 7.2.

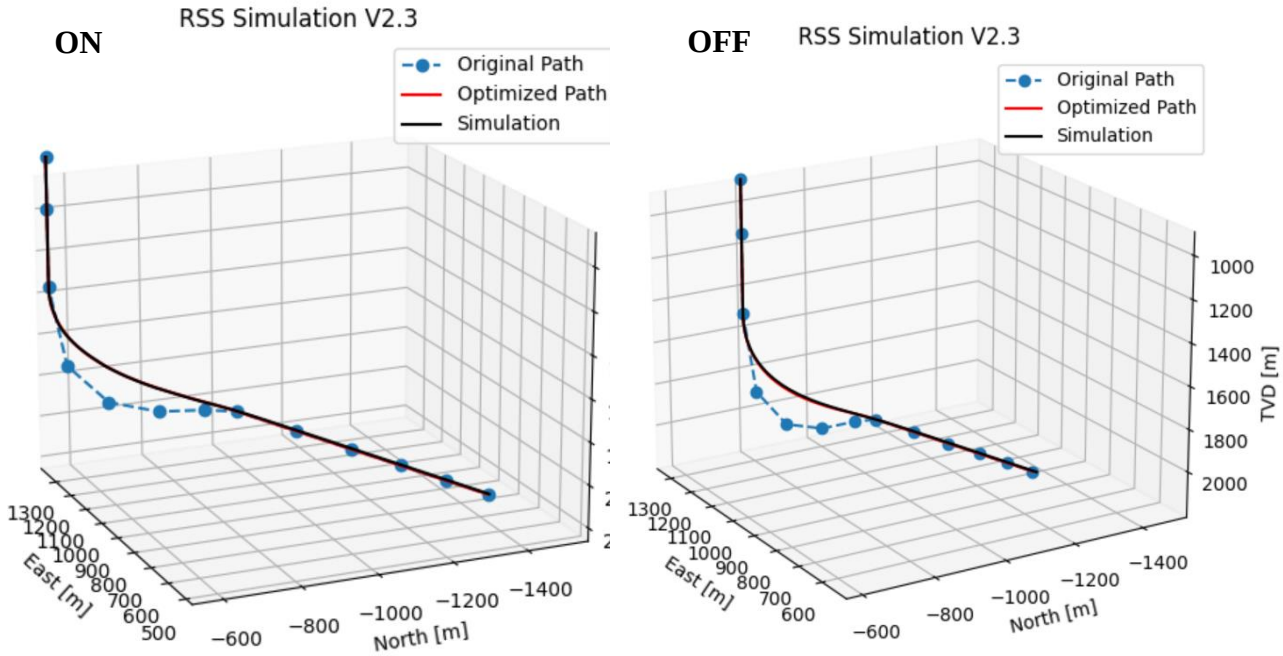

Figure 7.1: Difference of Trajectory Performances for the J-Shaped Well TCO On/Off.

Considering the corrections are done to assure the target will be hit as close as possible, it is safe to assume that because this well is quite simple and presents only a small build-up section, the simulator could perform well, even without the Deviation Control. However, such a trajectory can only be deemed acceptable if it stays within the tolerance limits set by the user.

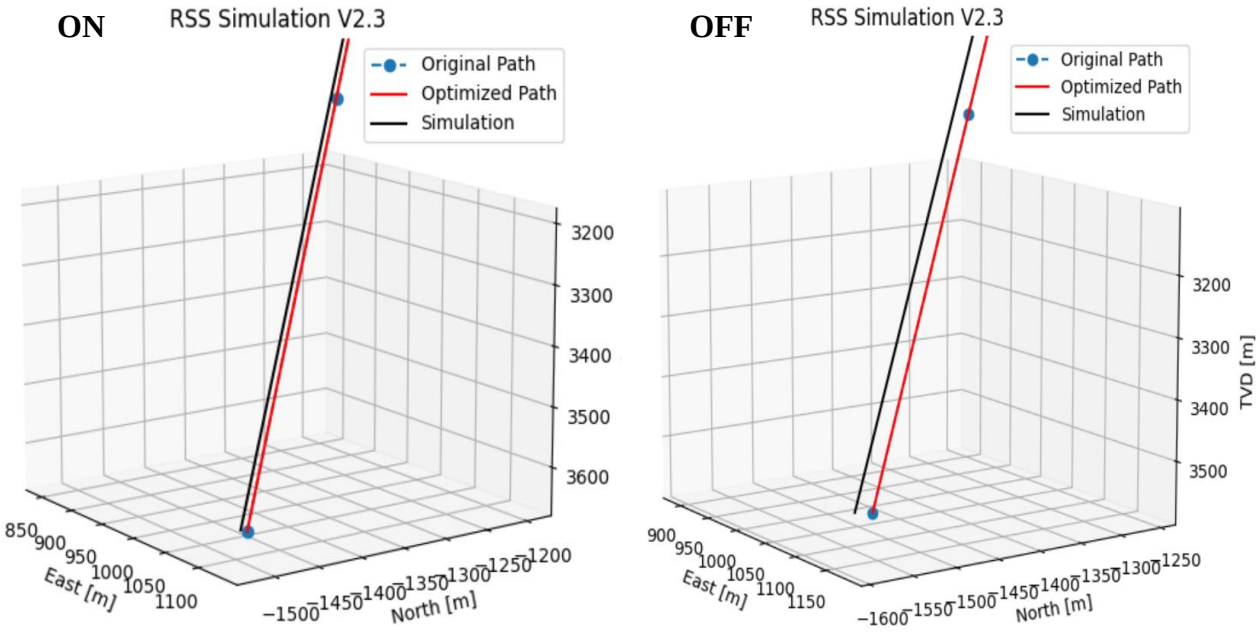

Figure 7.2: Final Target Comparison for J-Shaped Well TCO On/Off.

7.1.2. TCO Performance for S-Shaped Well

In this section, the 3D example for S-Shaped Well Trajectory was simulated without corrections on the survey points to see the differences within the trajectory and the target coordinates reached in both cases.

Figure 7.3 presents the trajectories for both cases; in the left well, the Deviation Control is active, while in the right well, it is inactive. While analyzing this Figure, it is possible to conclude that when inactive, the bit performs well in the vertical section but presents some differences in the curved sections.

Although small, these differences are larger than those found in the J-Shaped well, perhaps due to the more complex shape and larger changes in inclination and azimuth suffered in this well, the Deviation Control does not seem to perform as good as the previous case.

The difference in the PWP path and the simulation path for the first case with the TOC-On is on average 3.917426 m, reaching values between 15 m and 29 m on the curved section. On the other hand, although the TOC-Off presents a smaller maximum distance value of 26.705 m, the average distance value between both paths in the curved section is much higher, being 12.57 m, which can be seen in Figure 7.4.

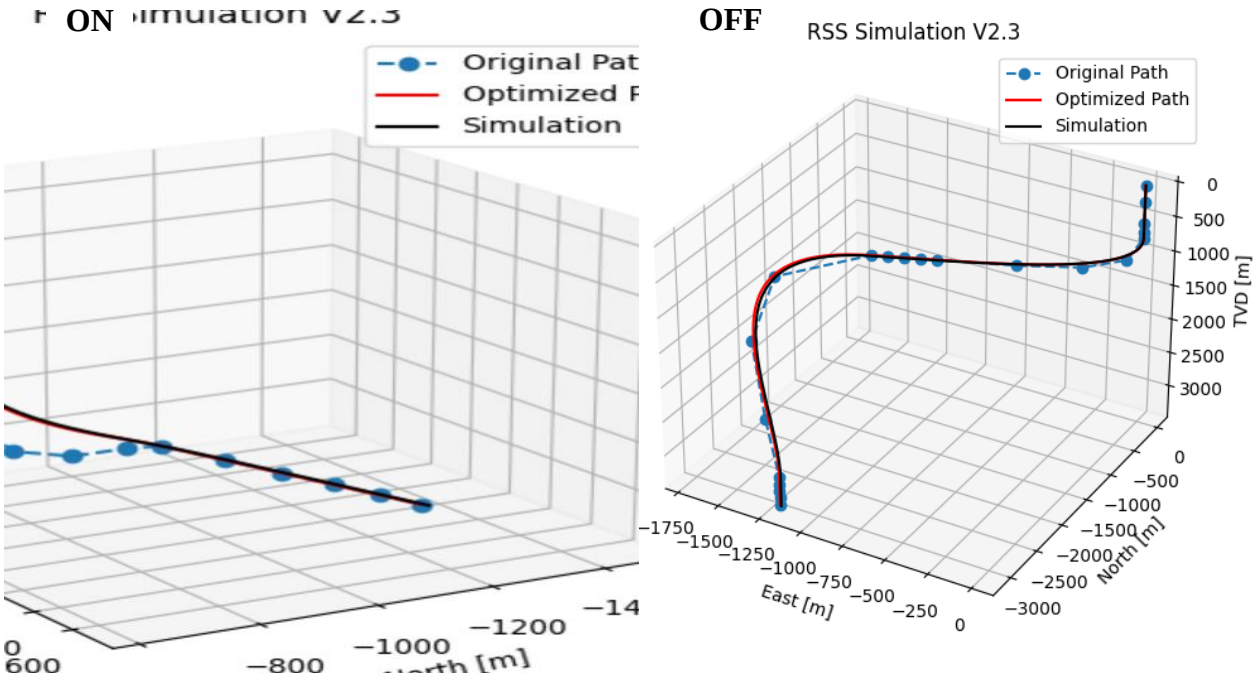

Figure 7.3: Difference of Trajectory Performances for the S-Shaped Well TCO On/Off.

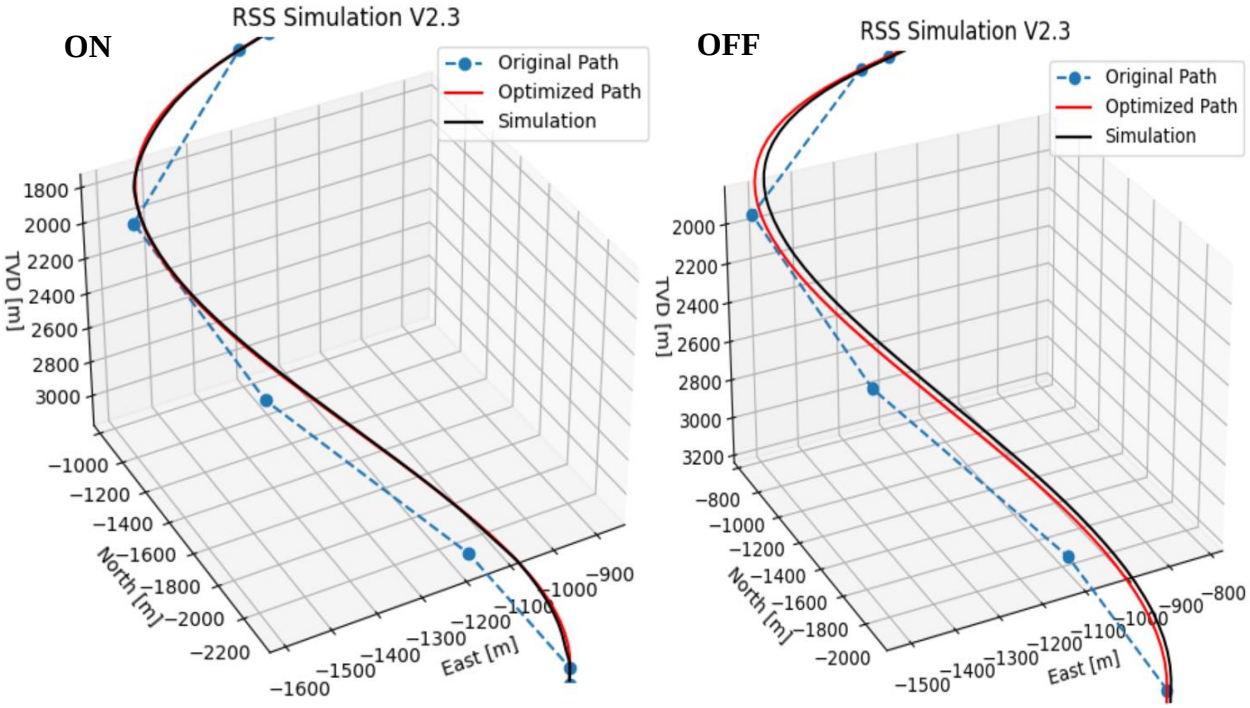

Figure 7.4: Difference of Trajectory Performances for the S-Shaped Well TCO On/Off, Curved Section zoomed-in.

On the target section of the trajectory, this case also displays a larger discrepancy from the target when having the TCO tool off. As shown in Figure 7.5, the TCO generates a simulated trajectory quite close to the PWP path, with a distance of 2.7 m from each other. On the other hand, this distance is increased to 17.5 m when the TCO is deactivated, which is higher than in the previous case.

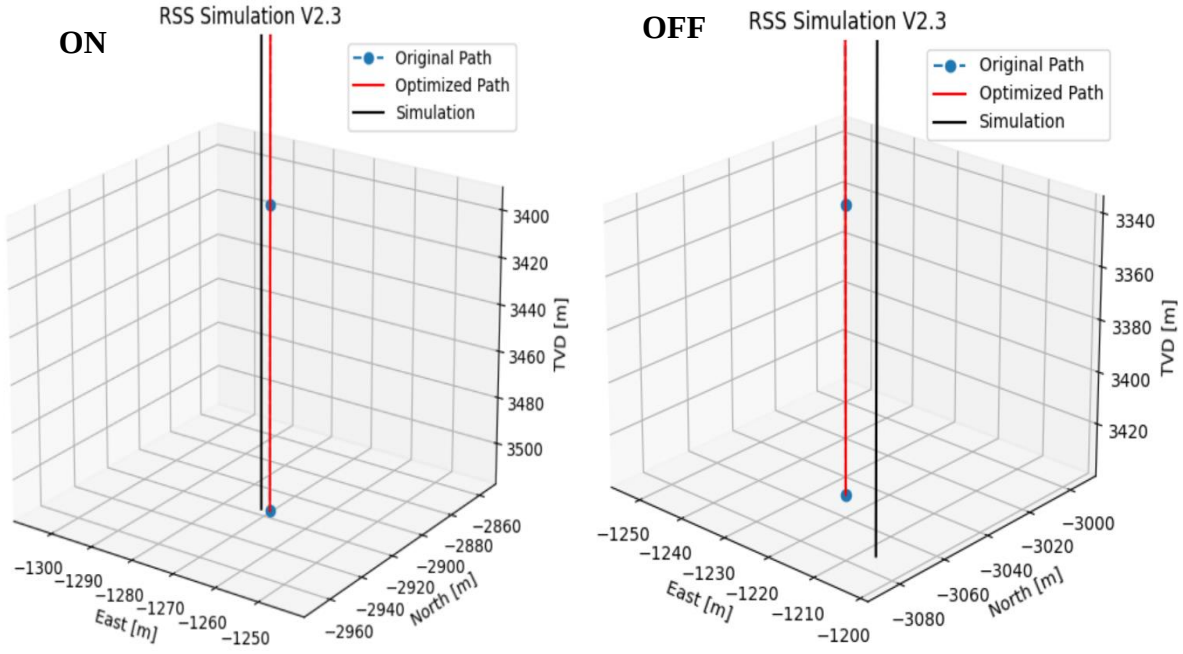

Figure 7.5: Final Target Comparison for J-Shaped Well TCO On/Off.

7.2. Sensitivity Analysis of RPM

The RPM is one of the parameters introduced in the PWP simulator to project the well trajectory. A sensitivity analysis on the RPM was performed for both wells, J-Shaped and S-Shaped.

Alongside the change in this parameter, the TOC was also evaluated by being activated and deactivated for each of the changes performed to find out if the parameter of RPM would affect the well trajectory.

The analysis was done by altering the values of RPM into both directions, negative and positive. The value was increased and decreased by 50% of the original, and the simulation was performed for both TOC On and OFF. Table 7.1 shows the values of RPM used for these simulations.

Table 7.1: Values of RPM used for Sensitivity Analysis.

Variable	Value	Unit
RPM – 50%	71	rpm
RPM – 0%	143	rpm
RPM + 50%	215	rpm

7.2.1. Sensitivity Analysis of RPM in J-Shaped Well

The first part of this analysis was done by decreasing the value of RPM by 50%. The simulator was run, and the results can be found in the plots shown in Figure 7.6. As seen in this figure, the decrease in RPM does not change the trajectory too much.

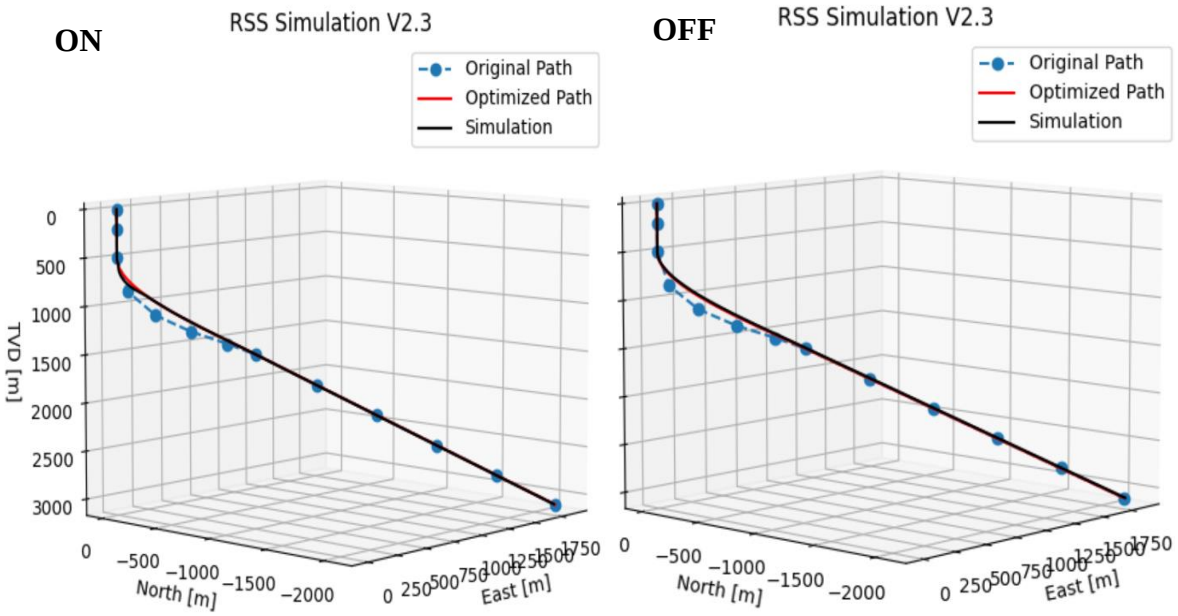

Figure 7.6: Sensitivity Analysis -50% RPM for J-Shaped Well.

However, it is possible to perceive that the TOC On presents a higher discrepancy between the PWP path and the simulation path in the curved section of the well path. At the same time, the

TOC Off appears to have a larger distance between both paths throughout the entire bottom part of the well, as seen in Figure 7.7.

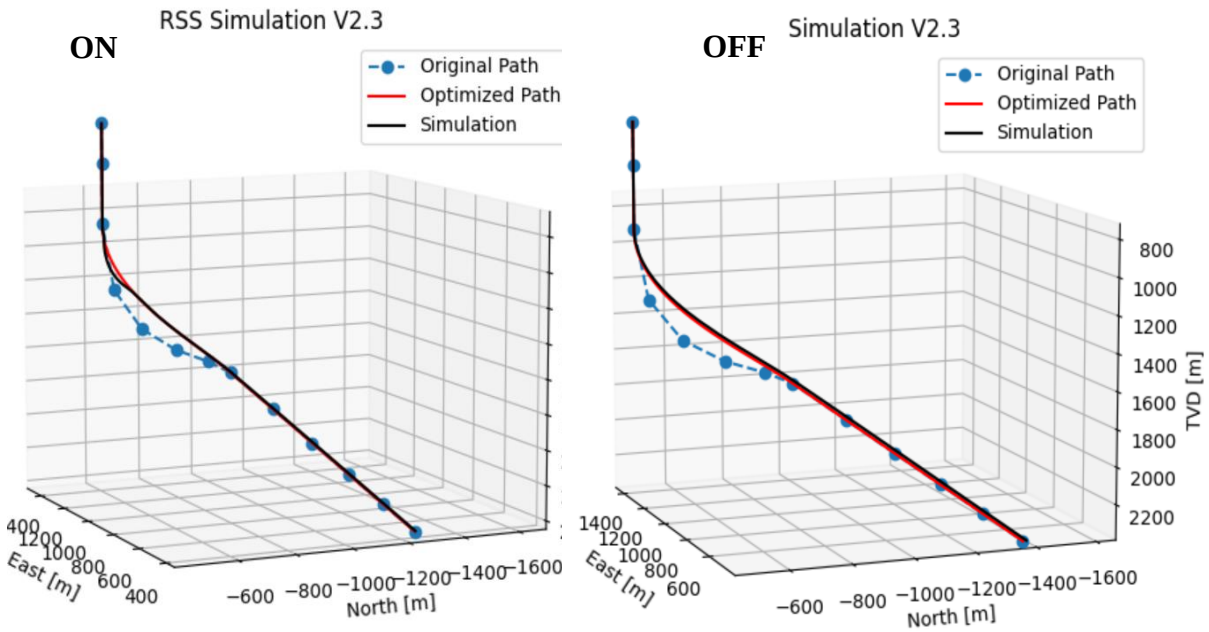

Figure 7.7: Sensitivity Analysis -50% RPM for J-Shaped Well, zoomed-in.

Identical to the analysis of the decreasing RPM, the increasing RPM seems not to change much of the trajectory either. As seen in Figures 7.8 and 7.9, despite providing some deviations in the simulation results, these are so minor that they can be neglected for both cases. The trajectories are, therefore, similar to the ones found previously in section 7.1.1.

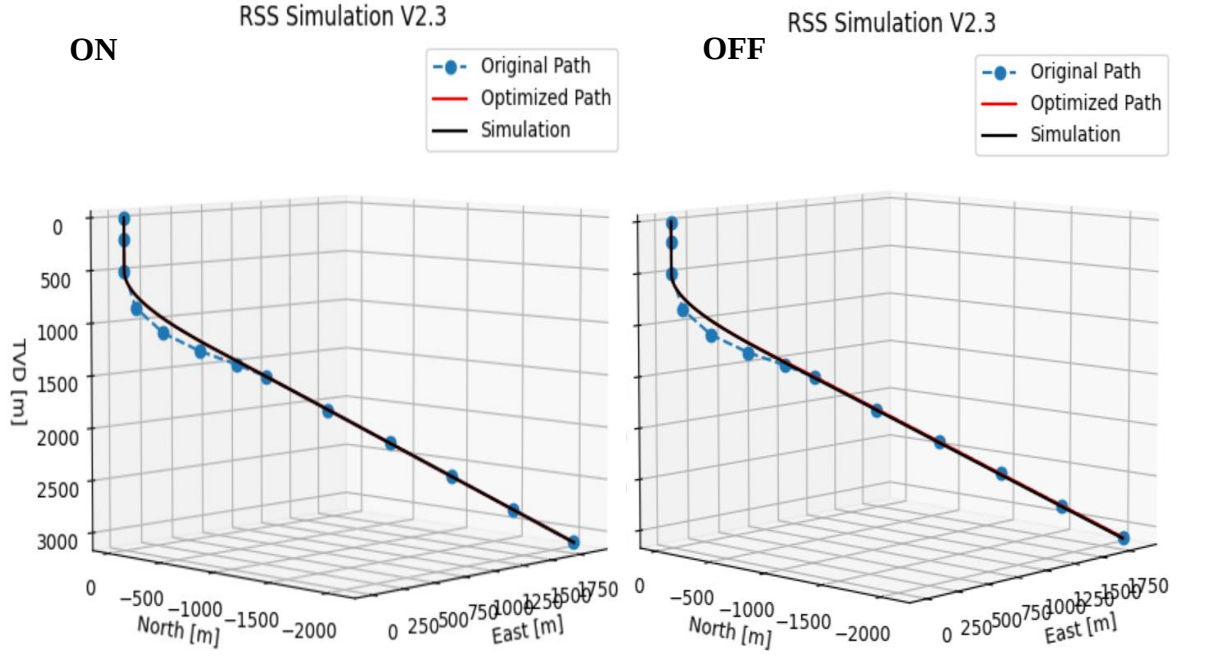

Figure 7.8: Sensitivity Analysis +50% RPM for J-Shaped Well.

In this case, it is possible to assume that the change in the value of RPM does not affect the trajectory considerably. The major change was seen in the analysis of the decreasing RPM if

compared to the increasing RPM, which provided no major differences from the original case, therefore, decreasing the RPM affects the well trajectory on a higher level than increasing it.

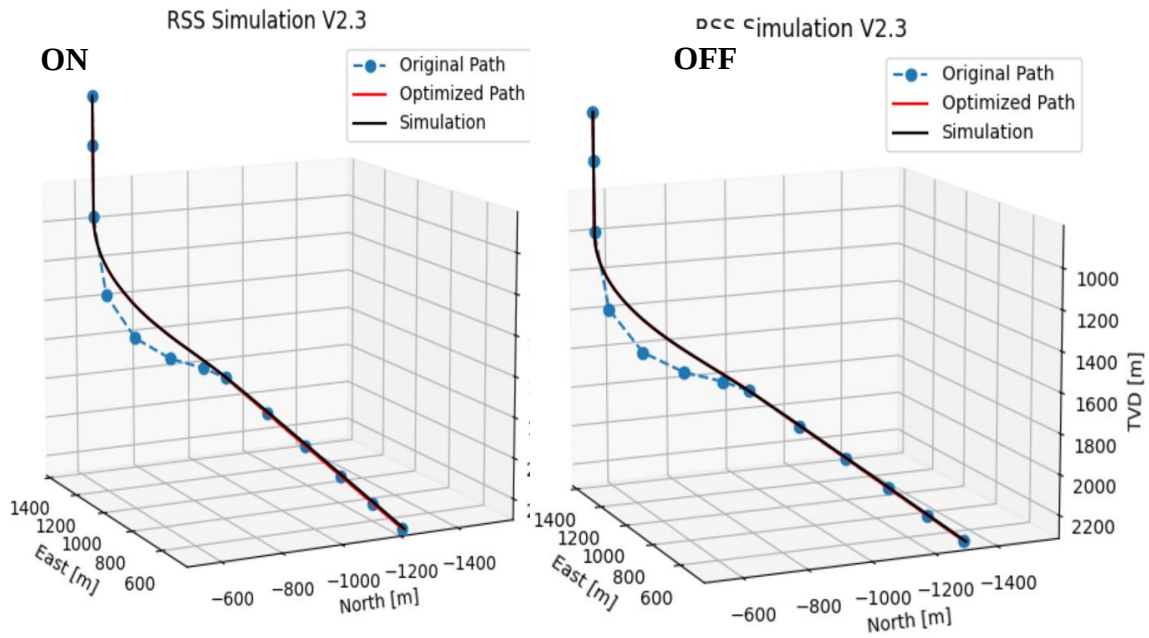

Figure 7.9: Sensitivity Analysis +50% RPM for J-Shaped Well, zoomed-in.

7.2.2. Sensitivity Analysis of RPM in S-Shaped Well

The same parameter was evaluated for the second case, the S-Shaped well. The values of RPM are provided in Table 7.1 and are the same as the J-Shaped Well. The first analysis was done by decreasing the value of RPM by 50%. The results can be found in the plots shown in Figure 7.10. As seen in this figure, the decrease in RPM does not provide any major changes in the trajectory compared to the initial evaluation of the simulator.

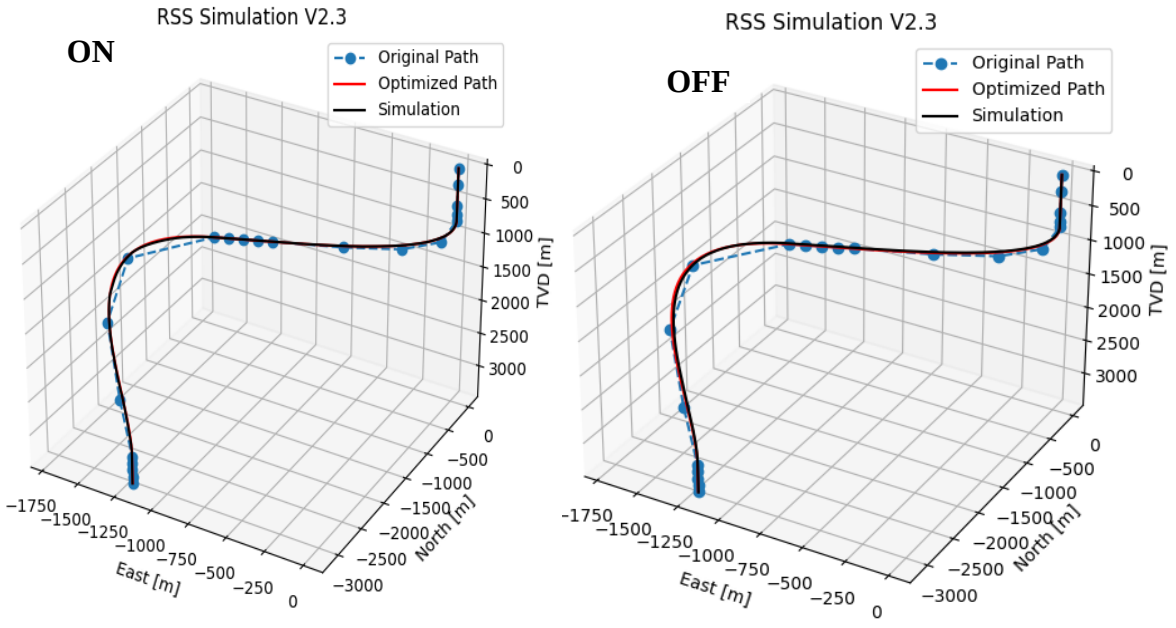

Figure 7.10: Sensitivity Analysis -50% RPM for S-Shaped Well.

As seen with the first case, the changes are minor and, therefore, can be neglected. Although the RPM decrease presented a small but perceptible change in the J-Shaped well, this does not happen in the S-Shaped well. The TOC analysis does not seem to change either, providing similar results to the original simulation, as seen in Figure 7.11.

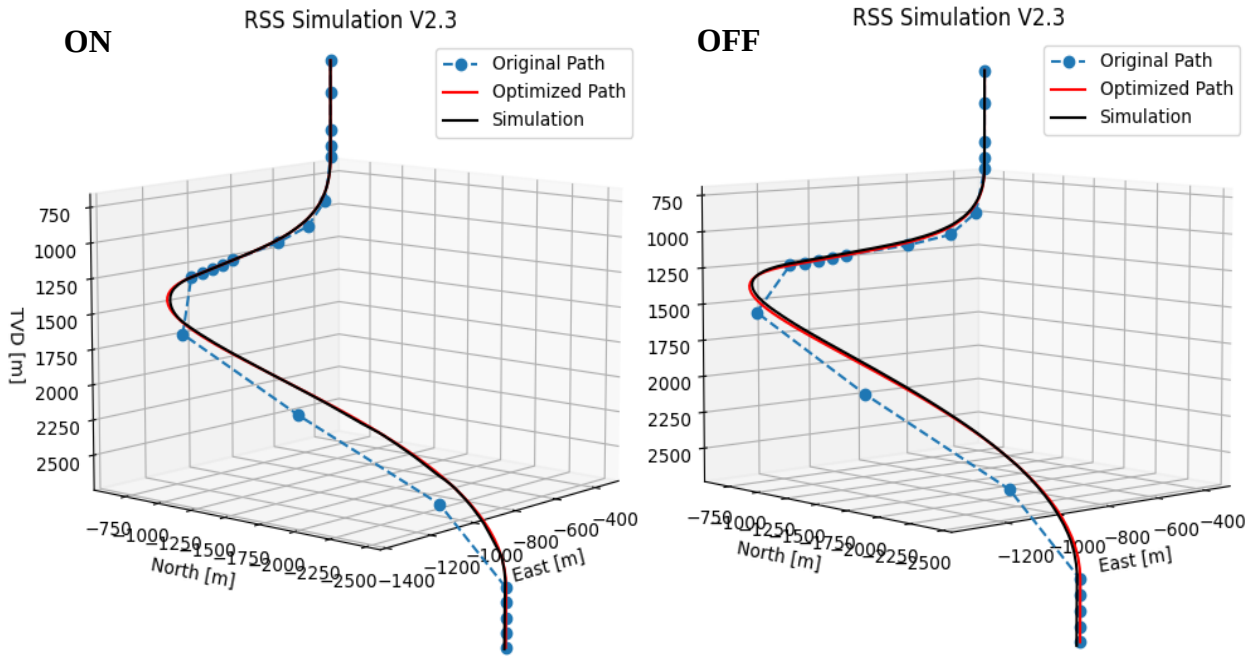

Figure 7.11: Sensitivity Analysis -50% RPM for S-Shaped Well, zoomed-in.

The second analysis, the RPM increase by 50%, presents the same results as the decreased RPM and the J-Shaped. Again, the trajectory barely variates from the original simulation, providing good simulation results regardless of the changes in RPM values, as seen in Figure 7.12.

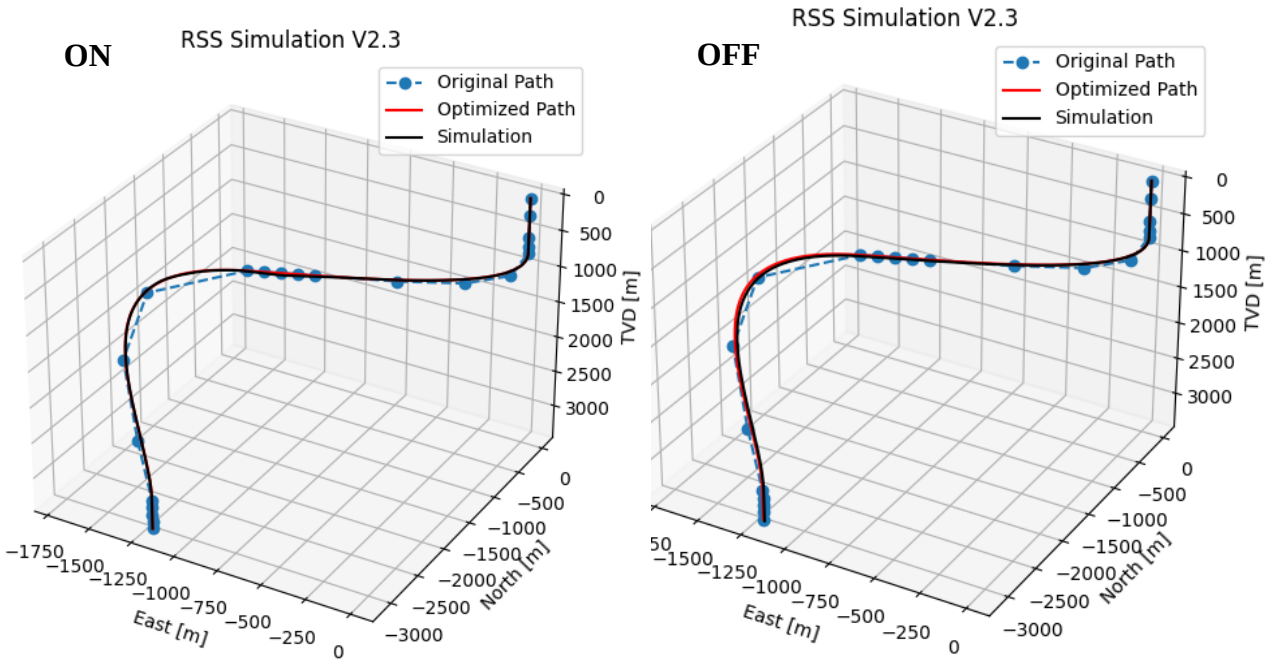

Figure 7.12: Sensitivity Analysis +50% RPM for S-Shaped Well.

However, differently from the J-Shaped well, where the decrease in RPM seems to show a larger variation, the S-Shaped well appears to be the contrary, where the RPM increase seems to affect the well more, at least for the TOC Off case, as seen in Figure 7.13.

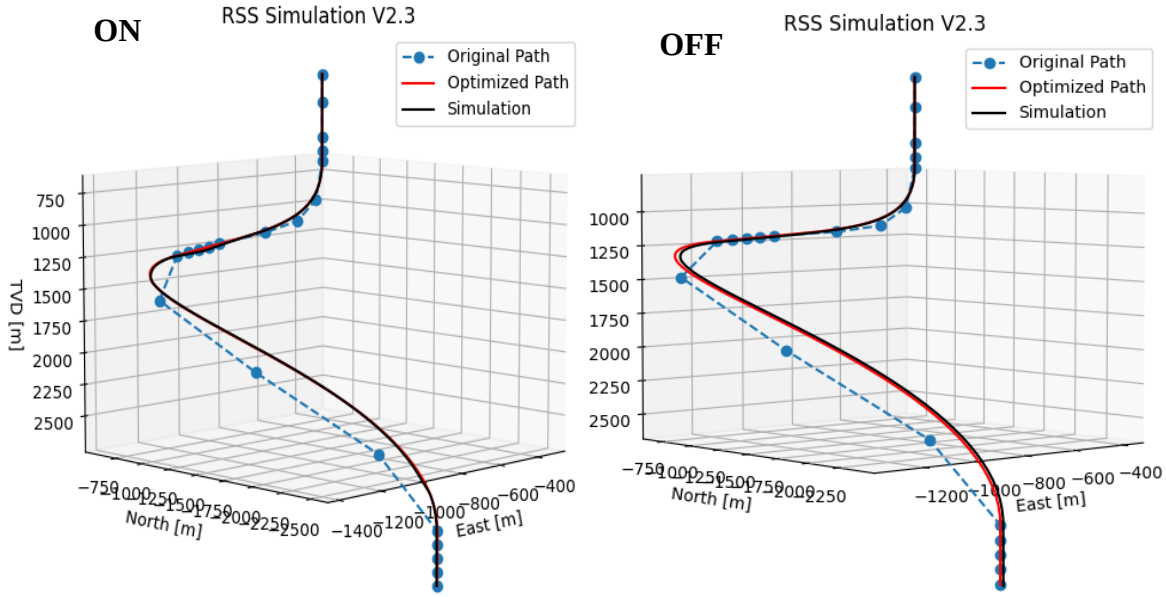

Figure 7.13: Sensitivity Analysis +50% RPM for S-Shaped Well, zoomed-in.

This difference might come from the shape of each well. Since this case provides a more complex well shape, perhaps a smaller RPM better contributes to this well's trajectory design than a larger RPM.

7.3. Sensitivity Analysis of μ

The μ, also known as the sliding factor, is another parameter introduced in the PWP simulator to project the well trajectory. It is defined as the product of the formation aggressiveness and the bit aggressiveness factor. A sensitivity analysis was performed on μ for both wells, J-Shaped and S-Shaped.

Similar to the RPM analysis, a change in the TOC was also evaluated for each of the changes performed to determine if μ's parameter would affect the well trajectory or, like the RPM, would provide no major changes in the trajectory.

The analysis was in the same manner as the RPM analysis, by altering the values of μ into both directions, negative and positive. In addition, the original value was increased and decreased by 50%, and the simulation was performed for both TOC On and OFF. Table 7.2 shows the values of μ used for these simulations.

Table 7.2: Values of μ used for Sensitivity Analysis.

Variable	Value	Unit
μ (sliding_factor) – 50%	0.115	dimentionless
μ (sliding_factor) – 0%	0.23	dimentionless
μ (sliding_factor) + 50%	0.345	dimentionless

7.3.1. Sensitivity Analysis of μ in J-Shaped Well

The initial part of this analysis was done by decreasing the value of μ by 50%. The results are found in the plots shown in Figure 7.14. As seen in this figure, the decrease in μ does not alter the trajectory. In fact, the parameter μ appears to affect the trajectory even less than the RPM.

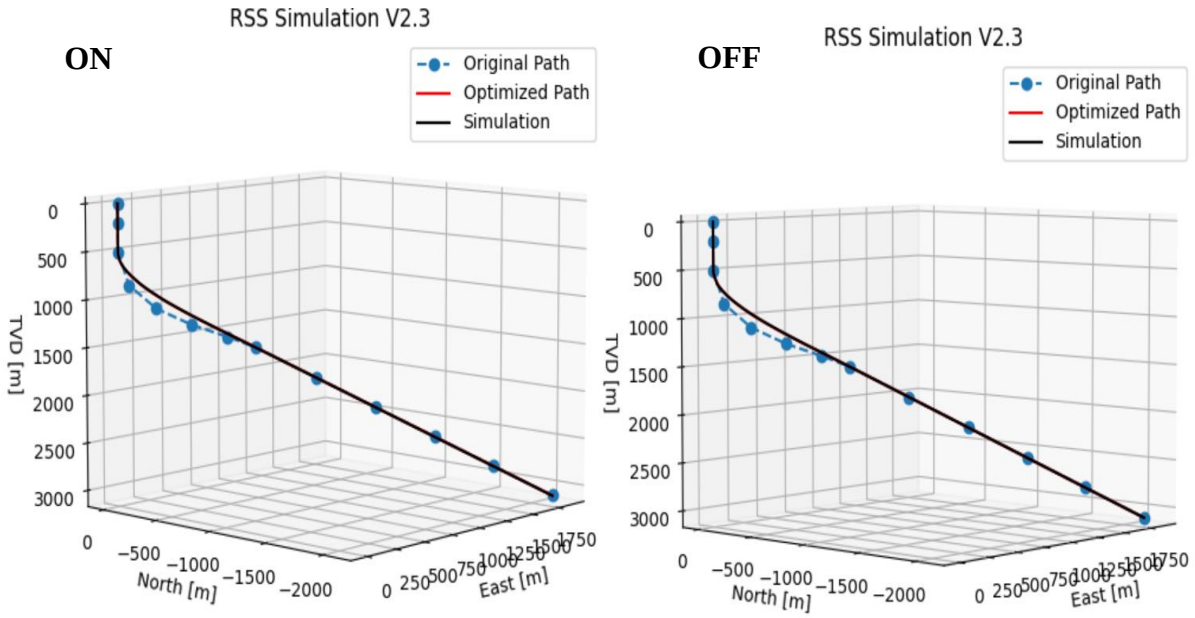

Figure 7.14: Sensitivity Analysis -50% μ for J-Shaped Well.

It is possible to assume that the differences are too small. The trajectory is the same as the one presented in the original simulation case; having the same principle is valid to the TOC analysis.

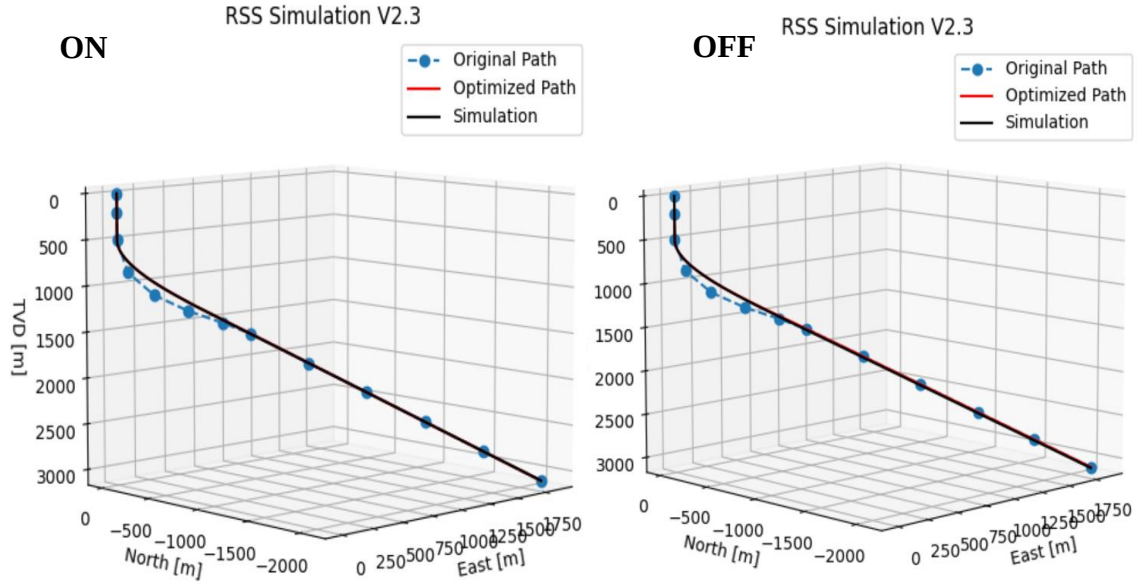

Figure 7.15: Sensitivity Analysis +50% μ for J-Shaped Well.

Identical to the analysis of the decreasing μ, the increasing μ seems not to change much of the trajectory either. As seen in Figures 7.15, these are so minor that they can be neglected for both cases with TOC On/Off. The trajectories are, therefore, similar to the ones found previously in

the original simulation. In this case, it is safe to assume that the change in the value of μ will not affect the trajectory.

7.3.2. Sensitivity Analysis of μ in S-Shaped Well

The parameter was evaluated for the second case, the S-Shaped well, to observe if, in a more complex well shape, μ would behave differently. The values of μ are provided in Table 7.2 and are the same as the J-Shaped Well.

The initial analysis was done by decreasing the value of μ by 50%. The results can be found in the plots shown in Figure 7.16. The decrease in μ does not provide any major changes in the trajectory compared to the initial evaluation of the simulator, the same result found by the J-Shape μ analysis.

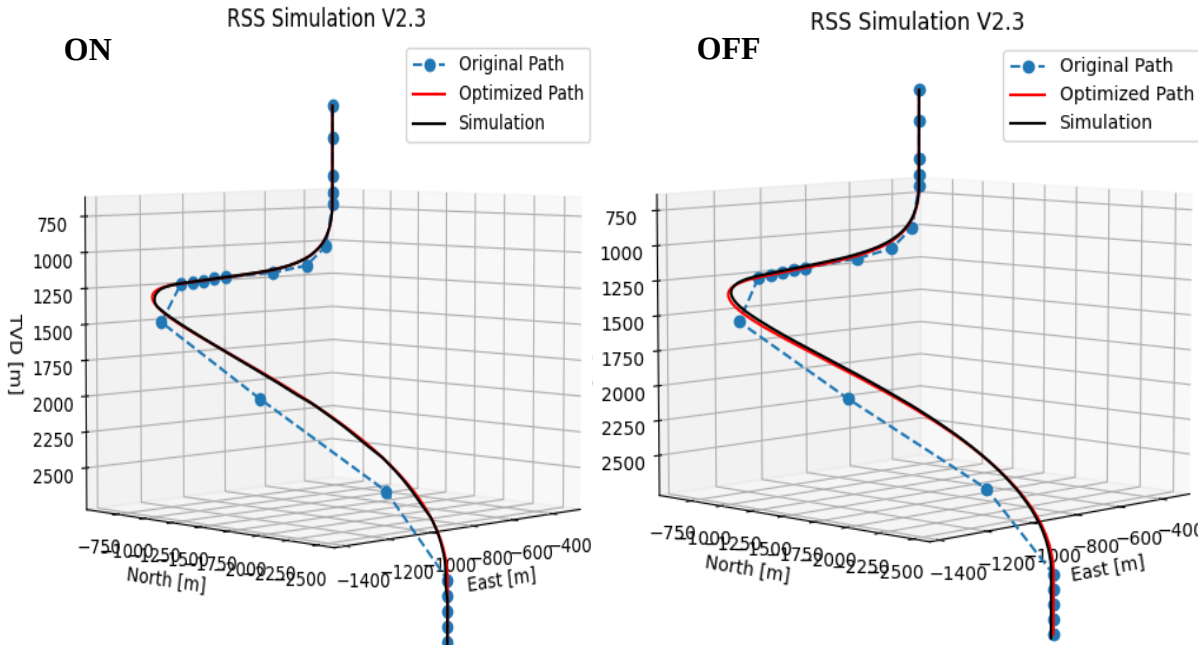

Figure 7.16: Sensitivity Analysis -50% μ for S-Shaped Well.

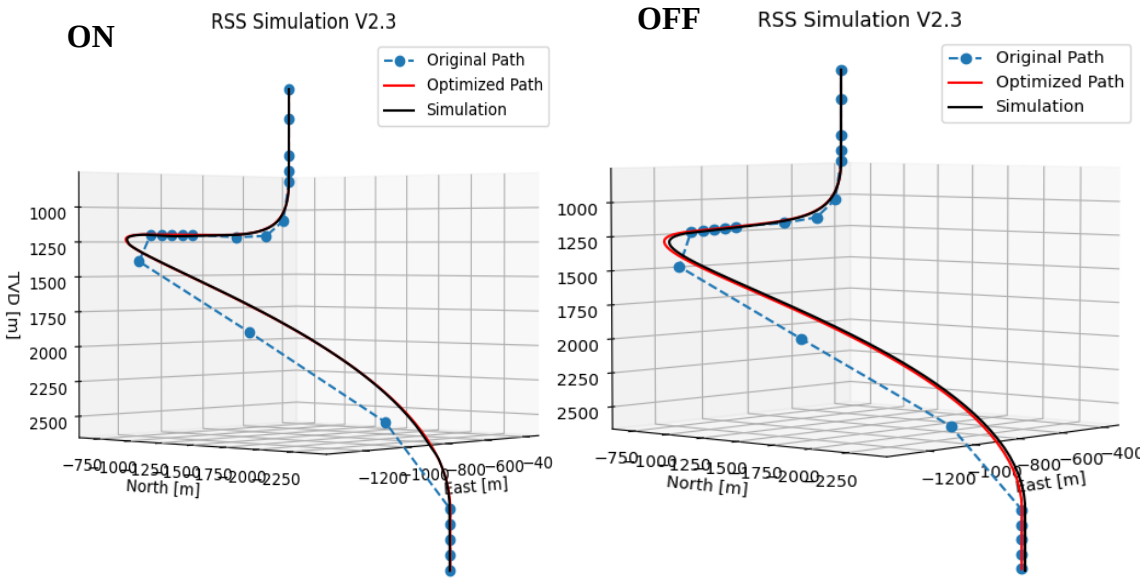

Figure 7.17: Sensitivity Analysis +50% RPM for S-Shaped Well, zoomed-in.

For the second case, the increase of 50% on μ value, the same results are found, yet again. The change in μ value does not appear to alter the trajectory for either TOC On/Off case, as seen in Figure 7.17. As well as it was found with the J-Shaped well, it is safe to assume that the S-Shaped well trajectory is not affected by the change in μ either.

7.4. Sensitivity Analysis of WOB

Finally, the last sensitivity analysis is made, the WOB analysis. The WOB is an important parameter for the trajectory design; as shown in this section modifying this parameter causes great alterations to the trajectory and the performance of the RSS Simulator.

These divergencies can be seen from the beginning of the analysis by altering the WOB value in the same aspect as the other parameters. Due to this occurrence, a further study was performed by providing more WOB values than the former parameters to find the simulator's limitations. These values are expressed in Table 7.3.

Table 7.3: Values of WOB used for Sensitivity Analysis.

Variable	Value	Unit
WOB – 50%	34933	N
WOB – 35%	45413	N
WOB – 0%	69 866	N
WOB + 50%	104 799	N
WOB +100%	139 733	N
WOB +150%	174 666	N
WOB +200%	209 599	N

As done for the previous analyses, these values were checked for trajectories designed with and without the TOC and compared against the original trajectory and the TOC performance trajectories.

7.4.1. Sensitivity Analysis of WOB in J-Shaped Well

The initial analysis performed was done in the J-Shaped well. A value of -50% of the WOB was chosen to evaluate the well trajectory design. However, the simulator presented a failure in its interations right from the start when trying to provide a trajectory with the TOC On.

The problem was found to be with the maximum DLS value set by the user. According to the simulator, the trajectory could not be optimized or found an adequate curve for the current maximum DLS value.

Accordingly, the test was performed with the TOC Off. Although this time the simulation could run without further problems, the well trajectory found by this run was far from the PWP and the original survey trajectories.

As seen in Figure 7.18, the trajectory simulated presents an extremely sharp angle in its build-up section, becoming a horizontal well after this section. Nonetheless, it presented a slightly similar shape although reduced in size and did not exhibit the same target coordinates.

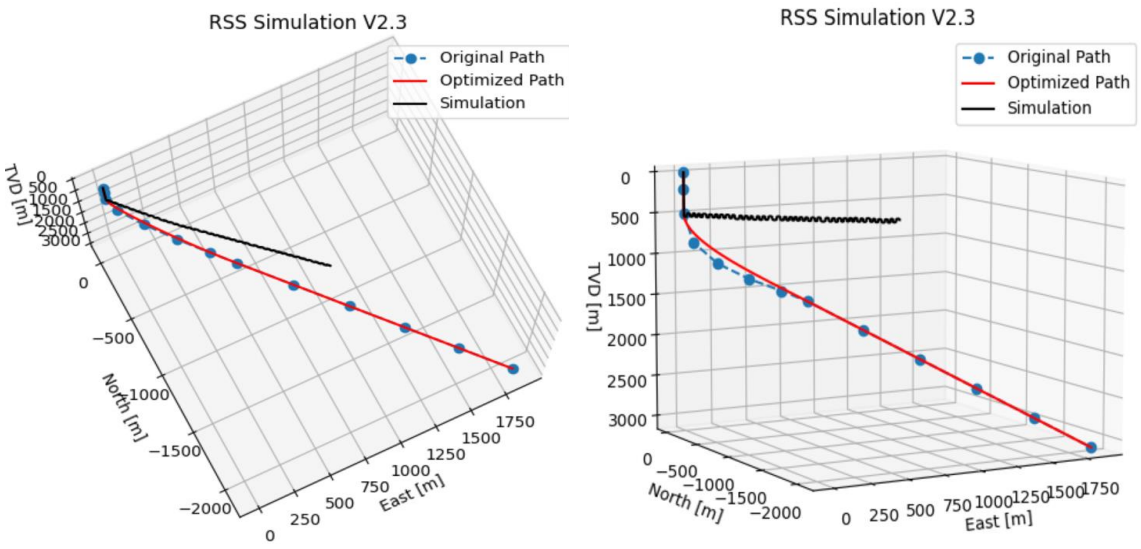

Figure 7.18: Trajectory simulation for J-Shaped well with TOC off.

Once this result was found, several analyses were performed to find the low limit of the WOB value. As a result, it was discovered that -35% of the original WOB value was the limitation for this parameter to provide an optimized DLS in the simulator. The results of the -35% WOB simulation are presented in Figure 7.19.

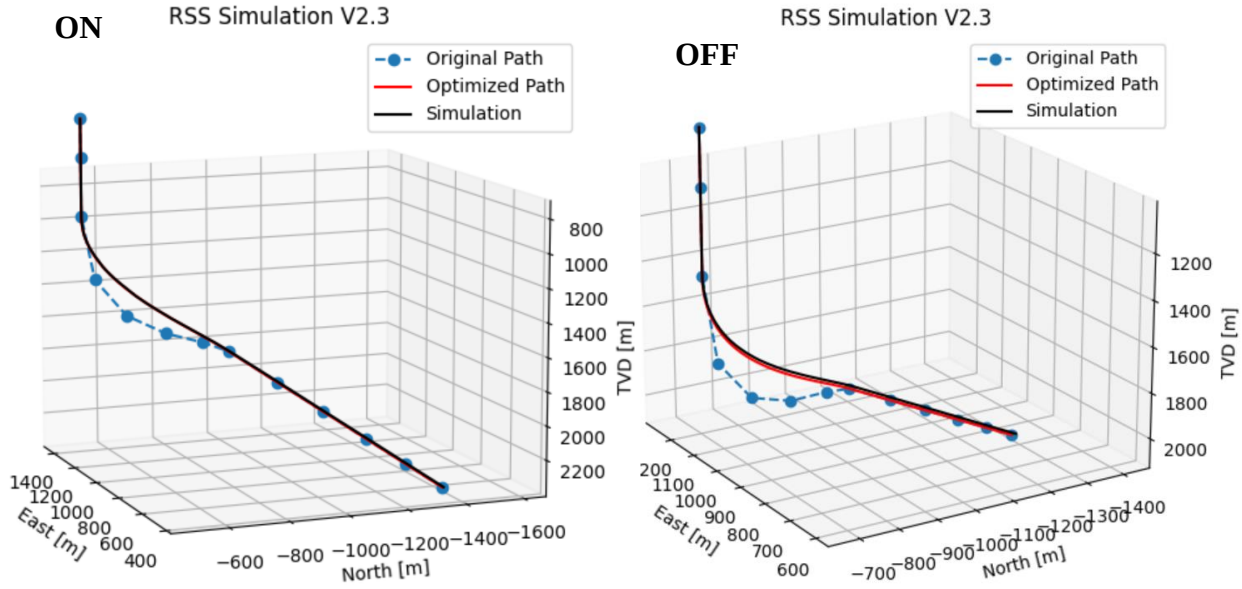

Figure 7.19: Sensitivity Analysis -35% WOB for J-Shaped Well.

Analyzing these plots, it is possible to observe that not a lot has changed between the case study results and the -35% WOB simulation results. The J-Shaped well simulation remains extremely close to the PWP path, and the TOC Off results still provide more deviation than the TOC On. This situation provides the conclusion that decreased WOB will only present major differences for cases where the TOC is off and the DLS cannot be optimized.

Following, the analysis of the increased WOB was done. The first value chosen was +50% WOB, and the results can be seen in Figure 7.20. As seen in the plot, a slight variation can be observed in the build-up section of the well for the TOC On.

For the TOC Off, the entire curved section presents a large deviation compared to the case study. Therefore, it is possible to assume that the increase in WOB will impact the bit steering. To prove this theory, more increasing the WOB analysis was done.

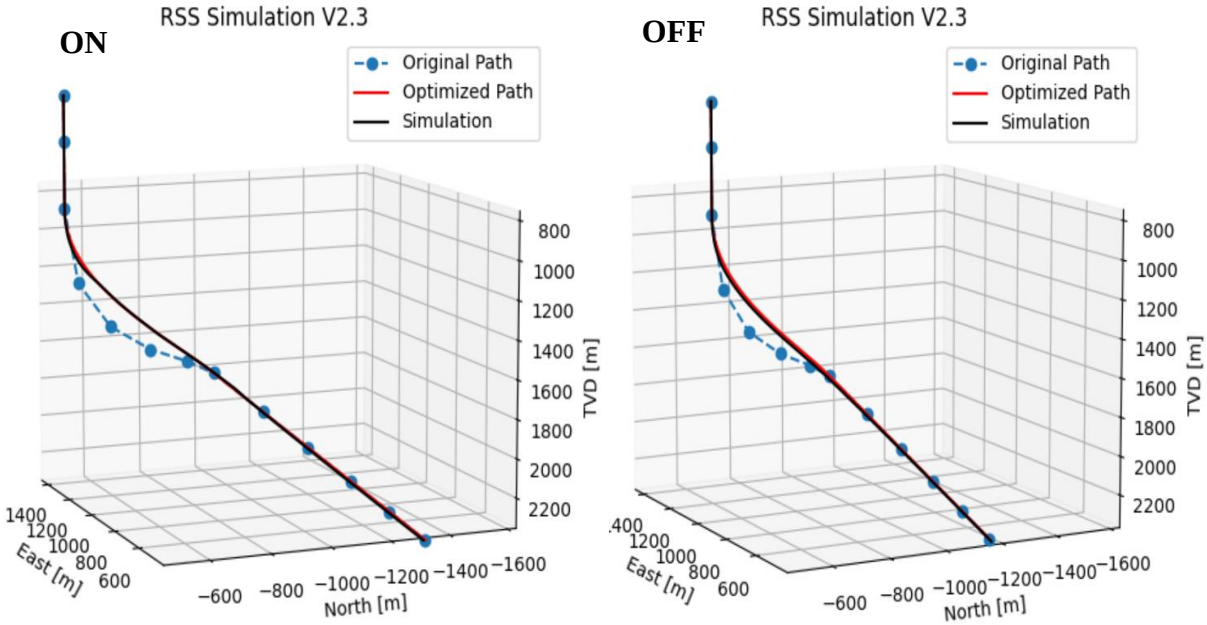

Figure 7.20: Sensitivity Analysis +50% WOB for J-Shaped Well.

The results for the analysis of the +100% WOB are shown in Figure 7.21. As seen, for the TOC On, the simulation has a good result for the vertical section of the well; however, it appears to follow the original path from the survey points instead of the PWP path for the curved section.

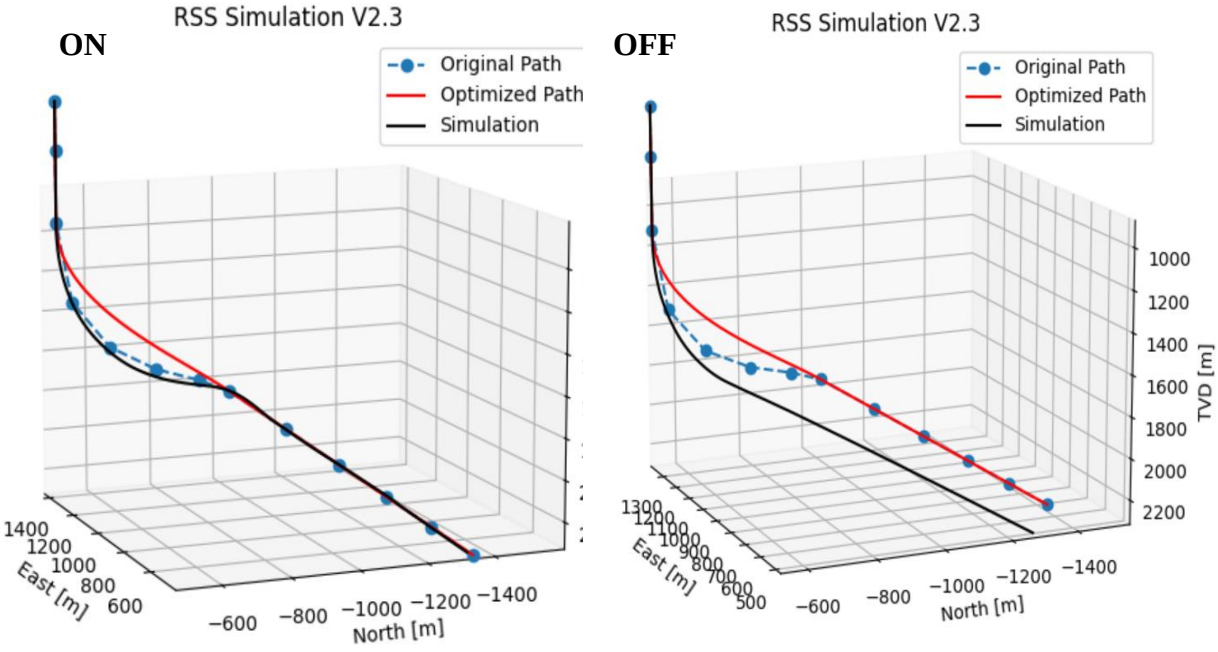

Figure 7.21: Sensitivity Analysis +100% WOB for J-Shaped Well.

For the TOC Off, the vertical section presents good results; nonetheless, the well following the KOP does not perform adequately. It presents an extreme deviation from both the PWP and the original paths and does not reach the target at the correct coordinates.

Continuing the investigation, the +150% WOB was executed. In like manner as the -50% WOB analysis, the results for this investigation show that the well trajectory cannot be performed with a WOB +150% above the original one. According to the simulator, the trajectory could not be optimized or found an adequate curve for the current maximum tortuosity value set by the user. However, the trajectory design was accomplished with the TOC Off, and the results are shown in Figure 7.22.

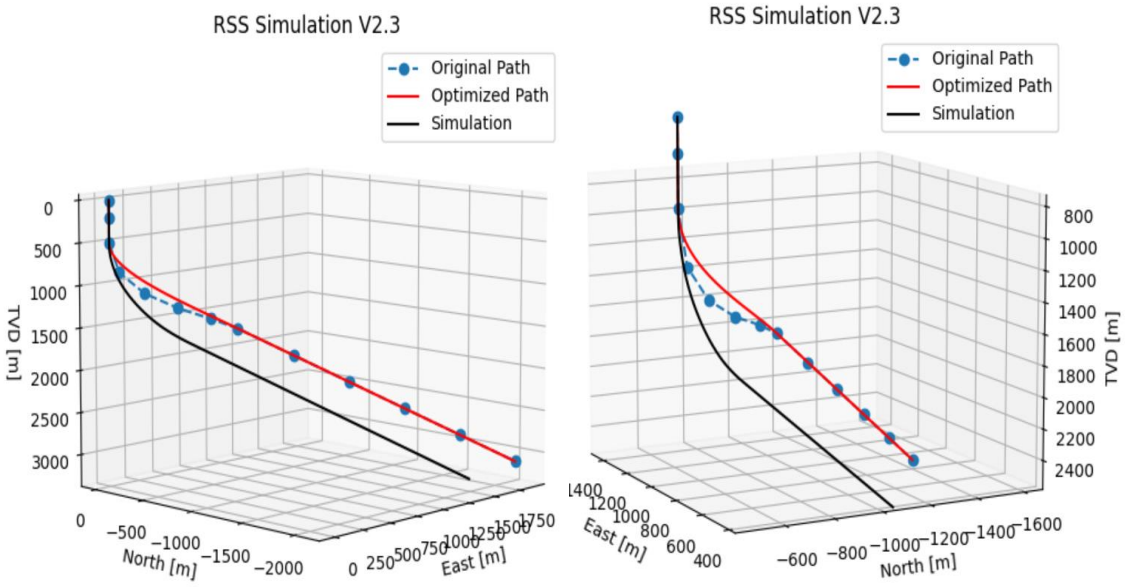

Figure 7.22: Sensitivity Analysis +150% WOB for J-Shaped Well, TOC Off.

As seen in the plots, the trajectory found here is quite similar to the one found in the +100% analysis for TOC Off; the difference appears to be in the distance between the simulation path and the other paths since, in this case, the path developed further away from the PWP and original paths if compared to the +100% case.

As for the 200% WOB analysis, this one also presents no results for the TOC On simulation due to the same problem found in the 150% WOB analysis. The maximum value of tortuosity could not be found. Therefore, the only result provided here is for the TOC Off.

Figure 7.23 shows the results of this investigation. From the plots, it is possible to observe that the higher the increase in the WOB, the larger the distance between the simulation path and the PWP and original paths. The zoomed-in version on the right shows how different the original target is from the simulated one; the gap between these points is extremely large. Therefore, is it safe to assume this is not a very reliable simulation.

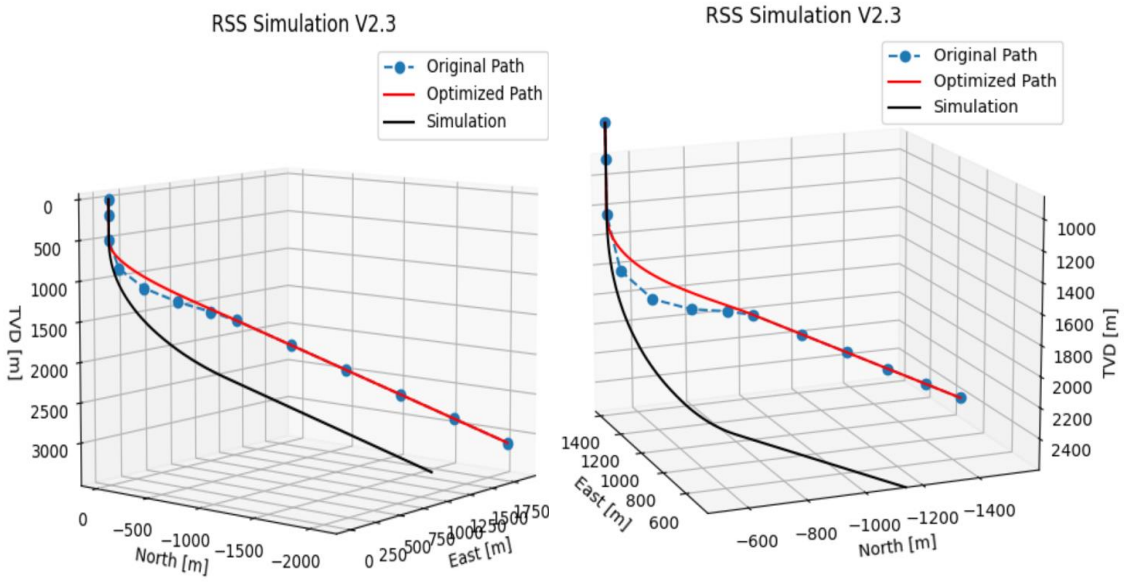

Figure 7.23: Sensitivity Analysis +200% WOB for J-Shaped Well, TOC Off.

7.4.2. Sensitivity Analysis of WOB in S-Shaped Well

The initial analysis for the S-Shaped well was done in the same way as the J-Shaped well. A value of -50% of the WOB was chosen to evaluate the well trajectory design. Alike the J-Shaped well, the simulator presented a failure in its interations right from the start while trying to provide a trajectory with the TOC On.

The problem was also found to be with the maximum DLS value set by the user. According to the simulator, the trajectory could not be optimized or found an adequate curve for the current maximum DLS value.

Respectively, the test was performed with the TOC Off. Albeit the simulation could run without further problems, the well trajectory found was far from the PWP and the original survey trajectories.

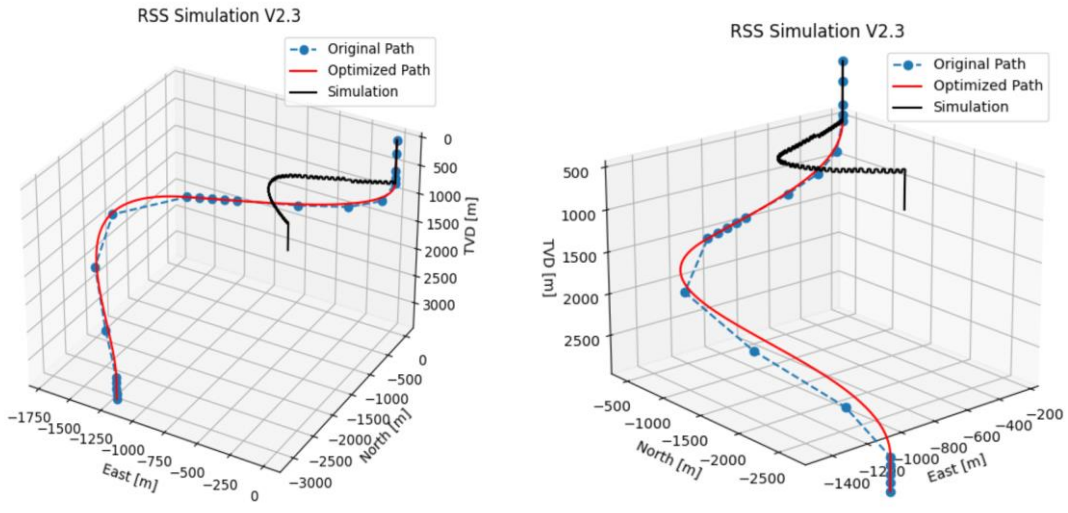

Figure 7.24: Sensitivity Analysis -50% WOB for S-Shaped Well, TOC Off.

As seen in Figure 7.24, the trajectory simulated presents the same shape as the PWP and original paths; nonetheless, it reduced in size and did not exhibit the same target coordinates as them. It is also possible to see that the curved sections of the well now present with a sharp inclination of apparently 90°, not fitted for a well trajectory design.

As discovered with the J-Shaped well that -35% of the original WOB value was the limitation for this parameter to provide an optimized DLS in the simulator, a new analysis was performed with this limit. The results of the -35% WOB simulation are presented in Figure 7.25.

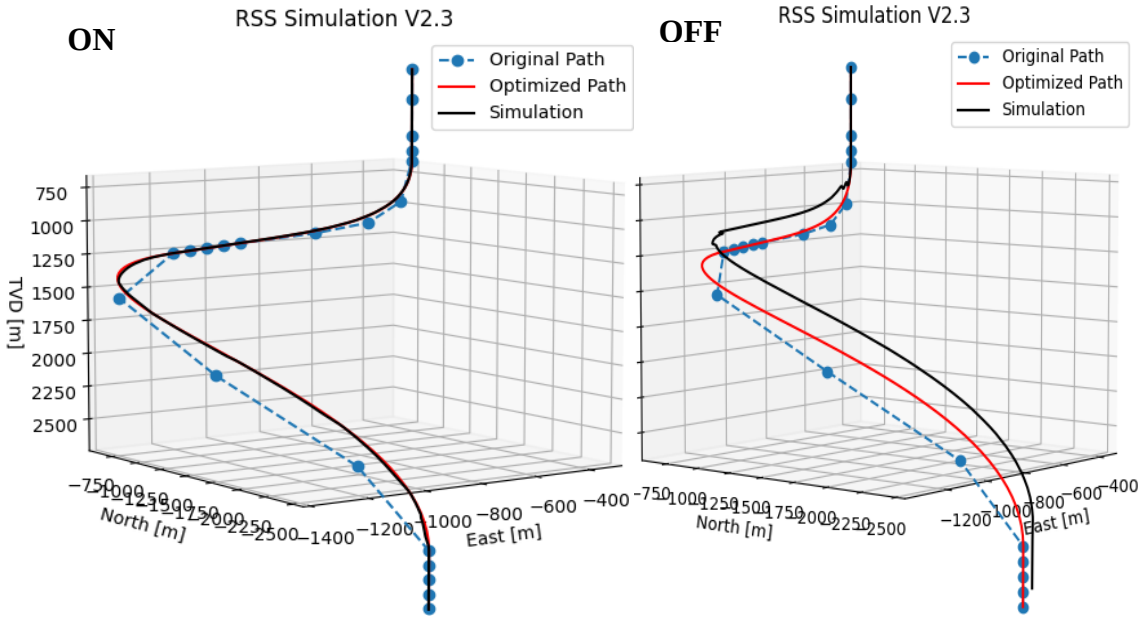

Figure 7.25: Sensitivity Analysis -35% WOB for S-Shaped Well.

Examining the TOC On plot, it is possible to observe that the simulator does a good job with the trajectory optimization; however, if compared with the original case, there is a small deviation from the simulation regarding the PWP path, although both simulations present final points extremely close to the original target.

The effect of the decreased WOB is better seen once the TOC is shut off; without this tool, the trajectory becomes highly deviated from the optimized one. The first problem found with this simulation is observed in the curved section of the well, where the KOP angle becomes remarkably sharp. The second problem is the deviation between the PWP and the simulation paths, which shifts the well up, causing the third problem, the final target being shifted to a different position.

The analysis further continued with investigating the increase in the WOB value by the same percentages presented in the J-Shaped well section. The first increment was +50%, and the results can be seen in Figure 7.26.

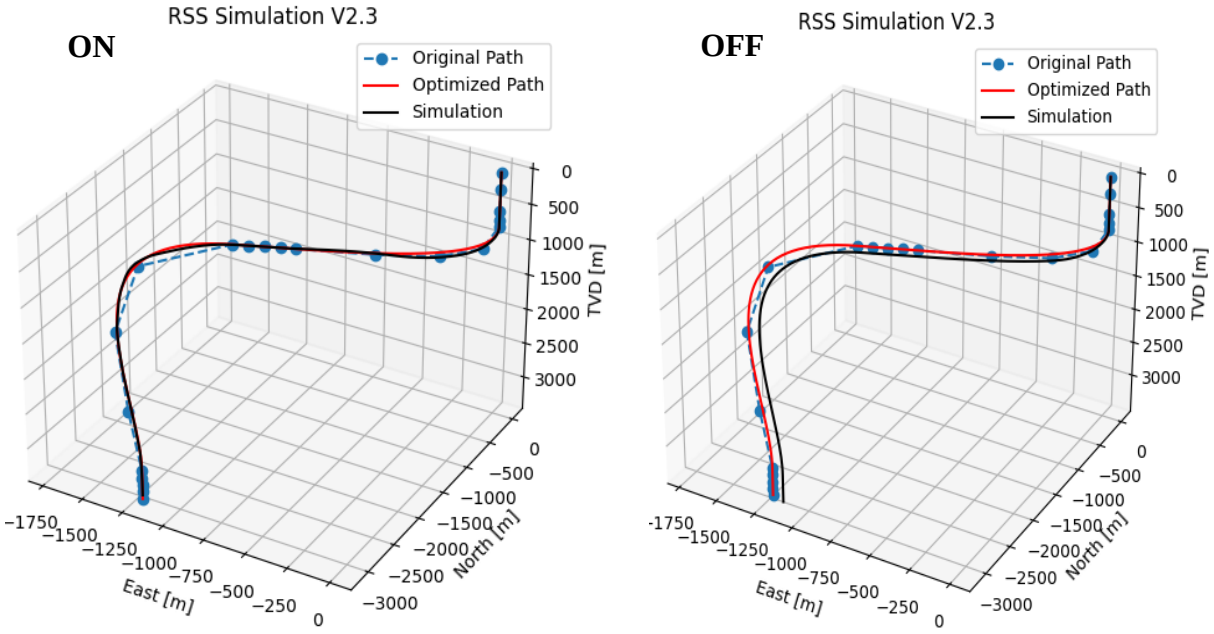

Figure 7.26: Sensitivity Analysis +50% WOB for S-Shaped Well.

As seen in the figure, the increase in WOB also provides a deviation in the well trajectory. This occurs in the curved section for the TOC On, where the trajectory shifts slightly towards the left of the PWP curve; nonetheless, the target point is very closely reached, and the trajectory does not appear to present any problems.

The TOC Off displays fewer problems than in the previous case but still displays some deviation from the PWP curve. The simulation curve follows the PWP curve until the beginning of the KOP, where it starts shifting its trajectory towards the north of the well; because of said shift, the final target is met with a deviation from the optimized one.

The second increment, the +100% WOB is then simulated to provide more data on the effect of the increase of WOB for the simulator. However, just like with the -50% WOB case, the simulator is unable to perform with the TOC On. As stated in the simulation, it could not be optimized or found an adequate curve for the current maximum tortuosity value.

Therefore the only simulation acquired was with the TOC Off; as seen in Figure 7.27, this increment in the WOB value has caused major problems with the simulation results. The vertical section of the well remains a good match for the simulation. However, the first problem is met when this section continues for longer, which causes the curved section to be shifted lower than the optimized path, providing a final target point with an extreme deviation down the original target.

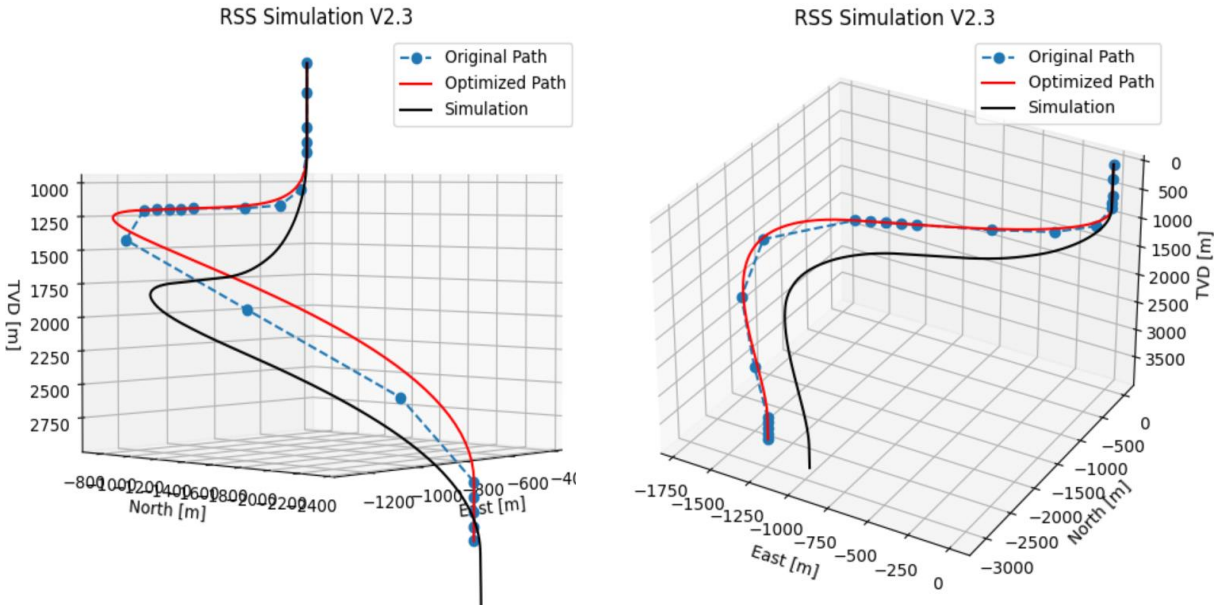

Figure 7.27: Sensitivity Analysis +100% WOB for S-Shaped Well, TOC Off.

The same results can be found when increasing the WOB by +150% and 200% as well. In both cases, the simulation with the TOC On cannot be achieved, this time due to problems with the maximum DLS. As stated in the simulation, the trajectory could not be optimized or found an adequate curve for the current maximum DLS value. Therefore, only the plots for the TOC Off can be analyzed.

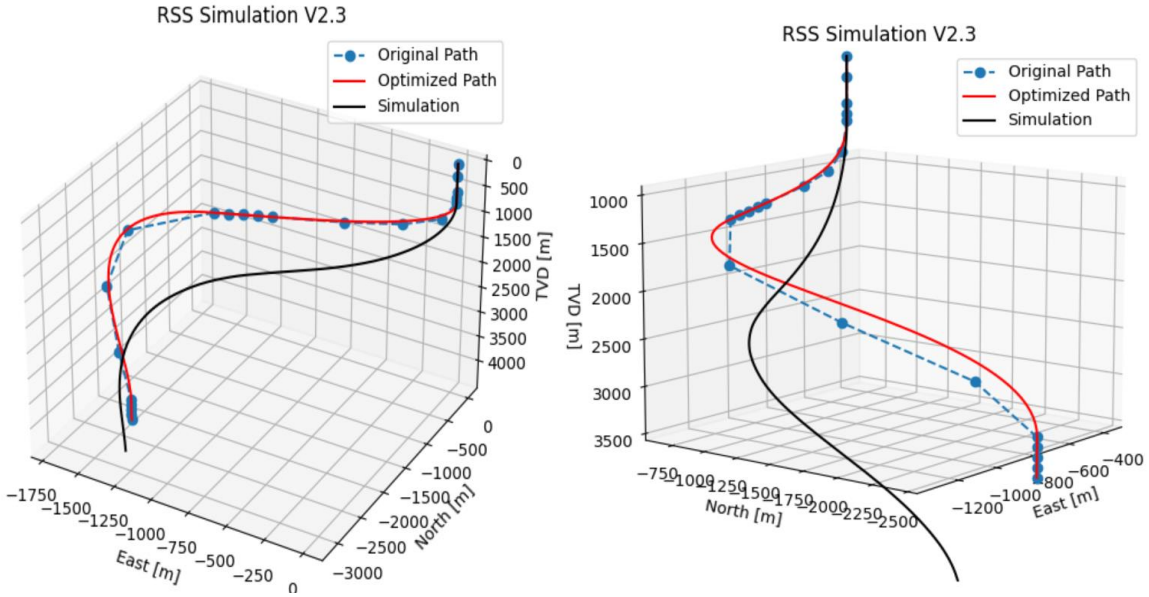

Figure 7.28: Sensitivity Analysis +150% WOB for S-Shaped Well, TOC Off.

Figure 7.28 shows the TOC Off at +150% WOB, where a huge discrepancy between the PWP path and the simulation path can be observed. Different from the previous cases where the trajectory kept its shape while shifting its coordinates, in this case, the shape suffers some alterations as well. The angles of the curved sections are larger and flatter than the original angles, and the final target is met at a greater distance from the original one.

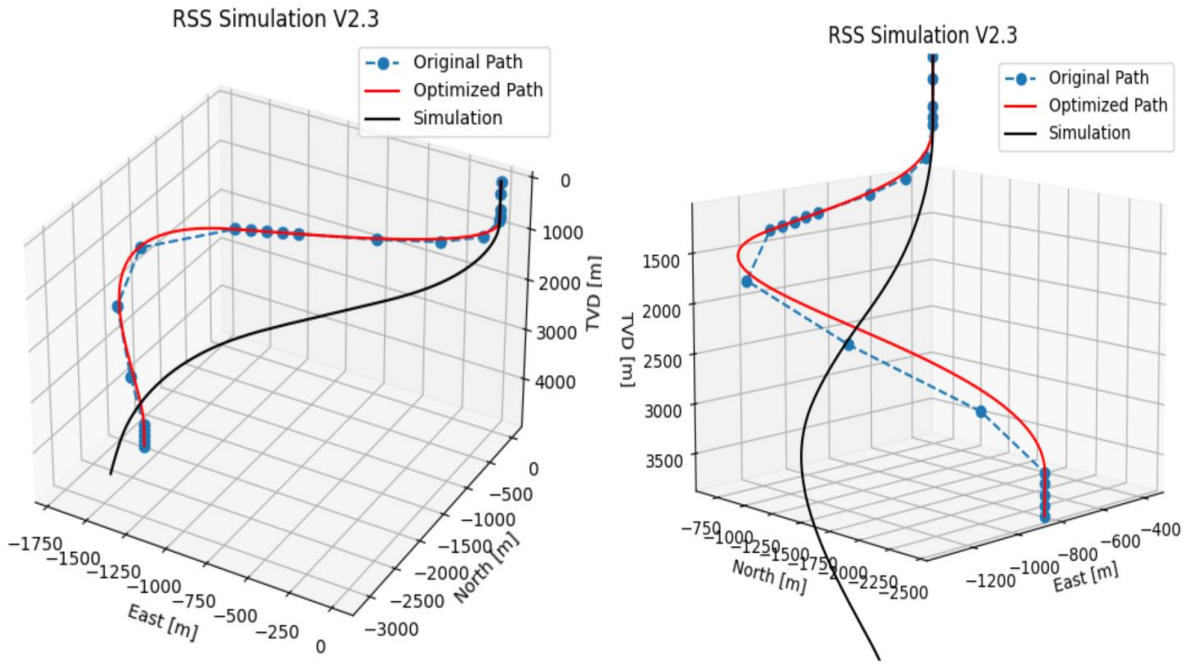

Figure 7.29: Sensitivity Analysis +200% WOB for S-Shaped Well, TOC Off.

The same phenomenon happens for the last case, the TOC Off +200% WOB; this time, the differences are accentuated. The angles of the curved sections are very dull; the trajectory is extremely flat if compared to the original, and the final target is not only far from the original coordinates but has also shifted down, meeting a lower TVD.

7.5 Discussions

The sensitivity analysis results demonstrate that although some small deviation might be expected, the trajectory does not seem to be sensitive to RPM or μ changes; however, it is quite sensitive to the change of WOB.

It appears that the choice of WOB will have an obvious impact on the real-time bit steering if no Real-Time Control scheme is implemented. The big deviations between true and planned bit are anticipated when the WOB is too large or too small. The selection of WOB shall also consider the severity deviation.

When interpreting the plots for the TOC Off, the severity of the gap between PWP, original and simulated paths can be represented with numbers (1 to 4), 4 meaning worse severity, and 1 meaning best severity. For each case, the severity can be evaluated as:

- Case 1. J-Shaped Well, WOB -50%, severity is 4
- Case 2. J-Shaped Well, WOB -35%, severity is 2
- Case 3. J-Shaped Well, WOB 0%, severity is 1
- Case 4. J-Shaped Well, WOB +50%, severity is 2
- Case 5. J-Shaped Well, WOB +100% severity is 3
- Case 6. J-Shaped Well, WOB +150% severity is 4
- Case 7. J-Shaped Well, WOB +200% severity is 4

For the S-Shaped well, the results of severity can be analyzed as:

- Case 1. S-Shaped Well, WOB -50%, severity is 4
- Case 2. S-Shaped Well, WOB -35%, severity is 3
- Case 3. S-Shaped Well, WOB 0%, severity is 1
- Case 4. S-Shaped Well, WOB +50%, severity is 2
- Case 5. S-Shaped Well, WOB +100% severity is 3
- Case 6. S-Shaped Well, WOB +150% severity is 4
- Case 7. S-Shaped Well, WOB +200% severity is 4

It was expected that for a smaller WOB, the severity to be higher. However, it seems this thought was not correct since the analysis of the increased WOB shows that by increasing the WOB, the severity also increases.

Some recommendations that can be done are performing further analysis on the RPM and μ for higher and lower increments until finding the limits of these and investigating if the trajectory will, eventually, be affected. Another recommendation is to perform this analysis after modifying the correction parameters of DLS and tortuosity and investigate if the limits for the simulator with the TOC On are altered.

8. Conclusion and Recommendations

The performance of the RSS simulator regarding the TOC has provided acceptable results for the trajectory optimization given three coordinate points. Albeit some areas could be improved, especially in regards to the curved sections of the well, these results are very promising.

Concerning the Well Design simulator, its capacity to use data from different offset wells, integrate different models in its calculations, and update in real-time the well plan are all good features that provide the simulations with encouraging results for the drilling design of challenging wells.

For the current stage of the Drillbotics Team A's work, the Well Design Web application and the Real-Time Drilling Simulator, although not in their initial stages any longer, still present themselves with many future improvements to be performed.

The main improvement needed by the current RSS Simulator is providing the formation model and the bit model integration into the code, an obligatory feature for the Drillbotics Competition. Another important improvement that should be addressed soon is designing a model to calculate the walk rate since the competition judges request said value.

The team also envisions transferring the codes from the Python platform into C++ and integrating all models into a singular GUI, which would allow the team and others to operate the simulator more intuitively.

Additionally, some future analysis can be done in the RSS Simulator to determine if other input parameters, such as the specific energy of the rock and the bit steerability, provide any alterations in the trajectory and if by changing the maximum values of DLS and tortuosity for the correction parameters the results found in section 7.4 would change.

9. References

Aadnoy, B.S., Fazaelizadeh, M., Hareland, G. (2010). A 3-Dimensional Analytical Model for Wellbore Friction. Journal of Canadian Petroleum Technology.

Abbas, A. K., Alameedy, U., Alsaba, M., & Rushdi, S. (2018, December 10). Wellbore Trajectory Optimization Using Rate of Penetration and Wellbore Stability Analysis. https://doi.org/10.2118/193755-MS

Abughaban, M. F., et al. (2016). Advanced Trajectory Computational Model Improves Calculated Borehole Positioning, Tortuosity, and Rugosity. IADC/SPE Drilling Conference and Exhibition, Society of Petroleum Engineers.

Ali A.M.B., Idris K.A., Shuk E.M.A, Abdo M.M. (2017). Bottom Hole Assembly Analysis Using Finite Element Analysis Software. M.S. thesis, Sudan University of Science and Technology.

Arabjamaloei, R., Edalatkhah, S., & Jamshidi, E. (2011). A New Approach to Well Trajectory Optimization Based on Rate of Penetration and Wellbore Stability. Petroleum Science and Technology, *29*(6), 588–600. https://doi.org/10.1080/10916460903419172

Barros L.M.L. (2015). ROP Modeling Chronology, Sensitivity Analyses, and Field Data Comparisons. The University of Texas at Austin. Retrieved June 11, 2021 from: http://hdl.handle.net/2152/63891

Belayneh, M. (2006). A review of Buckling in Oil Wells. University of Stavanger.

Bingham, G. (1965). A New Approach to Interpreting Rock Drillability. Tulsa: Petroleum Publishing Company.

Breyholtz, Ø., & Nikolaou, M. (2012). Drilling Automation: Presenting a Framework for Automated Operations. SPE Drilling & Completion, 27(01), 118–126. https://doi.org/10.2118/158109-PA

Burgoyne, A., Millhein, K., Chenevert, M., & Young Jr., F. (1991). Applied Drilling Engineering. Second Edition ed., Vol. 2. Richardson, TX, US: SPE textbook series.

Chen et al. - Modeling of the Effects of Cutting Structure, Impa. (2007). Retrieved June 2, 2021, from https://www.aade.org/application/files/8415/7303/7685/AADE-07-NTCE-10.pdf

Dawson, R., Paslay, P.R. (1984). Drill Pipe Buckling in Inclined Holes, J. Pet. Tech. (Oct.1984), 1734-38.

DeWardt, J. & C. Wolf (1981). Borehole Position Uncertainty-Analysis of Measuring Methods and Derivation of Systematic Error Model. Journal of Petroleum Technology.

Drillbotics®. (2021). Guidelines. Retrieved June 11, 2021, from https://drillbotics.com/ wp-content/uploads/simple-file-list/Guidelines/Guidelines-2021/2021-Drillbotics-Guidelines-v3.pdf

eDrilling. (2019). Artificial Intelligence, Predictive Analytics, and our Digital Tw Artificial Intelligence, Predictive Analytics, and our Digital Twin at IADC/SPEin at IADC/SPE. February 26, 2019. https://edrilling.no/news/artificial-intelligence-predictive-analytics-and-our-digital-twin-at-iadc-spe/

eDrilling. (2021). Products. Retrieved April 26, 2021, from https://eDrilling.no/products/

Eid E. (2020). Workshop: Well Trajectory Optimization, Stavanger, RO, Norway: Drillbotics UiS.

Ekseth, R. (1998). Uncertainties in Connection with The Determination of Wellbore Positions. Ph.D. Thesis, ISBN 82-471-0218-8 ISSN 0802-3271, Ph.D. Thesis no 1998 28 IPT report 1998.2, The Norwegian University of Science and Technology, Trondheim, Norway, March 1998.

Equinor. (2021). Technology, digitalisation and innovation—A new wave of digital transformation is driving sweeping change. Retrieved June 14, 2021, from https://www.equinor.com/en/what-we-do/digitalisation-in-our-dna.html

Farah, F. O. (2013). Directional Well Design, Trajectory and Survey Calculations, with a Case Study in Fiale, Asal Rift, Djibouti. 34. United Nations University.

Farmanbar, P., Revheim, O., Uberg, A. S., Chekushev, A., Cayeux, E., Gravdal, J. E., & Hauge, E. (2020). Digitalization of Detailed Drilling Operation Plans and Verification of Automatic Progress Tracking with an Online Drilling Simulator Environment. Day 2 Wed, March 04, 2020, D091S013R004. https://doi.org/10.2118/199666-MS

Grieves M. (2006). Product Lifecycle Management: Driving the Next Generation of Lean Thinking, McGraw-Hill Education.

Gulyayev, V., & Shlyun, N. (2016). Influence of Friction on Buckling of a Drill String in the Circular Channel of a Bore Hole. Research Gate. Petroleum Science.

Halliburton. (2016). WellPlan Software. H012161 datasheet, 4//16. Retrieved April 27, 2021, from https://www.landmark.solutions/Portals/0/LMSDocs/Datasheets/WellPlan_Software_DATASHEET-.pdf

Halliburton. (2020a). DecisionSpace® 365. Retrieved April 27, 2021, from https://www.landmark.solutions/Portals/0/LMSDocs/PDF/DecisionSpace365.pdf?ver=2021-04-13-194707-547

Halliburton. (2020b). Digital Well Program. Retrieved April 28, 2021, from https://www.landmark.solutions/Portals/0/LMSDocs/PDF/DigitalWellProgram.pdf?ver=2021-03-10-034253-547

Halliburton. (2020c). Holistic Field Development Planning. Retrieved April 28, 2021, https://www.landmark.solutions/Portals/0/LMSDocs/PDF/HolisticFieldDevelopment Planning.pdf?ver=2020-07-01-195325-620

Halliburton. (2020d). Real-Time Control – Edge. Retrieved April 28, 2021, from https://www.landmark.solutions/Portals/0/LMSDocs/PDF/RealTimeControlEdge.pdf?ver=2020-08-31-194845-317

Halliburton. (2020e). Real-Time Well Engineering. Retrieved April 28, 2021, from https://www.landmark.solutions/Portals/0/LMSDocs/PDF/RealTimeWellEngineering.pdf?ver=2021-04-12-193809-450

Halliburton. (2020f). Well Operations Monitor. Retrieved April 28, 2021, from https://www.landmark.solutions/Portals/0/LMSDocs/PDF/Well_Operations_Monitor.pdf?ver=2021-04-21-185132-760

Halliburton. (2021). About Landmark. Retrieved April 27, 2021, from https://www.landmark.solutions/About

Hareland, G., and P.R. Rampersad. (1994). Drag - Bit Model Including Wear. Paper presented at the SPE Latin America/Caribbean Petroleum Engineering Conference, Buenos Aires, Argentina. DOI: https://doi.org/10.2118/26957-MS

Hareland, G.., Wu, A.., and B. Rashidi. (2010). A Drilling Rate Model for Roller Cone Bits and Its Application. Paper presented at the International Oil and Gas Conference and Exhibition in China, Beijing, China. DOI: https://doi.org/10.2118/129592-MS

Hegde, C., Daigle, H., Millwater, H. et al.. (2017). Analysis of Rate of Penetration (ROP) Prediction in Drilling Using Physics-Based and Data-Driven Models. J Pet Sci Eng 159 (November): 295–306. DOI: https://doi.org/10.1016/j.petrol.2017.09.020.

Heriot-Watt professors, Department of Petroleum Engineering, Heriot-Watt University. https://www.software.slb.com/products/product-libraryv2?product=Drillbench&tab=Product%20Sheets

Hosseini, S., Ghanbarzadeh, A., & Hashemi, A. (2014). Optimization of Dogleg Severity in Directional Drilling Oil Wells Using Particle Swarm Algorithm. 48, 13.

Hsieh, L. (2011, September 21). Optimizing ROP through automation. Drilling Contractor. https://www.drillingcontractor.org/optimizing-rop-through-automation-2-10696

ISCWSA. (2017a, May 17). Standard Set of Wellpaths for Evaluating Clearance Scenarios—Excel Workbook. Www.Iscwsa.Net. https://www.iscwsa.net/articles/ standard-wellpath-revision-4-excel/

Jamieson A. (2012). Introduction to Wellbore Positioning. University of the Highlands & Islands Retrieved June 14, 2021, from https://pt.scribd.com/document/374722669/eBook-V9-10-2017-redux

Kahraman, S., Bilgin, N., and Feridunoglu, C. (2003). Dominant Rock Properties Affecting the Penetration Rate of Percussive Drills. Int. J. Rock Mech. Min. Sci., 40 (5), 711-723. https://doi.org/10.1016/s1365-1609(03)00063-7.

Kåre K. (2020). Cuttings transport. Course PET 510 Modellering av reservoar og brønnstrømning. University of Stavanger, UiS.

Kårstad, E. (2020). Buckling principles. Course PET 510 Modellering av Reservoar og Brønnstrømning. University of Stavanger, UiS.

Khadisov M. A. (2020). Directional Drilling: Trajectory Design and Position Uncertainty Study for a Laboratory Drilling Rig, University of Stavanger.

Khadisov, M., Hagen, H., Jakobsen, A., & Sui, D. (2020). Developments and Experimental Tests on a Laboratory-Scale Drilling Automation System. Journal of Petroleum Exploration and Production Technology, 10(2), 605–621. DOI: https://doi.org/10.1007/s13202-019-00767-6

Larsen, T. (1997). Development of a New Cuttings-Transport Model for High-Angle Wellbores Including Horizontal Wells. SPE, Unocal Corp.

Lei, L. (2014). Downhole Weight on Bit Prediction with Analytical Model and Finite Element Method. University of Calgary, Master Thesis. doi:10.11575/PRISM/25743.

Lubinski, A., and Althouse W.S. (1962). "Helical Buckling of Tubing Sealed in Packers." J Pet Technol 14. 655–670. DOI: https://doi.org/10.2118/178-PA

Masoomi, R., & Moghadasi, J. (2014). Mathematical modeling and prediction of drill string stability region. Journal of Petroleum Exploration and Production Technology, 4(4), 351–358. DOI: https://doi.org/10.1007/s13202-013-0097-3.

Mitchell, R.F., & Miska, S. (2011). Fundamentals of Drilling Engineering. Vol. 12. Society of Petroleum Engineers.

Mitchell, R.F. (1996). "Comprehensive Analysis of Buckling with Friction." SPE Drill & Compl 11: 178–184. DOI: https://doi.org/10.2118/29457-PA

Motahhari, H. R., Hareland, G., & James, J. A. (2010). Improved drilling efficiency technique using integrated PDM and PDC bit parameters. Journal of Canadian Petroleum Technology, 49(10), 45-52. DOI:10.2118/141651-PA

Nadhan, E. et al. (2018). Drilling with Digital Twins. SPE IADC Asia Pacific Drilling Technology.

Okpozo, P., & Samuel, O. (2016). The Use of Well Trajectory Design Illustration Tool Version 1.0 in the Design of Directional Well. https://doi.org/10.2118/184282-MS

Olaijuwon, M. (2012). A Study of Wellbore Position Uncertainty in the Ekofisk Field. Master's Thesis, Depth Issues in the Oil patch, University of Stavanger.

Oliasoft AS. (2021a). About. Retrieved April 26, 2021, from https://www.oliasoft.com/about/

Oliasoft AS. (2021b). Blowout & Kill Simulation Module. Retrieved April 26, 2021, from https://www.oliasoft.com/oliasoft-welldesign/blowout-kill-simulation/

Oliasoft AS. (2021c). Casing Design Module. Retrieved April 26, 2021, from https://www.oliasoft.com/oliasoft-welldesign/casing-design/

Oliasoft AS. (2021d). Hydraulics & S&S Module. Retrieved April 26, 2021, from https://www.oliasoft.com/oliasoft-welldesign/hydraulics-and-surge-and-swab/

Oliasoft AS. (2021e). Torque and Drag Module. Retrieved April 26, 2021, from https://www.oliasoft.com/oliasoft-welldesign/torque-and-drag/

Oliasoft AS. (2021f). Trajectory Design. Retrieved April 26, 2021, from https://www.oliasoft.com/oliasoft-welldesign/trajectory-design/

Oliasoft AS. (2021g). Tubing Design Module. Retrieved April 26, 2021, from https://www.oliasoft.com/oliasoft-welldesign/tubing-design/

Pessier R.C., Hughes Tool Co., & M.J. Fear, BP Exploration (1992). Quantifying Common Drilling Problems with Mechanical Specific Energy and a Bit-Specific Coefficient of Sliding Friction. Annual Technical Conference and Exhibition of the Society of Petroleum Engineers held in Washington, DC, October 4-7.

Pessier, R. C., & Fear, M. J. (1992). Quantifying Common Drilling Problems with Mechanical Specific Energy and a Bit-Specific Coefficient of Sliding Friction. All Days, SPE-24584-MS. https://doi.org/10.2118/24584-MS

PetroMehras Directory. (2019a). WellAhead. Retrieved April 26, 2021, from https://www.petromehras.com/petroleum-software-directory/drilling-completion-software/wellahead

PetroMehras Directory. (2019b). WellBalance. Retrieved April 26, 2021, from http://petromehras.com/petroleum-software-directory/drilling-completion-software/wellbalance

PetroMehras Directory. (2019c). WellPlanner. Retrieved April 26, 2021, from http://petromehras.com/petroleum-software-directory/drilling-completion-software/wellplanner

PetroMehras Directory. (2019d). WellSim. Retrieved April 26, 2021, from http://petromehras.com/petroleum-software-directory/drilling-completion-software/wellsim

Pirovolou, D., Chapman, C., Chau, M., Arismendi, H., Ahorukomeye, M., Peñaranda, J., & Schumberger. (2011). Drilling Automation: An Automatic Trajectory Control System. Society of Petroleum Engineers, SPE-143899-MS, 8. DOI: https://doi.org/10.2118/143899-MS

Ren, & Wang. (2017). Modeling and Analysis of Stick-Slip Vibration and Bit Bounce in Drill Strings. In: Journal of Vibroengineering 19.7, pp. 4866–4881.

Richard et al. (2002). Influence of Bit-Rock Interaction on Stick-Slip Vibrations of PDC Bits. In: SPE Annual Technical Conference and Exhibition. Society of Petroleum Engineers.

Rishyank C. (2021). Modelling and analysis of Drill string dynamics using finite element model. University of Stavanger.

Rocha L. A. d. S. (2011). Perfuração Direcional. Editora Interciência. Rio de Janeiro, RJ, Brazil.

Ruiz, R. (2021). Real Time Data Driven ROP and Torque Modelling using Machine Learning. UiS, Faculty of Science and Technology, MSc Drilling and Well Engineering.

Sampaio Jr, J. H. B. (2006). Designing Three-Dimensional Directional Well Trajectories Using Bézier Curves. Journal of Energy Resources Technology, vol. 139.

Sampaio Jr, J. H. B. S. (2007). Planning 3D Well Trajectories Using Spline-in-Tension Functions. Journey of Energy Resources Technology, ASME.

Saramago, C. (2020). Rotary Steerable System Modelling and Simulator. University of Stavanger.

Saavedra L.A.J. (2021). Trajectory Control Optimization Using the RSS Model. University of Stavanger.

Schlumberger. (2015a). DrillBench Dynamic Drilling Simulation Software. Retrieved April 27, 2021, from https://www.software.slb.com/products/drillbench

Schlumberger. (2016). DrillBench Underbalanced and Managed Pressure Drilling. Retrieved April 27, 2021, from https://www.software.slb.com/products/drillbench/ drillbench-underbalanced

Schlumberger. (2021). What is the DELFI Environment? Retrieved April 27, 2021, from https://www.software.slb.com/delfi/what-is-delfi

Schlumberger. (26 June, 2015b). DrillBench Blowout Control. Retrieved April 27, 2021, from https://www.software.slb.com/products/product-library-v2?product=Drillbench &tab=Product%20Sheets

Schlumberger. (2016a, August 19). DrillBench Dynamic Well Control. Retrieved April 27, 2021, from https://www.software.slb.com/products/product-library-v2?product= Drillbench&tab=Product%20Sheets

Schlumberger. (July 22, 2016b). DrillBench Dynamic Hydraulics. Retrieved April 27, 2021, from https://www.software.slb.com/products/product-library-v2?product= Drillbench%20Dynamic%20Hydraulics&tab=Product%20Sheets

Schlumberger. (November 18, 2020). DrillPlan. Retrieved April 27, 2021, from https://www.software.slb.com/products/product-library-v2?product=DrillPlan&tab= Product%20Sheets

Schlumberger. (October 6, 2016c). DrillBench Rigsite Kick. Retrieved April 27, 2021, from https://www.software.slb.com/products/product-library-v2?product= Drillbench&tab=Product%20Sheets

Siemens. (2020). Digitalization for Oil and Gas. Siemens-Energy.Com Global Website. Retrieved June 15, 2021, from https://www.siemens-energy.com/global/en/offerings/industrial-applications/oil-gas/digital.html

Strømhaug, A. H. (2014). Directional Drilling—Advanced Trajectory Modeling. NTNU – Norwegian University of Science and Technology.

Sui, D., and Langåker, V. H. (2018). Downhole Temperature Modeling for Non-Newtonian Fluids in ERD Wells. Modeling, Identification, and Control: A Norwegian Research Bulletin, 39(2), 131–149. https://doi.org/10.4173/mic.2018.2.7

Sunny. (2015a, September 17). Art of Directional Drilling: Basic Terminologies. Art of Directional Drilling. https://directionaldrillingart.blogspot.com/2015/09/basic-terminologies-below-are-listed.html

Sunny. (2015b, September 18). Art of Directional Drilling: Types of Directional Well Profiles. Art of Directional Drilling. https://directionaldrillingart.blogspot.com/2015/09/ types-of-directional-well-profiles-in.html

Tang L. (2019), Stick-Slip Vibrations in Oil Well Drill String. From: https://journals.sagepub.com/doi/10.1177/1461348419853658.

UiS Drillbotics. (2021a). UiS Drillbotics. University of Stavanger. Retrieved June 11, 2021, from https://www.uis.no/en/energy/uis-drillbotics

UiS Drillbotics. (2021b). Team A - UiS Drillbotics, University of Stavanger. Retrieved June 11, 2021, from https://www.uis.no/en/energy/team-uis-drillbotics

Wiktorski, E., & Sui, D. (2020), Investigation of Stick-Slip Severity in a Coupled Axial-Torsional Drillstring Dynamics Using a Two DOF Finite Element Model. OMAE June 28-July 3, 2020, Fort Lauderdale, Florida, USA.

Wiktorski, E., Kuznetcov, A., & Sui, D. (2017). ROP Optimization and Modeling in Directional Drilling Process. Day 1 Wed, April 05, 2017, D011S003R002. https://doi.org/10.2118/185909-MS

Williamson, H. (2000). Accuracy Prediction for Directional Measurement While Drilling. SPE Drilling & Completion 15(04): 221-233.

Wilson, A. (2015). Drilling Modeling and Simulation: Current State and Future Goals. *J Pet Technol* 67: 140–142. doi: https://doi.org/10.2118/0915-0140-JPT

Winters, W. J., Warren, T. M., & Onyia, E. C. (1987). Roller Bit Model with Rock Ductility and Cone Offset. 12. DOI: https://doi.org/10.2118/16696-MS

Wolff, C., & De Wardt, J. (1981). Borehole Position Uncertainty-Analysis of Measuring Methods and Derivation of Systematic Error Model. Journal of Petroleum Technology 33(12): 2,338-332,350.

Wu, J., and Juvkam-Wold, H.C. (1993). "Study of Helical Buckling of Pipes in Horizontal Wells." Paper presented at the SPE Production Operations Symposium, Oklahoma City, Oklahoma. DOI: https://doi.org/10.2118/25503-MS.

Yigit, A. & Christoforou A. (2006). Stick Slip and Bit Bounce Interaction in Oil Well Drill String. Journal of Energy Resources Technology, 128: 268–274.

Zhang Y. (2013). Side Force and Directional Tendency of BHA with Eccentric Components. M.S. thesis, University of Houston.

Appendixes

Appendix A

2D Wellbore Trajectory Design Example

A 2D wellbore trajectory can be designed by applying the parameters represented by the variables used in the following equations are described in the figure below.

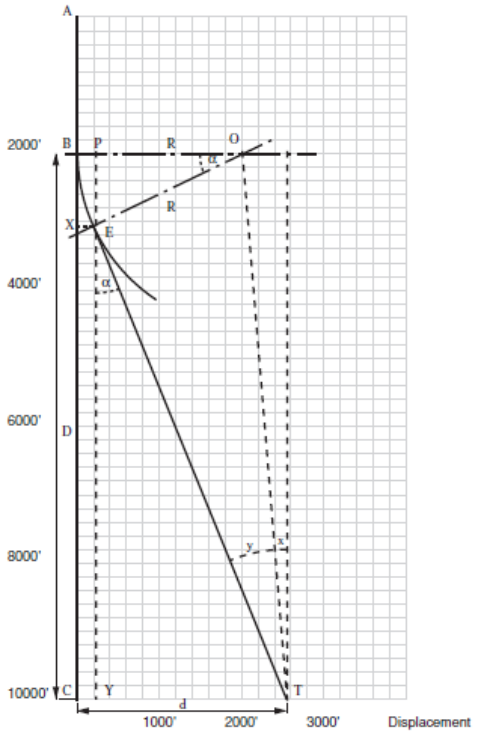

Figure 1: 2D Trajectory Calculation.
Source: (Heriot-Watt University, n.d)

Table 3.1, shown below, gives an insight into what is needed for 2D trajectory design and which outputs the model calculated. The simple calculations for such 2D well trajectory prediction are given to briefly demonstrate the numerical effort and steps involved in such work.

Table 1: Inputs and outputs

Inputs	TVD, KOP, HD, BUR
Outputs	INC, AZ, MD

A simple example for 2D well trajectory design:

In the figure above, the radius of curvature R can be calculated from the build-up rate:

$$R = \frac{180}{\pi} * \frac{100}{BUR} \quad (1)$$

$$Tan\ x = \frac{(d - R)}{D} \quad (2)$$

$$Sin\ y = \frac{R * Cos\ x}{D} \tag{3}$$

$$\alpha = x + y \tag{4}$$

The length of the build section can be given by:

$$\frac{BE}{2 * \pi * R} = \frac{\alpha}{360} \tag{5}$$

The TVD at the end of the build section is expressed as:

$$PE = R * Sin\ \alpha \tag{6}$$

$$AX = AB + PE \tag{7}$$

The horizontal displacement at the end of the build section is calculated by:

$$XE = OB - OP \tag{8}$$

where OB = R

$$OP = R * Cos\alpha \tag{9}$$

$$XE = R * (1 - Cos\ \alpha) \tag{10}$$

The MD at the end of the build section is given by:

$$AE = AB + BE \tag{11}$$

Furthermore, the total MD at the target can be expressed as:

$$AT = AE + ET \tag{12}$$

Where:

- α is the angle of inclination.
- R is the radius of curvature.
- BUR is the build of Rate.
- d is the horizontal displacement.

Appendix B

List of Inputs and Outputs

Following are the inputs and outputs for the models from section 4.

B.1. Inputs and outputs table from section 4.1

Table 1: Inputs for the T&D Model

Parameter	Notation	Unit
Length of the pipe (30m)	L	m
Unit pipe weight	w	N/m
Inclination	incl	degree (º)
Coef. of friction (0.2)	mi	-
Mud density (water => 1 sg)	Rho_mud	sg
Pipe density (steel =>7.85 sg)	Rho_pipe	sg
Dogleg (DL (Incl, Az))	DL	degree (º)
Axial velocity	Vh	m/s
Rotary pipe speed	RPM	RPM
Diameter of the pipe	d	m
Internal diameter casing (0.219075m)	D	m

Table 2: Outputs for the T&D Model

Parameters	Notation	Unit
Dynamic parameters		
Simple Drag profile – Tripping in drill string	F_in	N
Simple Drag profile – Tripping out drill string	F_out	N
Drag profile – Tripping in drill string (Combined motion)	Fc_in	N
Drag profile – Tripping out drill string (Combined motion)	Fc_out	N
Simple Torque profile	T	Nm
Torque profile – (Combined motion)	Tc	Nm

B.2. Inputs and Outputs table from section 4.2

Table 3: Flow Model constant inputs

Parameter	Notation	Unit
ID of drill pipe	r_pi	SI
OD of drill pipe	r_p	SI
ID of casing	r_ci	SI
Roughness of pipe and casing	roughness	
Surface viscosity of fluids	visc_f	SI
Surface density of fluids	rho_f	SI
Measured depth	depth	SI

Table 4: Flow model constant outputs

Parameters	Unit
Pressure profile of fluids inside pipe	SI
Pressure profile of fluids inside annulus	SI
Density profile of fluids inside pipe	SI
Density profile of fluids inside annulus	SI

B.3. Inputs and Outputs table from section 4.3.

Table 5: Inputs of the Model

Constant inputs		
Parameter	**Notation**	**Unit**
Diameter of the pipe	di	SI (m)
Diameter of the hole	do	SI (m)
Cutting's diameter (applied to the correction factor equation---- dismiss this input ?)	dcutt	SI (m)
Yield point	yp	SI – cp
Plastic viscosity	pv	SI – N/100m^2
Cuttings bed porosity (cuttings concentration)	fi_bed	SI
Adjustable inputs		
Parameter	**Notation**	**Unit**
Rate of penetration	rop	SI (m/s)
Mud weight	mw	SI (sg)
RPM	rpm	SI
Flow rate	Q0	SI
Inputs from other modules		
Parameter		**Modules**
Inclination, azimuth, TVD		Trajectory model

Table 6: Outputs of the Model

Parameters	**Unit**
Critical flow rate	SI (m/s)
Cutting's concentration	SI

B.4. Inputs and Outputs table from section 4.4.

Table 7: Inputs of the Model

Constant inputs		
Parameter	**Notation**	**Unit**
Density of steel	rho_steel	SI (sg)
Youngs modulus	E	psi
Weight of the drill string (DS)	wDP	SI (kN/m)
Outer diameter of the DS	OD	SI (m)
Inner diameter of the DS	ID	SI (m)
Casing inner diameter/open hole diameter	csgID	SI (m)
Drill pipe grade (API)	grades	psi
Friction factor	mu	SI
Adjustable inputs		
Parameter	**Notation**	**Unit**
Mud weight	mw	SI (sg)
Inputs from other modules		
Parameter		**Modules**
Inclination, azimuth, TVD		Trajectory model

Table 8: Outputs of the Model

Parameters	**Unit**
Dynamic forces acting on the drill string	SI (kgf)
Effective axial load	SI (kgf)
Maximum helical buckling limit along the well	SI (kgf)
Minimum helical buckling along the well	SI (kgf)
Sinusoidal buckling limit	SI (kgf)
Permanent corkscrewing (for given Feff)	SI (kgf)